HIGH TEMPERATURE PYROLYSIS AND GASIFICATION OF BIOMASS AND BLENDS

A Dissertation
Presented to
The Academic Faculty

by

Mohmed Akil Syed

In Partial Fulfillment
of the Requirements for the Degree
Doctor of Philosophy in the
School of Chemical & Biomolecular Engineering

Georgia Institute of Technology
May 2016

HIGH TEMPERATURE PYROLYSIS AND GASIFICATION OF BIOMASS AND BLENDS

Approved by:

Dr. Pradeep K. Agrawal, Advisor
School of Chemical & Biomolecular Engineering
Georgia Institute of Technology

Dr. Carsten Sievers, Co-advisor
School of Chemical & Biomolecular Engineering
Georgia Institute of Technology

Dr. Jerry M. Seitzman
School of Aerospace Engineering
Georgia Institute of Technology

Dr. John D. Muzzy
School of Chemical & Biomolecular Engineering
Georgia Institute of Technology

Dr. Ryan P. Lively
School of Chemical & Biomolecular Engineering
Georgia Institute of Technology

Dr. Derrick W. Flick
Lead R&D Manager
The Dow Chemical Company

Date Approved: April 2, 2016

ACKNOWLEDGEMENTS

I would like to thank my advisors, Dr. Pradeep Agrawal and Dr. Carsten Sievers, for the guidance through graduate school and the research projects. I would also like to thank my research group members for useful discussions and assistance through the years: Gautami Newalkar, Olga Simakova, Sireesha Aluri, Ildar Musin, John Copeland, Jessica Ewbank, Sarah Schimming, Guo Shiou Foo, Jungseob So, Chukwuemeka Okolie, and Alex Brittain. I would like to extend my special thanks to Dr. Scott Sinquefield for providing operational assistance for running the pressurized entrained flow reactor (PEFR), and Steve Lien for providing guidance on building different equipment's and for assisting in biomass feedstock preparation. I would like to thank my thesis reading committee for the constructive comments on this work.

I would like to acknowledge "The Dow Chemical Company" for their support of this research. I would also like to acknowledge the help of Dr. Christopher Jones group members for training me on different analytical instruments: Shilpa Mahamulkar, Taylor Sulmonetti, and Miles Sakwa-Novak.

I would also like to acknowledge the technical support from the Center for Nanostructure Characterization (CNC) and Microanalysis centre (MAC), both located on the Georgia Institute of Technology campus. I would like to thank TI: GER program (Technological innovation: Generating economic results) for providing 50% graduate tuition fee waiver for two years and $25,000. Finally, the support from the following undergraduate researchers is highly appreciated: Yurancy Quinones, Christopher Schmitt, Andrew Tricker, Leigh Anne Tuck, Erin Hogan, Karina Psareva, Marion Juren, Isil Deniz Aydin, and Yiquiong Zhang.

TABLE OF CONTENTS

LIST OF TABLES

LIST OF FIGURES

LIST OF SYMBOLS

R_{app}	Apparent reaction rate
R_{in}	Intrinsic reaction rate
S	Char surface area
η	Effectiveness factor
D_{eff}	Effective diffusion coefficient
V_{avg}	Average velocity of gas in the PEFR or LEFR
Q	Total inlet gas flow rate in the PEFR or LEFR
r_i	Inner radius of the reactor tube of the PEFR or LEFR
H	Height of the collector tube for reaction in the PEFR or LEFR
t_R	Residence time in the PEFR or LEFR
X	Char conversion
R	Instantaneous char reactivity
dm/dt	Rate of char weight loss
m_o	Initial mass of the char at the onset of gasification
m_t	Instantaneous mass of the char at time t
m_{ash}	Remaining mass of ash after completion of gasification and burning
S_{DR}	Surface area by Dubinin- Radushkevich equation
S_{BET}	Surface area by Brunauer–Emmett–Teller theory
C_{cs}	Concentration of carbon (re)active sites
X_{calc}	Calculated or predicted conversion of the mixture
W_{BB}	Weight fraction of BB char in the mixture
X_{BB}	Conversion of pure brazil bagasse
X_{BL}	Conversion of pure brazil leaves

R_{calc}	Calculated or predicted instantaneous reactivity of the mixture
R_{exp}	Experimentally measured instantaneous reactivity of the mixture
N	Number of data points for calculating RMS deviation

LIST OF ABBREVIATIONS

PAH	Polycyclic aromatic hydrocarbons
HACA	Hydrogen abstraction acetylene addition
PEFR	Pressurized entrained flow reactor
EFR	Entrained flow reactor
LEFR	Laminar entrained flow reactor
IGCC	Integrated gasification combined cycle
DTF	Drop tube furnace
SEM-EDX	Scanning electron microscope- energy dispersive X-ray analysis
XRD	X-ray diffraction
ICP-OES	Inductively coupled plasma- optical emission spectrometry
HHV	High heating value
db	Dry basis
daf	Dry and ash free basis
TGA	Thermogravimetric analyzer
DFT	Density functional theory
SCT	Sugarcane leaves and tops
LB	Louisiana bagasse
BB	Brazil bagasse
LL	Louisiana leaves
BL	Brazil leaves
AI	Alkali index
ASA	Active surface area
TSA	Total surface area

RSA	Reactive surface area
AAEM	Alkali and alkaline earth metals
NREL	National renewable energy laboratory
TPD	Temperature programmed desorption
RMS	Root mean square deviation
MFC	Mass flow controller

SUMMARY

Biomass is regarded as a truly renewable resource, and is expected to play an important role as a future energy feedstock. Biomass can supplement the energy required to meet the continuous increase in energy demand while mitigating climate change. The lignocellulosic components in biomass can be gasified to produce syngas for the sustainable production of electricity, chemicals and fuels.

The gasification process, in general, includes a devolatilization step (pyrolysis) and a char gasification step. During gasification, much of the initial mass loss from biomass consists of volatiles released by pyrolysis while the char gasification reactions of the carbonaceous char with steam and carbon dioxide are comparatively slow. Due to the drastic difference in the time scales for the pyrolysis and char gasification steps, the approach chosen here involves experimental study of these two steps separately, so that each step may be independently optimized. Since char gasification is the rate-limiting step in the gasification process, a considerable effort is being made to understand the char gasification reactivity.

One of the major challenges involved in commercialization of biomass gasifiers is the lack of fundamental studies which can help in generalizing the results among different biomass feedstocks and different gasification conditions used in various studies. So, the research theme of this project focuses on providing a fundamental understanding of the four major parameters that affect char gasification kinetics in a gasification reactor. These parameters lead to four major research objectives of this project and these are: a) Evaluating the effect of pyrolysis operating conditions on the char physicochemical properties and gasification reactivity (study 1); b) Reconciliation of the char reactivity of

different biomass species (study 2 and study 3); c) Co-gasification of two biomasses (study 4); and d) Char gasification study in steam, CO_2, and their mixtures (study 5). High temperature pyrolysis and gasification of different biomass species is studied in this work by utilizing two complementary reactors for experiments: entrained flow reactor (EFR) for pyrolysis, and thermo-gravimetric analyzer (TGA) for char gasification.

The *first* study uses a pressurized entrained flow reactor (PEFR) to study the pyrolysis of sugarcane bagasse at different pressures, temperatures, and residence times (at high heating rates relevant for biomass gasifiers). The aim of this study is to evaluate the effect of pyrolysis operating conditions (under relevant commercial gasifier conditions) on the char morphology, char physicochemical properties, and the subsequent char gasification reactivity. An increase in pyrolysis severity in the PEFR causes a decrease in char surface area and formation of more polyaromatic char. This led to a decrease in char gasification reactivity. Also, a complex char reactivity dependence on pyrolysis pressure was observed with a minimum char reactivity at 1.5 MPa and at a high pyrolysis residence time. These observations can be helpful in choosing efficient biomass gasifier design conditions.

The *second* study focuses on two different sugarcane residues (bagasse and cane leaves) to identify the similarities and differences during the evolution of char gasification reactivity with conversion. Experimental results showed that even though bagasse and cane leaves come from the same biomass species, their gasification reactivities differ. It was found that the (K + Ca)/Si ratio correlated well with the initial char reactivity, but not with the overall char reactivity. The overall char reactivity profile with char conversion level can be correlated to the dispersion of active inorganics in char,

and the active surface area defined by CO_2 chemisorption was found to be a measurable descriptor of char gasification reactivity.

The third study focuses on correlating the initial reactivity of different types of biomass chars with the fundamental char properties. Formulating a correlation to predict gasification reactivity of chars from a wide variety of biomass can be used for predicting the gasification reactivity when processing chars from different biomasses in a gasifier. In this study, the physiochemical properties of chars (namely, surface area, ash content, ash composition, and H/C atomic ratio) from a wide variety of biomasses were measured and correlated with its gasification reactivity. Based on the results none of the aforesaid char properties could solely explain the char reactivity for different biomasses. However, the active surface area (ASA) of the chars, as measured by CO_2 chemisorption, represents the cumulative effect of the properties above, and therefore it is a better descriptor.

The *fourth* study focused on co-processing of bagasse with cane leaves since it can lead to potential improvements in the economy of scale and fuel availability, and also there is the possibility of a potential synergistic increase in the mixture reactivity due to interaction between two different biomass chars. This study was focused on co-gasification of various mixtures of Brazilian bagasse (BB) and cane leaves/tops (BL) chars to determine if co-gasification is a favorable processing scheme. It was found that co-gasification of these two chars led to a lower than expected gasification performance. This inhibition effect is attributed to the migration of potassium from K-rich BB char to BL char, followed by the reaction of some of the migrated potassium with silica in BL char to form inactive potassium aluminosilicates. It was found that a staged reactor flow

scheme, where BB ash from a first reactor is used to catalyze BL char gasification in a second reactor, is a more favorable processing scheme.

The last part of this thesis *(the fifth study)* involves studying char gasification of potassium rich bagasse char in steam, CO_2, and their mixtures. The aim of this study is to provide a fundamental understanding about the differences in the evolution of char reactivity in steam as compared to CO_2, and to find the char reactivity in a mixture of steam and CO_2 since the gasification atmosphere inside a commercial gasifier is a mixture of steam and CO_2. Based on the results the *initial* char gasification reactivity in steam is higher than in CO_2 (about 2.4 times), as is commonly reported in the literature. However, the *overall* reactivity (defined by the time for 90% char conversion) is higher in CO_2 than in steam, thus making CO_2 an attractive gasification agent compared to steam. It was also shown that the initial active sites for steam and CO_2 gasification are likely to be the same. However, as the char gasification progresses in pure steam, the active sites are likely to be blocked by in-situ hydrogen product formation, which does not happen during CO_2 gasification. On the contrary, there is an enhancement in char reactivity with increasing conversion in CO_2 due to the increasing K/C ratio, thus creating more active sites. This explains why the *overall* reactivity is lower in steam than in CO_2. Finally, gasification of bagasse char in a mixture of steam and CO_2 is not additive. Therefore, mixed atmosphere gasification reactivity should be measured experimentally by conducting experiments with different $H_2O/CO_2/N_2$ mixtures.

CHAPTER 1

INTRODUCTION

1.1 Driving factors for biomass gasification research

Gasification is a complex thermochemical process in which a carbonaceous solid fuel (coal, biomass, and wastes) is transformed at high temperatures (700-1500 °C) and in the presence of a gasifying agent into a gas, called a producer gas or synthesis gas. The key advantage of gasification is the possibility of converting a solid fuel into a gas (easier to clean, transport and burn efficiently) which keeps 70-80% of the chemical energy of the original fuel [1]. Moreover, syngas from gasification can be used in a wide range of applications: production of heat and power, and for the synthesis of fuels and chemicals [2].

In recent years, a growing demand for renewable energy to reduce excessive dependence on fossil fuels and to reduce global CO_2 emissions has resulted in higher production of first generation biofuels which uses food crops such as sugarcane, grains and vegetable oil. However, the increasing concern about the sustainability of first generation biofuels, primarily due to competition with feed and food production, has raised attention to the potential of using renewable lignocellulosic biomass waste for the production of second generation fuels and chemicals [3,4]. Second generation biofuel technologies are broadly classified into thermochemical and biochemical conversion technologies. The advantages of thermochemical technology are robustness and the ability to accept a wide range of feedstocks, making thermochemical processes like gasification much more attractive than biochemical conversion processes [5]. The

potential for using more than one feedstock and widely different feedstocks in a single gasification facility also reduces the project risk.

Pressurized biomass gasification processes (to produce alternative liquid fuels) can reduce downstream syngas compression requirements as well as processing equipment size, in addition to enhancing the rate of gasification reactions [6]. Therefore, in recent years, increasing interest has been shown in pressurized gasification systems due to their potentially high thermal efficiency and reduced environmental impact [7]. The need for advanced gasification technologies which can increase efficiency and consequently reducing greenhouse gas emissions led to the investigation of char structures formed during high pressure gasification.

One of the major lignocellulosic agro-industrial materials found in great quantities, especially in tropical countries, which can be used as a feedstock for a gasification process is sugarcane bagasse [8]. Bagasse is a fibrous residue obtained after extracting the juice from sugarcane stalk in the sugar production process. The strategic value proposition of using sugarcane waste is that it is available at one location – a sugar mill. This eliminates the need for collecting biomass from a much wider area, and reduces transportation and preprocessing cost. These factors lead to lower delivered bagasse cost compared to many other biomass feedstocks [9]. In addition to the bagasse produced from sugar mill operations, an equivalent amount of fiber is produced by the sugarcane plant in the form of cane trash, the leaves and tops that are usually burned or left in the field during the harvest operations. Cane trash has long been recognized as a significant potential source of biomass [10]. Utilizing cane trash effectively through gasification, either separately or as a mixture with bagasse, can provide value-added

products from waste. Thus this research project focuses on utilizing sugarcane bagasse and cane trash for gasification research. However, to gain more insight into the effect of different variables on char reactivity, data from other feedstocks will also be utilized when required.

1.2 Advantages of gasification over combustion

The gasification process has superior environmental performance vis-à-vis combustion processes in dealing with the solid feeds such as biomass [11]. Gasification plants can capture carbon dioxide more efficiently than combustion-based power plants because of the high pressure of produced syngas by gasification [1]. Captured CO_2 can then either be utilized (for example, in enhanced oil recovery) or stored, thus reducing the emission of CO_2 to atmosphere. All the combustion processes that use solid fuels, apart from gas emissions, produce solid residues (slag and fly ash) which have been found to be hazardous. Unlike those from combustion processes, the by-product ash and slag from the gasification technologies have been shown to be non-hazardous [11].

1.3 Overview of steps in gasification

The gasification process, in general, includes a devolatilization step (pyrolysis) and a char gasification step. During pyrolysis, the carbonaceous material is heated and rapidly loses volatiles to generate char, gas and tars [11], as shown in Figure 1.1. The first organic species vaporized from the biomass during pyrolysis are termed primary pyrolysis tars. Secondary pyrolysis tars are formed from cracking of primary tars, and tertiary pyrolysis tars are those species formed at high temperatures (>750 °C). The tertiary products are polycyclic aromatic hydrocarbons (PAH's) and are often the species found during gasification [12]. PAH then leads to soot/coke formation. HACA (hydrogen

abstraction acetylene addition) route to PAH formation has been proposed as the likely mechanism for soot formation [13].

The char gasification step involves reactions with the various gaseous species present in the gasifier such as H_2O, CO_2 and O_2 (oxygen remaining after the combustion of the volatile species). Figure 1.1 shows the schematic of steps involved in biomass gasification. The pyrolysis step is much faster than the char gasification step. Consequently, char gasification is the rate limiting step during gasification of solid fuels. Accordingly its kinetics highly impact the design of the gasifier [14].

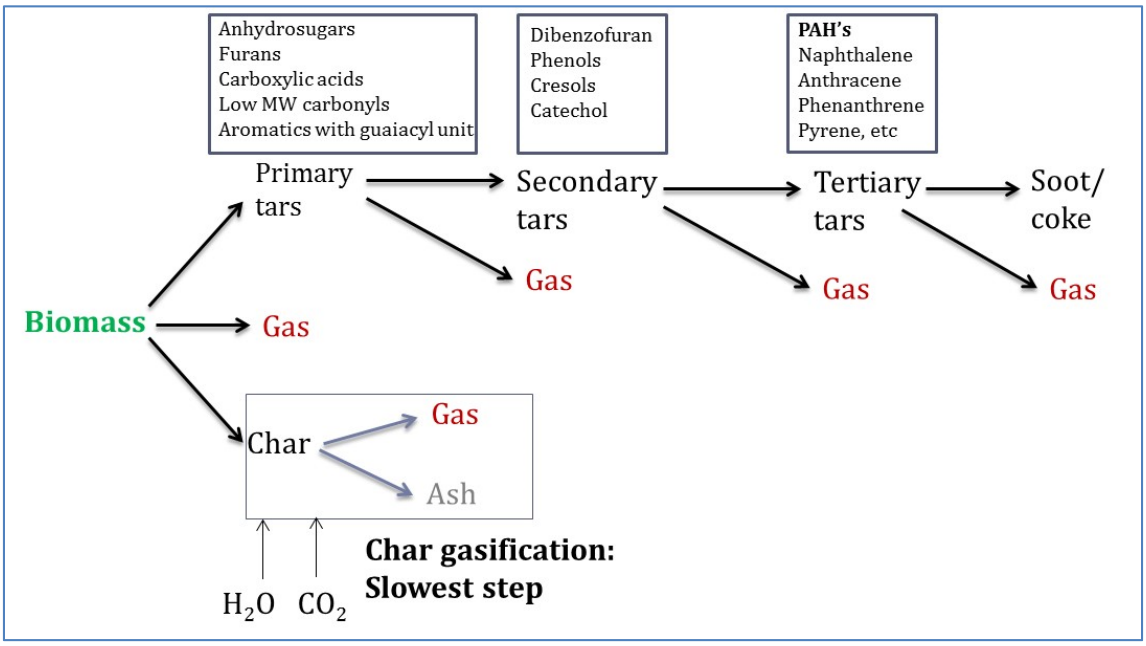

Figure 1.1 Schematic of reaction steps involved in biomass gasification [11,12]

1.4 Major challenges in biomass gasification research

The major challenges involved in the commercialization of biomass gasifiers are as follows:

a) Biomass heterogeneity and lack of fundamental studies: The biomass gasification technologies are currently under development, but because of the heterogeneity of the biomass sources (e.g., wood, agricultural waste, forest residue, etc.), there can be significant variations in the composition and quantity of syngas, and reactivity and conversion of biomass char. Flexibility of using feedstocks from difference sources is important as old fuel sources can dwindle and new sources become available. However, owing to the wide variations in the composition of biomass from different sources or from different feedstocks, and incomplete characterization, the results do not lend themselves to generalization. The uncertainties associated with any quantitative description of the gasification suggest that one needs to approach the problem from a basic understanding level. This means that the research study should focus on identifying and measuring fundamental parameters controlling biomass gasification by rational design of experiments to deconvolute the effect of different parameters.

b) Lack of high pressure gasification kinetic data: It is apparent that there is extensive literature on the kinetics of devolatilization and gasification [11]. However, some of the gasification kinetics at high pressures has been carried out on char samples generated at atmospheric pressure or slow heating conditions and that are therefore not representative of chars present in commercial gasifiers. This renders the

experimental data to be less useful for design. The aim of lab scale research should be to build and utilize a reactor set up that mimics commercial gasifiers.

c) High capital cost and limited economy of scale: The most significant economic challenge for the commercialization of biomass gasification is the relatively high capital costs of gasification plants per unit of product, and the limited quantity of biomass feedstock that can be economically collected. Lab scale research and development (R&D) to lower capital costs is inherently difficult and is limited to choosing moderate (or less severe) gasification operating conditions. The other effective method of lowering costs per unit of product is by achieving economy of scale [15]. Gasification plants designed to handle a mixture of biomass, or co-processing biomass and low-rank coal is one possible solution for meeting the requirement of economy of scale. Co-processing can also mitigate the effect of short term variations in feedstock.

d) Equipment reliability issues: Improvement in reliability and dependability of gasification equipment is needed to ensure profitable operation and to ensure commercial acceptability [15].

e) Tar (PAH) removal: Development of high-efficiency processes for syngas cleaning and conditioning that operate at moderate to high temperatures is needed to provide multi-contaminant mitigation to extremely low levels. This is needed to ensure stable operation of downstream syngas conversion processes. Tar formation remains the main technical hurdle at commercial scale, due to its associated operating problems (condensation, deactivation of catalysts, polymerization, etc.)

[2]. Therefore, tar elimination from the product gas, either during gasification or after gasification, is required to make gasification an attractive option [13].

The aim of the current research project is focused at addressing the first three issues listed above.

1.5 Objectives and Organization

The approach chosen here involves experimental study of the pyrolysis and char gasification processes separately, so that each step may be independently optimized. For this purpose, biomass will be first pyrolyzed in a reactor which operates under commercially relevant operating conditions (pressurized entrained flow reactor, PEFR; and laminar entrained flow reactor, LEFR) to generate chars, which are then characterized. Char gasification is then studied separately. Since char gasification is the slowest step, extensive effort will be made to understand fundamental descriptors that affect char reactivity. It is again noted here that this research project focuses primarily on utilizing sugarcane bagasse and cane trash for gasification research. However, to gain more insight into the effect of different variables on char reactivity, data from other biomass feedstocks will also be utilized when required.

At present, biomass-based gasification processes are largely based on the experience of coal gasification. Understanding the relation between char structure and reactivity is largely based on the studies of coal chars and/or highly ordered carbon materials. However, derived from biomass, biochar has a highly heterogeneous and disordered structure, which can be prone to changes during the course of char

gasification. And therefore, the knowledge of coal chars may not be entirely applicable to biochars [16].

The parameters affecting char reactivity in an industrial gasifier are broadly classified in different sections below, and these parameters are the focus of this research project for improving the fundamental understanding of char gasification kinetics in a gasification reactor. These parameters are as follows:

a) Effect of pyrolysis conditions on initial char properties: The initial char properties which are fundamental in understanding char reactivity are carbon structure, pore structure/morphology, inorganic content and type, and the dispersion of inorganics [17]. These properties are determined by the pyrolysis conditions employed in the gasifier, and it determines the *initial* char reactivity. The effect of pyrolysis conditions, under commercially relevant gasifier operating conditions, on char initial physicochemical properties and thus char reactivity is discussed in Chapter 2. This study can help in choosing favorable operating conditions for gasifier design.

b) Conversion level of char: The char properties mentioned above do not remain constant during the progression of gasification. Therefore, it is important to identify the evolution of char properties, and therefore char reactivity as a function of conversion. Structural models, like the random pore model (RPM), account only for the changes in pore size and distribution but do not account for the changes in carbon structure, inorganic content and the dispersion of inorganics with conversion [18]. These parameters also play a role in determining the evolution of char gasification reactivity, and need to be assessed [17]. Changes in

physicochemical properties of char, and its effect on char reactivity with increasing conversion level are studied for a potassium rich and calcium rich char in Chapter 3. The aim is to correlate the char reactivity at different conversions with the corresponding active surface of char measured using CO_2 chemisorption at 300°C. The char reactivity is determined by the char physical surface area, the content of K, Ca and Si (or the active inorganics which are not deactivated by minerals in biomass), and the dispersion of K and Ca (all of which changes with char conversion). It is hypothesized that the active site area (ASA) can combine these individual effects to measure the dispersion of active catalytic species on the char surface.

c) Feedstock characteristics: Biomass varies widely in terms of inorganic content and type. Formulating a correlation to predict gasification reactivity of chars from a wide variety of biomass feedstocks requires an understanding of the fundamental descriptor(s) of char gasification reactivity. However, the major hurdles to achieve this objective are the inherent complexity of biomass and the concurrent variations in many char properties. These factors prevent the deconvolution of the effect of different char properties on its gasification reactivity. To partially overcome these limitations, Chapter 4 focuses on studying chars from different biomass feedstocks in an effort to segregate the effect of different char properties on its initial reactivity. The aim of this study is to obtain fundamental predictors of char gasification reactivity in order to predict reactivity of different biomass chars. Also, within the same biomass, biomass properties and thus char reactivity varies between different sources of biomass. Thus Chapter 3

focuses on determining the fundamental char descriptors to reconcile the reactivity of sugarcane residue from two different sources (sugarcane residue from Louisiana and Brazil).

d) Interactions during co-gasification of two different biomass feedstocks: As discussed before, gasification plants designed to handle a mixture of biomasses is one possible solution for meeting the requirement of economy of scale, and also to reduce the effect of short term variations in biomass feedstock availability. Also, the interaction between two char components can cause a synergistic or inhibitive effect on gasification of the mixture rather than an additive effect [19–21]. Since the sugarcane bagasse quantity available at a given location is limited, co-processing sugarcane leaves and tops with bagasse can potentially double the gasifier feedstock quantity [22]. Thus Chapter 5 focuses on co-gasification characteristics of sugarcane residues to determine the optimum flow scheme for co-processing of sugarcane residues (bagasse with cane trash) to maximize the char reactivity.

e) Gas composition in gasifier: The gasification atmosphere inside a commercial gasifier includes steam, CO_2, air/oxygen (for supplying heat), and their mixtures. Char gasification reactivity in CO_2 and steam are different [23–26]. Also, the char gasification reactivity is not only a function of partial pressure of reactant gases (like CO_2, H_2O) but also a function of other gases generated during pyrolysis and gasification, such as H_2 which inhibits reaction rate [27–29]. Thus, the aim of Chapter 6 is to provide a fundamental understanding about the differences in the evolution of char reactivity in steam compared to CO_2.

f) Intra-particle pore diffusion limitations: The char gasification reaction is limited by gas diffusion within the porous char matrix as the gasification temperature is increased. An effectiveness factor η, which is the ratio of the actual rate to the rate attainable if no pore diffusion resistance existed, is often used to quantify pore diffusion limitations. The apparent reaction rate R_{app} (s^{-1}) is then calculated by: $R_{app} = \eta R_{in} S$

where R_{in} ($g\ m^{-2}\ s^{-1}$) is the intrinsic reaction rate, and S ($m^2\ g^{-1}$) is the internal surface area of the char particles

The effectiveness factor, η, primarily depends on particle temperature and size, as well as gas phase partial pressure of reactants and inhibiting products [30]. The pore diffusion becomes dominant with increasing gasification temperature. Thus, an effective diffusion coefficient, D_{eff}, is required for the calculation of the effectiveness factor, and is strongly dependent on the pore size within the particle [30]. In all the studies discussed in this thesis, the aim is to obtain the intrinsic char reaction kinetics, i.e., char kinetics in the absence of internal and external mass transfer limitations. To remove internal mass transfer limitations, crushed char particles and moderate gasification temperatures are used in all studies.

g) External mass transfer limitations: If diffusion through the particle film is not fast enough, the actual gasification rate differs from the intrinsic one evaluated under bulk-gas conditions. The overall gasification rate of a char particle is then determined by combining the intrinsic chemical reaction rate with intra-particle (part f above) and external diffusion rates. Therefore, the actual gasification rate may be strongly dependent on the particle size, effective properties of the char (if

intra-particle resistance is limiting), and fluid-dynamic conditions (if film resistance is important) [31]. To obtain intrinsic kinetic data in all the studies, the operating conditions, particle size and sample mass would be chosen such that the effect of intra-particle and external diffusional rates is removed.

Figure 1.2 shows a brief summary of the four main research objectives of this thesis. These four objectives incorporate the above mentioned parameters that affects char reactivity in a gasifier.

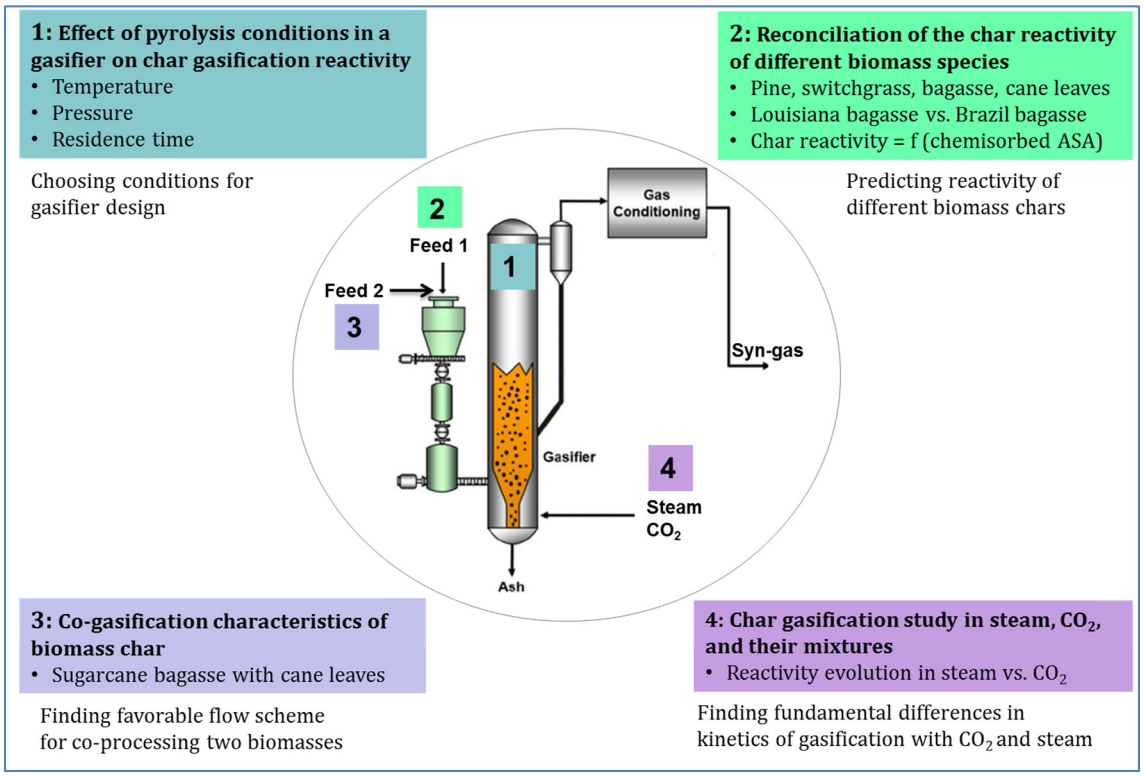

Figure 1.2 Schematic showing the four main research objectives for this project. The gasifier figure is adapted from reference [32].

The first research objective of Figure 1.2 focuses on part a. mentioned above, the results of which is discussed in Chapter 2. The second research objective focuses on part b. and c., the results of which is discussed in Chapter 3 and 4. The third research objective focuses on parts d., the results of which is discussed in Chapter 5. The fourth and final research objective focuses on parts e., the results of which is discussed in Chapter 6. Lastly, Chapter 7 summarizes the key learnings from each of these studies and discusses the broader impact of the research. This chapter concludes with recommendations for future studies.

1.6 References

[1] Higman C, Van Der Burgt M. Gasification, Gulf Professional Publishing 2008.

[2] Hernández JJ, Ballesteros R, Aranda G. Characterisation of tars from biomass gasification: effect of the operating conditions. Energy 2013;50:333–42.

[3] Eisentraut A. Sustainable Production of Second-Generation Biofuels: Potential and perspectives in major economies and developing countries. No 2010/1 OECD Publ 2010.

[4] Naik SN, Goud V V, Rout PK, Dalai AK. Production of first and second generation biofuels: a comprehensive review. Renew Sustain Energy Rev 2010;14:578–97.

[5] Milne TA, Abatzoglou N, Evans RJ. Biomass gasifier "tars": Their nature, formation, and conversion. vol. 570. National Renewable Energy Laboratory Golden, CO; 1998.

[6] Stevens C, Brown RC. Thermochemical processing of biomass: conversion into fuels, chemicals and power. John Wiley & Sons; 2011.

[7] Fermoso J, Stevanov C, Moghtaderi B, Arias B, Pevida C, Plaza MG, et al. High-pressure gasification reactivity of biomass chars produced at different temperatures. J Anal Appl Pyrolysis 2009;85:287–93.

[8] Martín C, Klinke HB, Thomsen AB. Wet oxidation as a pretreatment method for enhancing the enzymatic convertibility of sugarcane bagasse. Enzyme Microb Technol 2007;40:426–32.

[9] Joyce J, Dixon T, da Costa JCD. Characterization of sugar cane waste biomass derived chars from pressurized gasification. Process Saf Environ Prot 2006;84:429–39.

[10] Lau FS, Bowen DA, Dihu R, Doong S, Hughes EE, Remick R, et al. Techno-economic analysis of hydrogen production by gasification of biomass. Dep Energy Natl Renew Energy Lab DE-FC36-01GO11089; 2003, p. 37.

[11] Murthy BN, Sawarkar AN, Deshmukh NA, Mathew T, Joshi JB. Petroleum coke gasification: A review. Can J Chem Eng 2014;92:441–68.

[12] Jarvis MW, Haas TJ, Donohoe BS, Daily JW, Gaston KR, Frederick WJ, et al. Elucidation of biomass pyrolysis products using a laminar entrained flow reactor and char particle imaging. Energy Fuels 2010;25:324–36.

[13] Palma CF. Modelling of tar formation and evolution for biomass gasification: a review. Appl Energy 2013;111:129–41.

[14] Wang L, Sandquist J, Varhegyi G, Matas Güell B. CO_2 gasification of chars prepared from wood and forest residue: a kinetic study. Energy Fuels 2013;27:6098–107.

[15] http://www.netl.doe.gov/research/coal/energy-systems/gasification/gasifipedia/challenges. Accessed 15th Jan 2016.

[16] Wu H, Yip K, Tian F, Xie Z, Li C-Z. Evolution of char structure during the steam gasification of biochars produced from the pyrolysis of various mallee biomass components. Ind Eng Chem Res 2009;48:10431–8.

[17] Wang M, Roberts DG, Kochanek MA, Harris DJ, Chang L, Li C-Z. Raman spectroscopic investigations into links between intrinsic reactivity and char chemical structure. Energy Fuels 2013;28:285–90.

[18] Struis R, von Scala C, Stucki S, Prins R. Gasification reactivity of charcoal with CO_2. Part I: Conversion and structural phenomena. Chem Eng Sci 2002;57:3581–

92.

[19] Nemanova V, Abedini A, Liliedahl T, Engvall K. Co-gasification of petroleum coke and biomass. Fuel 2014;117:870–5.

[20] Habibi R, Kopyscinski J, Masnadi MS, Lam J, Grace JR, Mims CA, et al. Co-gasification of biomass and non-biomass feedstocks: synergistic and inhibition effects of switchgrass mixed with sub-bituminous coal and fluid coke during CO_2 gasification. Energy Fuels 2012;27:494–500.

[21] Tchapda A, Pisupati S. A Review of Thermal Co-Conversion of Coal and Biomass/Waste. Energies 2014;7:1098–148.

[22] Pippo WA, Garzone P, Cornacchia G. Agro-industry sugarcane residues disposal: the trends of their conversion into energy carriers in Cuba. Waste Manag 2007;27:869–85.

[23] Tomita A, Ohtsuka Y, Tamai Y. Low temperature gasification of brown coals catalysed by nickel. Fuel 1983;62:150–4.

[24] Ren L, Yang J, Gao F, Yan J. Laboratory study on gasification reactivity of coals and petcokes in CO_2/steam at high temperatures. Energy Fuels 2013;27:5054–68.

[25] Fan D, Zhu Z, Na Y, Lu Q. Thermogravimetric analysis of gasification reactivity of coal chars with steam and CO_2 at moderate temperatures. J Therm Anal Calorim 2013;113:599–607.

[26] Zhang L, Huang J, Fang Y, Wang Y. Gasification reactivity and kinetics of typical Chinese anthracite chars with steam and CO_2. Energy Fuels 2006;20:1201–10.

[27] Pineda DI, Chen J-Y. Modeling hydrogen inhibition in gasification surface reactions. Int J Hydrogen Energy 2015;40:6059–71.

[28] Hüttinger KJ, Merdes WF. The carbon-steam reaction at elevated pressure: Formations of product gases and hydrogen inhibitions. Carbon 1992;30:883–94.

[29] Molina A, Mondragon F. Reactivity of coal gasification with steam and CO_2. Fuel 1998;77:1831–9.

[30] Liu G, Tate AG, Bryant GW, Wall TF. Mathematical modeling of coal char reactivity with CO_2 at high pressures and temperatures. Fuel 2000;79:1145–54.

[31] Gomez-Barea A, Ollero P, Villanueva A. Diffusional effects in CO_2 gasification experiments with single biomass char particles. 2. Theoretical predictions. Energy Fuels 2006;20:2211–22.

[32] https://www.andritz.com/products-and-services/pf-detail.htm?productid=14969. Accessed 18th Jan 2016.

CHAPTER 2

EVOLUTION OF CHAR PHYSICOCHEMICAL PROPERTIES AND REACTIVITY DURING PYROLYSIS OF BAGASSE IN AN ENTRAINED FLOW REACTOR

2.1 Background

A growing demand for sustainable energy coupled with increasing questions about the sustainability of first generation biofuels, which use food crops such as sugarcane, grains and vegetable oil, has raised attention to the potential of renewable lignocellulosic biomass waste as an attractive option for the production of second generation fuels and chemicals [1,2]. One of the major lignocellulosic agro-industrial materials found in great quantities to be considered, especially in tropical countries, is sugarcane bagasse, a fibrous residue obtained after extracting the juice from sugarcane stalk in the sugar production process [3]. The utilization of bagasse has the advantage of low cost availability at centralized sugarcane processing facilities, which allows a great reduction of biomass collection and transportation costs when compared to other biomass resources. As a result, there has been an interest in utilizing sugarcane waste for electricity generation, by both conventional and integrated gasification combined cycle (IGCC) processes [4]. The power efficiency of biomass fueled power plants can be enhanced by performing gasification under elevated pressure in an IGCC plant [5]. In addition, biomass gasification at elevated pressure to produce alternative liquid fuels can reduce the size of downstream clean-up units and enhance the rate of gasification

reactions [6]. Therefore, in recent years, increasing interest has been shown in pressurized gasification systems due to their potentially high thermal efficiency and reduced environmental impact [7].

The gasification process consists of two steps: (i) pyrolysis or devolatilization, and (ii) char conversion to gas. Pyrolysis conditions in large scale gasifiers are characterized by high heating rate, high temperature, continuous feeding, low residence time and high pressure for IGCC and Fischer-Tropsch applications [8]. Experimental facilities and techniques to achieve operating conditions similar to practical applications are preferred to provide design data for optimizing parameters for large scale systems [8]. A lab or pilot-scale pressurized entrained flow reactor (PEFR) is well suited to mimic these practical operating conditions. The use of entrained flow reactors to study the characteristics of biomass pyrolysis and gasification under high temperature (700-1000 ^{0}C) and high heating rate (10^4 K/s) is important for biomass industrial applications, such as a cyclone gasifier, a fluidized-bed or a circulating fluidized bed gasifier [9].

Since char conversion is the slowest step and pyrolysis conditions affect char reactivity, extensive effort has been made in the past to understand the influence of pyrolysis conditions on biomass char characteristics and subsequent char gasification reactivity. However, in these studies not all operating variables were within relevant practical limits in a single experiment due to limitations of the reactor set-up. In the literature, rapid heating rate studies in a drop tube furnace (DTF) to determine the effect of pyrolysis operating conditions on biomass char morphology and char gasification reactivity were performed at atmospheric pressure [10-13]. The effect of pyrolysis pressure on char structure and reactivity is studied: (1) at moderate heating rate (500

K/min) in a wire mesh reactor [10], (2) in a continuous downdraft fixed bed reactor with heating rates of 1600 K/s [14], and (3) in a pressurized thermobalance at a low heating rate of 15 K/min [15]. There is a complex interdependence of the effect of operating conditions and reactor type on char structure and reactivity. This implies that to predict the effect of operating conditions in a PEFR on char structure and reactivity, the individual effects of different operating conditions from past studies cannot be readily combined. This necessitates an experimental study of biomass pyrolysis in the PEFR.

There were two studies which utilized a PEFR or a reactor set-up similar to a PEFR. Zanzi et al. [16] studied the effect of residence time (0.6 to 2.7 sec) on wood char reactivity at 0.26 to 0.30 MPa in a free fall reactor. The reactivity was found to decrease with an increase in residence time. Fjellerup et al. [5] studied the effect of pyrolysis pressure on char combustion reactivity in a PEFR using wheat straw as feedstock at 1000 ^{0}C and a 2.5 sec residence time. The char combustion reactivity was reduced when pressure was increased from 1.0 to 2.0 MPa. However, these two studies did not investigate a wider range of pyrolysis operating conditions and more importantly, the char characteristics responsible for decreased char gasification reactivity were not identified. These char characteristics are important for understanding the impact of pyrolysis conditions on char properties and reactivity. Thus, the objectives of this work are 1) to characterize the char formed under different pressurized pyrolysis conditions in a PEFR, 2) to relate pyrolysis operating conditions in a PEFR to char physical and chemical features and, in turn, to char gasification reactivity, and 3) to identify the differences between PEFR char generated under commercially relevant operating

conditions in this study versus the chars generated in previous literature studies for biomass pyrolysis.

In this study, the pyrolysis of sugarcane bagasse is carried out in a PEFR at different pressures (0.5 to 2.0 MPa), temperatures (600- 1000 ^{0}C) and residence times (2 sec and 25 to 29 sec). Char obtained from the PEFR is characterized extensively (by SEM-EDX, N_2 and CO_2 physisorption, XRD, ICP-OES, and ultimate analysis) to understand the changes in char physicochemical characteristics and their impact on char CO_2 gasification reactivity. The results from this study can assist in choosing favorable operating conditions for the design of gasifiers.

2.2 Experimental Methods

2.2.1 Experimental materials

Sugarcane bagasse from Louisiana (U.S.) was used in this study. Bagasse samples were dried in an oven at 105 ^{0}C for 6 hours and then ground and sieved to obtain 180-250 μm particles. This size range was used for all experiments. Proximate and ultimate analyses, ash composition and high heating value (HHV) of these particles are listed in Table 2.1.

Table 2.1. Ultimate analysis, proximate analysis and ash composition of Louisiana bagasse (180-250 μm)

Parameter	Value	Parameter	Value
Proximate analysis	*wt %*	*Ash Composition*	*wt ppm (db)*[a]
Moisture	6.5	K	3182
Fixed Carbon	10.8	Na	94
Volatile matter	75.4	Mg	745
Ash	7.2	Fe	1547
Ultimate analysis	*wt % (daf)*[a]	Ca	2718
C	46.30	Al	3205
H	6.38	S	1219
O[a]	46.81	P	354
N	0.36	Mn	45
S	0.16	Si	21396
HHV (*MJ/kg- db*[a])	18.47		

[a] by difference; db= dry basis; daf= dry and ash free basis

2.2.2 Pyrolysis experiments

Pyrolysis of bagasse under pressurized conditions was performed in a PEFR which was originally designed and located at Risø National laboratory and then moved to Georgia Institute of Technology (Atlanta) in 1999 [17]. Fjellerup et al. [5] explains briefly about the operation of this PEFR. This PEFR can provide a heating rate of ~10^4 ^{0}C/s and the residence time can be varied from 1 to 40 sec. Since the bagasse particle size is small, it moves with the same velocity as the nitrogen gas (99.999 %) used as the pyrolyzing medium. Average velocity of the gas in the PEFR (V_{avg}, in m/s) and the particle residence time (t_R, in s) is calculated by:

$$V_{avg} = \frac{Q}{\pi r_i^2} \tag{2.1}$$

$$t_R = \frac{H}{V_{avg}} \tag{2.2}$$

where Q (in m^3/s) is total inlet gas flow rate at the reactor operating temperature and pressure; r_i (in meters) is the inner radius of reactor tube; H (in meters) is the distance from the top of reaction tube to the top of collector probe where reacted particles are collected. Residence time can be varied by changing H (by moving the collector probe up or down) and/or by varying V_{avg} (by changing Q).

Two key characteristics of the PEFR help in precisely knowing the residence time. 1) The gas velocity is controlled in order to keep the flow in a laminar regime. By having a laminar flow, biomass particles follow a well-defined flow path and therefore have a well-defined residence time. 2) The collector probe is water cooled and a nitrogen quench gas is added at the top of the probe to stop any chemical reaction instantaneously. This provides a well-defined particle residence time at high temperature. Another important feature of the PEFR is that the gas volumetric flow rate is several orders of magnitude higher than the biomass mass flow rate, which means pyrolysis is done at constant gas temperature and at nearly constant gas composition. One limitation of the PEFR is that the direct calculation of char yield is not possible because not all the char can be collected in the collector since some of the char falls to the bottom of the reactor and sticks to the interior surface of the collector during quenching of the reactor outlet stream. Char yield estimation using ash tracer techniques did not yield reliable results, possibly due to significant ash loss from char particles in the PEFR.

In addition to PEFR runs, low heating rate (15 K/min) – low pressure (1 atm) pyrolysis runs were also conducted in a horizontal quartz tube reactor heated by a horizontal furnace. About 1 gram of sample was kept in a quartz boat inside the quartz tube reactor, and then the furnace was heated at 15 K/min to the desired pyrolysis

temperature (800 or 1000 ^{0}C) and held there for 10 min. Then the reactor was cooled slowly to below 60 ^{0}C to collect the char. Figure 2.1 shows the schematics of the PEFR and the quartz tube reactor.

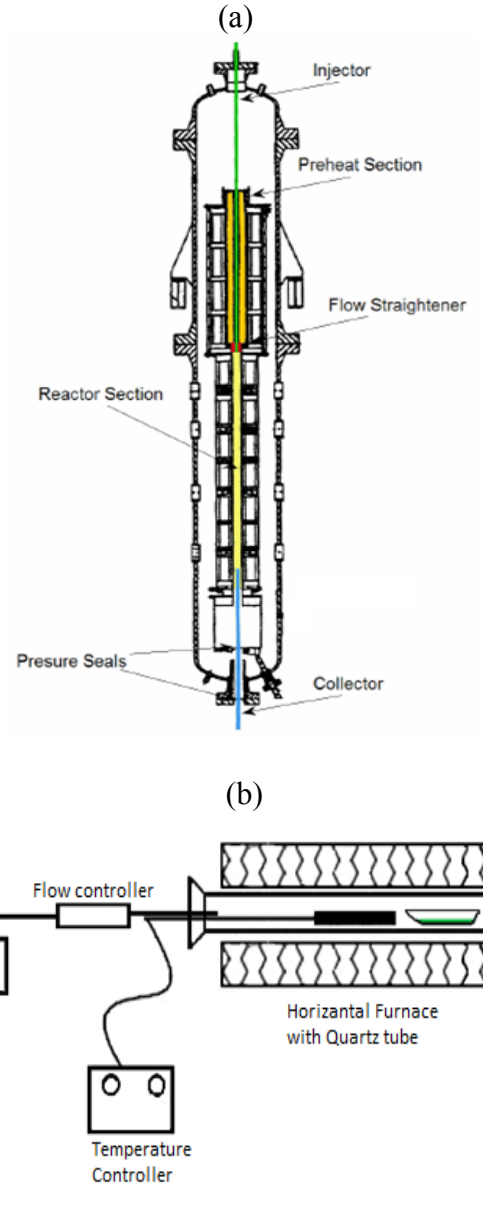

Figure 2.1 Schematics of reactors for pyrolysis experiments: (a) pressurized entrained flow reactor, and (b) horizontal quartz tube reactor

Table 2.2 shows the details of operating conditions used for different PEFR and quartz tube reactor runs. For ease of comparison, chars are designated as follows: 1st character stands for reactor type used for preparing char ("P" stands for PEFR char and "Q" for Quartz reactor char), then the 1st number stands for temperature in ^{0}C, the 2nd number is pressure in MPa and the 3rd number is residence time in seconds (only for PEFR chars). For the quartz reactor chars, the 3rd number is left vacant (NA-Not applicable). The experimental conditions corresponding to P-800-1.0-26, for example, refers to PEFR char generated at 800 ^{0}C, 1.0 MPa, and 26 s of residence time.

Table 2.2. Pyrolysis operating conditions for preparing different chars in the PEFR and quartz tube reactors, and the physical properties of these chars

Char Designation	T (˚C)	P (MPa)	t_R (s)	$V_{micropore}$ (cm^3/g)	$V_{mesopore}$ (cm^3/g)	Total pore volume[a] (cm^3/g)	Volatiles (wt% db)[b]
P-600-0.5-29	600	0.5	29.2	0.089	0.015	0.125	13.6 ± 1.6
P-600-1.5-26	600	1.5	26.1	0.072	0.007	0.082	10.7 ± 3.0
P-800-0.5-26	800	0.5	26.3	0.072	0.011	0.102	9.5 ± 2.3
P-800-1.0-26	800	1.0	26.0	0.041	0.021	0.080	4.5 ± 0.4
P-800-1.5-26	800	1.5	26.3	0.045	0.021	0.083	2.4 ± 0.3
P-800-2.0-25	800	2.0	24.9	0.052	0.018	0.088	3.6 ± 1.6
P-1000-0.5-2	1000	0.5	2.0	0.077	0.010	0.108	21.8 ± 1.5
P-1000-0.5-29	1000	0.5	29.2	0.037	0.030	0.088	5.6 ± 0.6
P-1000-1.5-28	1000	1.5	27.5	0.023	0.027	0.071	1.2
Q-800-0.1-NA	800	0.1	NA[c]	0.161	0.011	0.202	8.1 ± 0.3
Q-1000-0.1-NA	1000	0.1	NA[c]	0.161	0.012	0.196	4.2 ± 0.6

[a] Total pore volume obtained by combining micropore volume (by CO_2 physisorption), and meso and macropore (till approximately 150 nm) volume (by N_2 physisorption)
[b] Volatiles refers to the wt% of volatiles released from char during heating up of the char sample in N_2 at 25 K/min to 800 ˚C
[c] NA: Not applicable; T: Temperature, P: Pressure, t_R: Residence time

2.2.3 Char CO_2 gasification experiments

To assess the impact of pyrolysis operating conditions on char reactivity, isothermal CO_2 gasification experiments of chars generated by different pyrolysis runs were carried out in an atmospheric thermogravimetric analyzer (TGA) manufactured by TA Instruments (SDT Q-600). To ensure there was no external mass transfer resistance, sample mass was varied in gasification experiments until no change in reactivity is observed by further reducing the sample mass. To avoid internal mass transfer resistance, crushed char particles were used. About 0.8 to 2 mg of sample was used in each run to minimize mass transfer resistance at a gasification temperature of 800 ^{0}C. In each experiment, the sample was kept in a 90 μL alumina crucible and heated in N_2 (flowing at 200 ml/min) at 25 K/min to 800 ^{0}C and held there for 10 minutes to stabilize the sample mass measurement. The gas flow was then switched to pure CO_2 (99.99 %) at 200 ml/min to start gasification. The weight loss of the char sample was recorded continuously as a function of gasification time. For char with very low reactivity which did not convert fully even after 4-5 hours, air was injected to burn off the remaining char to find the final mass of ash. The carbon conversion (X) is defined as:

$$X = \frac{(m_o - m_t)}{(m_o - m_{ash})} \tag{2.3}$$

where m_o represents the initial mass of the char at the onset of gasification, m_t is the instantaneous mass of the char at time t and m_{ash} is the remaining mass of ash after completion of gasification and burning. Repeatability of data between the runs was good with a deviation of less than 5 %.

2.2.4 Characterization techniques

Complementary N_2 and CO_2 physisorption techniques were conducted at 77 K and 273 K, respectively. These were used to characterize the char for pore surface area, pore volume and pore size distribution. The measurements were performed in a Micromeritics ASAP 2020 instrument with an operating pressure range of 0 to 950 mm Hg. Nitrogen physisorption can provide meso and macropores surface area contributions accurately. But diffusional limitations at a low nitrogen adsorption temperature of 77 K limit access into ultramicropores (pores smaller than 0.7 nm in width). Alternatively, CO_2 molecules can easily access ultramicropores [18]. Micropore volume and surface area is obtained by applying the Dubinin- Radushkevich (DR) equation to the CO_2 physisorption data [19,20]. The Brunauer–Emmett–Teller theory (BET) is applied to obtain the surface area from N_2 physisorption data [21]. Nitrogen physisorption data is used to obtain mesopores (2 to 50 nm) surface area, macropores (>50 nm) surface area and mesopore volume, by applying the original density functional theory (DFT) model, assuming N_2 adsorption on carbon slit pores. Ultramicropores (<0.7 nm) and supermicropores (0.7 to 2.0 nm) surface areas are extracted from CO_2 physisorption data by applying the DFT model assuming CO_2 adsorption on carbon slit pores. DFT models installed in the ASAP 2020 instrument were used. Chars were outgassed first in a nitrogen flow of 500 ml/min in an atmospheric quartz tube reactor by heating at 25 K/min to 800°C (same as the gasification temperature) for 1 hour to remove trapped volatiles inside char. Final degassing is done again under vacuum at 50°C at a final pressure of < 0.7 Pa for 5 hours prior to the gas adsorption experiments.

SEM–EDX analysis of char was carried out in a LEO 1530 thermally-assisted field emission (TFE) scanning electron microscope (SEM) with energy dispersive X-ray analysis (EDX) capability. Other SEM images to study morphology of the char were taken in Hitachi S-800 and Hitachi SU8010 instruments. To investigate the carbon structure of the char samples, X-ray diffraction (XRD) spectra were recorded in the 2θ scan range of 10 to 90^0 on a PANalytical B.V. X'Pert Pro X-ray diffractometer operating at 45 kV, 40 mA with Cu Kα radiation. Proximate analysis of biomass is carried out in TGA (SDT Q-600). Ultimate analysis is done by Huffman Laboratories (Colorado, US). Trace element analyses were performed by the analytical testing lab located at the Renewable Bioproducts Institute (Atlanta, Georgia). Trace metal analysis of biomass (except sodium) was done by using a caustic fusion digestion method followed by ICP-OES (Inductively coupled plasma - optical emission spectroscopy). For the analysis of sodium in biomass, an acid digestion method is used followed by ICP-OES.

2.3 Results and Discussion

2.3.1 Morphological characteristics of char

2.3.1.1 Effect of heating rate and pressure

Figures 2.2a and 2.2b show the char morphology (by SEM) for chars prepared at a low heating rate - low pressure at 800 ^{0}C in a quartz tube reactor (Q-800-0.1-NA) and at high heating rate- high pressure at 800 ^{0}C in the PEFR (P-800-2.0-25), respectively. Figure 2.2a shows that Q-800-0.1-NA char retains the original fibrous structure of bagasse. However, P-800-2.0-25 char evolved into a swollen spherical morphology (Figure 2.2b).

Biomass pyrolysis at high heating rate in the PEFR caused simultaneous melting of the solid matrix and devolatilization. This allows the particle to swell and evolve into a round shape. Similar observations were made by Biagini et al. [12] during pyrolysis in an atmospheric drop tube reactor, and by Cetin et al. [10] during pyrolysis in a pressurized wire-mesh reactor. An increase in pyrolysis pressure decreases the driving force for the escape of volatiles trapped within the char. These trapped volatiles (primary pyrolysis products) inside the char particle would undergo secondary and tertiary reactions within the particle to form gases, tars, and coke. Due to the melting of the solid matrix, these gases generated inside char would lead to the formation of gas pockets in the char, thus giving char a foam like structure as shown by Figures 2.2c and 2.2d. These foam-like or honeycomb-like structures, as designated in coal gasification literature, are also formed during coal pyrolysis in a PEFR or in a pressurized drop tube furnace reactor [22]. Note that not all particles are spherical and many finer char particles can also be seen. These are likely formed by fragmentation of these spherical char particles due to the high residence time of these chars in the PEFR. Figure 2.2d shows a fragmented char foam structure which would lead to finer char particles. It is postulated that the fragmentation of these foam like char structures may be responsible for the higher inorganic component losses from char particles due to the formation of finer ash particles during fragmentation. Wu et al. [23] showed the formation of finer ash particles for combustion of coal in a pressurized drop tube furnace reactor.

2.3.1.2 Formation of carbon nano-spheres in the char

Figure 2.2e shows the SEM image of P-1000-0.5-29 char. It was observed that the solid matrix is really comprised of a majority of irregular-shaped char with a minority of

spherical nano-particles. Similar observations were made for P-800-0.5-26 char (Figure 2.2f) and other high pressure chars from the PEFR. SEM-EDX of these spherical shaped particles revealed that these particles are carbon (86 wt% C, 14% O) and the concentration of inorganic species was below the detection limit of EDX. These spherical particles can be seen even after P-800-0.5-26 char is 90-95% gasified in CO_2. The size of these spherical carbon particles ranges between 100 nm and a few microns. Agglomerated spherical particles can also be seen in SEM images (Figure 2.2f).

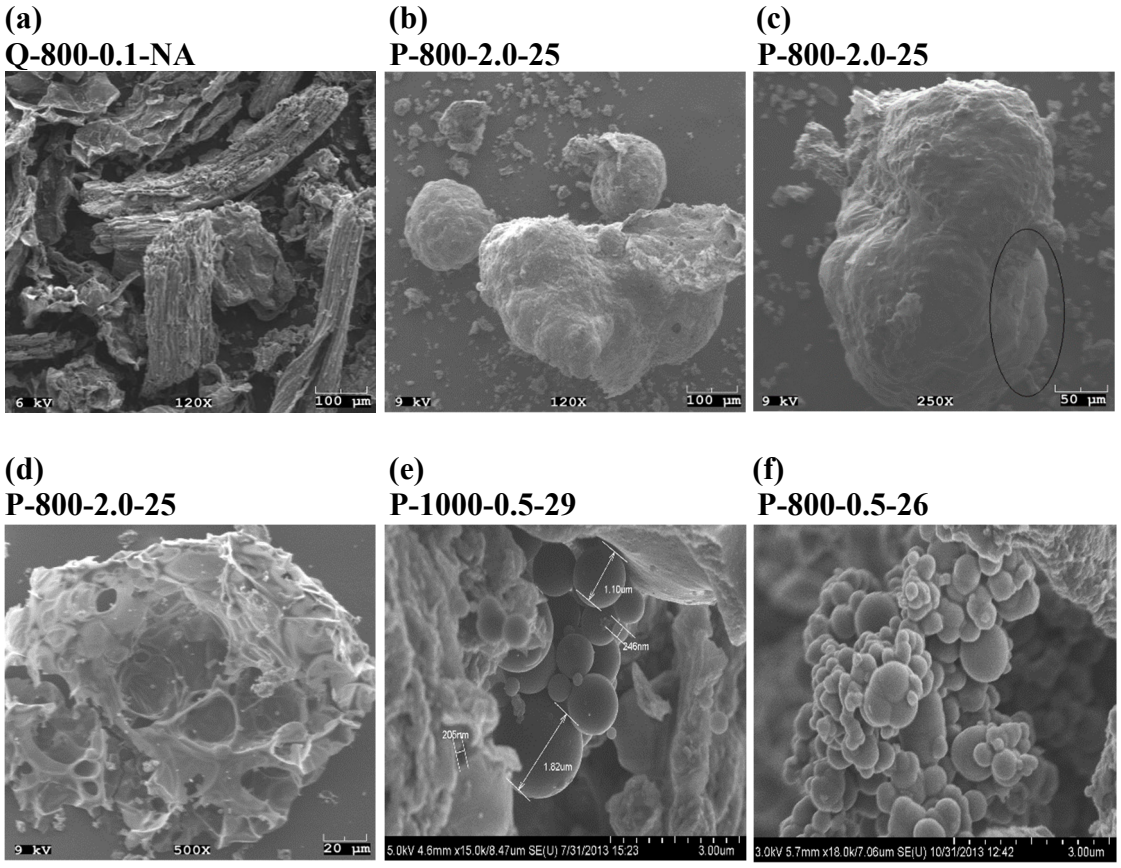

Figure 2.2 SEM images of char prepared at various pyrolysis conditions: (a) char prepared at a slow heating rate (15 K/min) in the quartz tube reactor; (b)-(d) char prepared in the PEFR showing spherical char morphology with (d) showing bursting of char foam structure; (e) nanospheres of carbon formed in the PEFR char particle, and (f) carbon nanosphere aggregates in the PEFR char

Spherical particles in similar size range were observed by Miura et al. [24] in the chars generated by high-temperature pyrolysis of "Bontang coal" in a pressurized drop tube furnace reactor operating at different temperatures (1200-1350 ^{0}C), pressures (0.15 to 2.1 MPa) and residence times (4.3 to 5.2 sec). They attributed the formation of these spherical carbon particles, which are referred to as coke by the authors, through the secondary pyrolysis of volatile matter and found this coke to be less reactive than char. Qin et al. [25] also observed these particles (referred to as soot by the authors) outside the char particles during atmospheric entrained flow gasification of beech saw dust and wheat straw at different temperatures (1000 to 1350 ^{0}C) and residence times (2.1 to 3.0 sec).

2.3.1.3 Mechanism of coke formation in char particles at elevated pressure

Coke is formed from the volatiles produced during the initial pyrolysis at high temperature (typically > 1000 ^{0}C). The inherent nature of plant cellular matter is known to restrict the mass transport of volatiles generated by pyrolysis. Baldwin et al. [26] have shown by microscopic imaging that some vapors can condense into tar microspheres inside the charred cells due to mass transport limitations by dense cell walls or the pits in these walls. An increase in pyrolysis pressure reduces the driving force for the volatiles to escape and reduces the release of higher molecular weight volatile tar molecules that would otherwise be released at low pressure. More volatiles trapped inside the particle due to elevated external pressure also causes swelling of the biomass particle as already seen by SEM images in Figures 2.2b to 2.2d. This would result in a larger quantity of volatiles trapped inside the char. These volatiles under pyrolysis conditions produce free radicals [27] and acetylene [27-29] which leads to the formation of polycyclic aromatic

hydrocarbons (PAH). PAH species then nucleate and grow to finally form soot [29]. Higher pyrolysis pressure would mean higher partial pressure of these radicals inside the char and thus a faster reaction rate. Coke deposition on char also happens by thermal cracking reactions of light hydrocarbons with a higher quantity of these inside char under typical PEFR conditions (high heating rate and higher pressure) enhancing coke deposition on char. Coke or carbonaceous deposits on char would likely be responsible for a decrease in char surface area. The mechanism of coke formation, both inside as well as outside the char particle, is expected to be the same. However, the key difference here is that while outside the char particles the concentration of free radicals is small due to dilution by the entraining gas stream, whereas inside the char particles there can be a much higher concentration of these free radicals, which leads to faster reaction rates for formation of PAH and thus coke. This would explain the coke formation in the char particles even at a lower pyrolysis temperature of 800 ^{0}C at elevated pressures.

2.3.1.4 Effect of pyrolysis conditions on coke formation and char reactivity

PAH formation is a relatively slow process and proceeds through temperature-sensitive, endothermic bimolecular reactions [26]. This means that the formation of coke in the char particles during devolatilization would depend on pyrolysis operating conditions because these would affect the residence time, temperature, and concentration of the volatiles inside the char particle. In a PEFR, which operates at high heating rate, most of the volatiles are released at high temperature and since high operating pressure restricts the evolution of these volatiles from the char particles, these trapped volatiles undergo secondary reactions to generate more coke and gases in the char particles. Higher residence time and/or higher temperature in the PEFR would convert more of

these trapped volatiles into coke. These coking reactions coupled with the difference in the reactivity of coke versus char, have important implications on the reactivity of chars generated under different pyrolysis operating conditions in the PEFR. This can be seen by the char gasification reactivity trends in Figure 2.3a and Figure 2.4a which will be discussed in more detail in the next section (2.3.2).

2.3.2 Effect of pyrolysis operating conditions

2.3.2.1 Effect of pyrolysis temperature

Figures 2.3 and 2.4 show the effect of pyrolysis temperature on char gasification reactivity and physicochemical properties at 1.5 MPa and 0.5 MPa, respectively. Chars were prepared at different temperatures (600, 800 and 1000 ˚C) at an average residence time of 27 sec in the PEFR (the residence time varied in a narrow range of 26 to 29 sec between different pyrolysis runs with a standard deviation of 1.4 sec). The char conversion profiles in Figure 2.3a and Figure 2.4a show that char reactivity decreases with increasing pyrolysis temperature from 600 to 1000 ^{0}C. Char reactivity can be gauged by the time required for approximately 20% conversion (a measure of initial reactivity) and 90% char conversion (a measure of total reactivity). This is an important consideration because the effect of pyrolysis conditions on char reactivity persists throughout the entire gasification of char, not just the initial char gasification. Figures 2.3b and 2.3c show the specific surface area of char and the fraction of surface area occupied by ultramicropores (<0.7 nm), supermicropores (0.7 to 2.0 nm), mesopores (2-50 nm) and macropores (>50 nm), respectively. BET surface area measured by N_2

physisorption, referred to as S_{BET}, showed an increasing trend with pyrolysis temperature between 600 ^{o}C and 800 ^{0}C, followed by a decrease in surface area from 800 ^{0}C to 1000 ^{0}C. However, surface area measured by CO_2 using the Dubinin- Radushkevich (DR) equation, referred to as S_{DR}, showed a continuous decrease with increasing pyrolysis temperature (Figure 2.3b). Also, S_{BET} was negligible compared to S_{DR} at 600 ^{0}C. This drastic difference in surface area values and the trends measured by N_2 versus CO_2 physisorption techniques are because of the highly ultramicroporous nature of chars at 600 ^{0}C. As pyrolysis temperature increases, more of these ultramicropores are converted to supermicropores, mesopores, and macropores where N_2 can diffuse easily. Therefore, S_{BET} increases with pyrolysis temperature. Since ultramicroporosity (<0.7 nm) and pore restriction in char lead to activated diffusion of N_2 at low adsorption temperatures, it implies that S_{DR} is a more important measure of char surface area. Figures 2.3a and 2.3b show that the change in S_{DR} with pyrolysis temperature correlates well with the char reactivity, although there might be other variables in play as well. A similar trend was observed at 0.5 MPa pyrolysis pressure as shown in Figure 2.4. Note that the char reactivity and S_{DR} at 0.5 MPa was always higher than the corresponding 1.5 MPa char. This shows that higher pressure leads to lower char surface area and lower reactivity, the effect of pressure is discussed in more detail in Section 2.3.2.3.

Another implication of the highly microporous nature of char is that the rate of diffusion of volatiles (including light gases like methane, ethane, etc.) formed during pyrolysis inside char would be restricted. This allows more time for these volatiles to undergo secondary reactions (e.g., cracking, free radical reactions to form PAH, etc) and get converted to carbon deposits, causing a reduction in both surface area and pore

volume. Kamishita et al. [30] also have shown (using methane as the volatile component) that methane, while diffusing out of the microporous structure of lignite char into a gas stream, undergoes cracking reactions on the carbon surface depositing carbon into the pores of char. This reduced the char surface area and pore volume and adversely affected subsequent char reactivity in air. They found the deposited carbon to be much less reactive to air than the lignite chars.

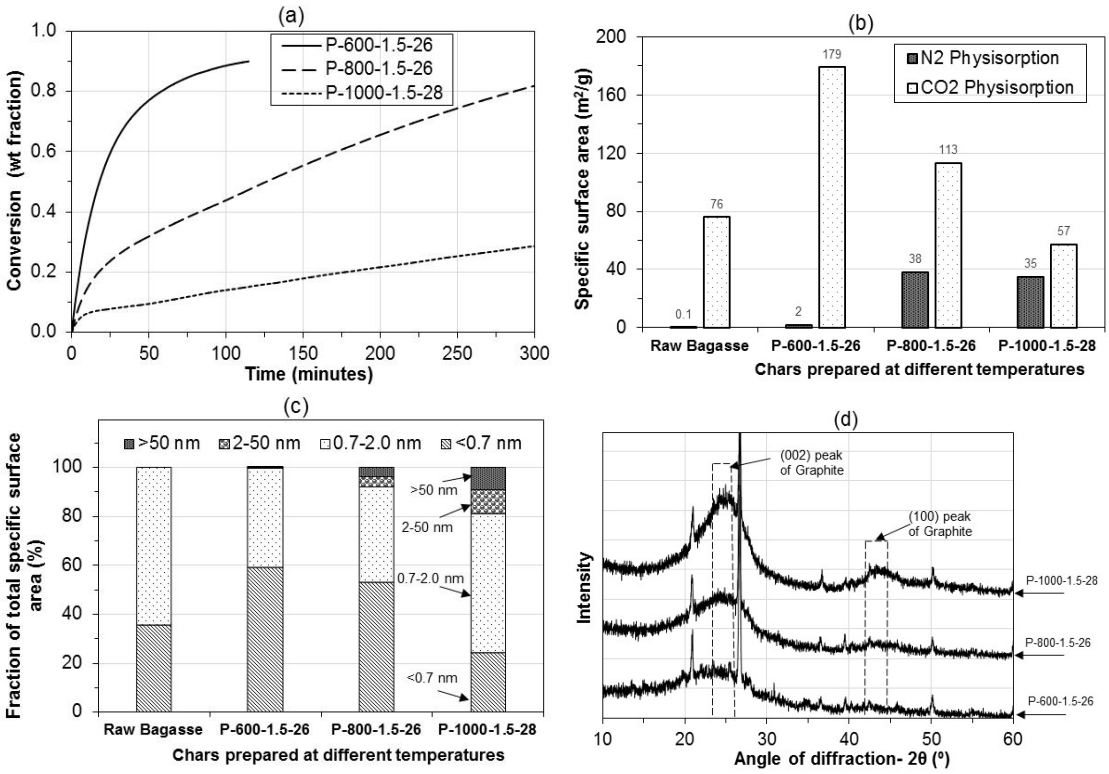

Figure 2.3 Effect of pyrolysis temperature at 1.5 MPa on the reactivity and physicochemical properties of chars: (a) isothermal gasification conversion profile of chars in pure CO_2 at 800 ˚C, (b) specific surface area of chars and raw bagasse, (c) fraction of the total surface area provided by pores of different widths, and (d) XRD spectra of chars

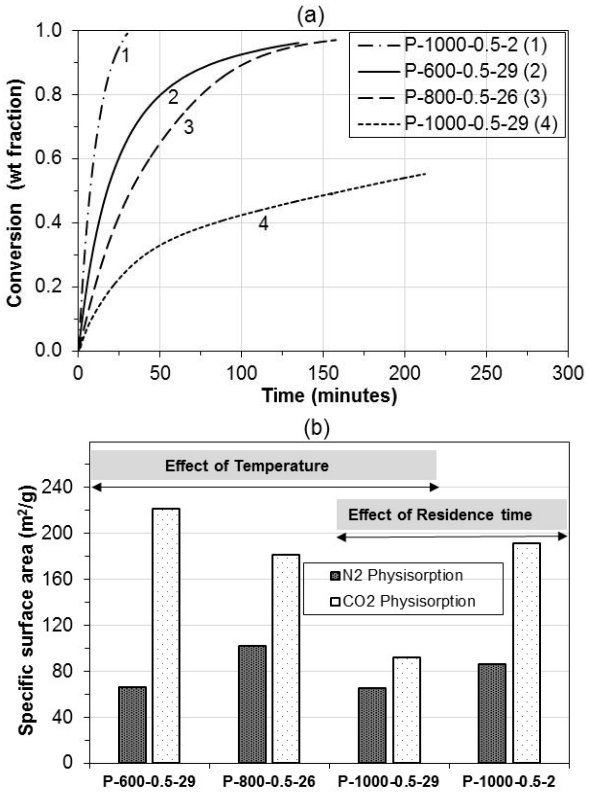

Figure 2.4 Effect of pyrolysis temperature and residence time at 0.5 MPa on the reactivity and physicochemical properties of chars: (a) isothermal gasification conversion profile of chars in pure CO_2 at 800 ˚C. Curves numbered 2, 3, and 4 show the effect of temperature while curves 1 and 4 show the effect of residence time, and (b) specific surface area of chars

The pyrolysis temperature not only affects the physical characteristics of char but also the chemical nature of carbon in char as seen by XRD spectra of Figure 2.3d. Peak intensity of (002) and (100) bands of graphite at 2θ of 22-25^0 and 44^0, respectively, gives a measure of aromaticity and structural order of char [10, 31]. Sharp peaks at 20.9° and 26.7° are attributed to silica. Figure 2.3d shows that with increasing pyrolysis temperature char becomes more polyaromatic and ordered. This also leads to a decrease in char reactivity at higher temperature. In addition, it was observed that the peak intensities of the (002) and (100) bands at 0.5 MPa are lower than the corresponding 1.5

MPa chars at the same temperatures and residence times. At a pyrolysis pressure of 0.5 MPa, XRD spectra did not change with increasing pyrolysis temperature from 600 to 1000℃.

2.3.2.2 Effect of residence time

Two different residence time chars were prepared in the PEFR at 2 and 29 sec at a constant pressure of 0.5 MPa and temperature of 1000 ˚C. Figure 2.4a shows that the low residence time char (P-1000-0.5-2) is highly reactive compared to a high residence time char (P-1000-0.5-29). In fact, P-1000-0.5-2 is the most reactive char of all chars studied in this work. The surface area (S_{DR}) of P-1000-0.5-2 char (191 m^2/g) was about twice that of P-1000-0.5-29. The pore volume of P-1000-0.5-2 was also higher than P-1000-0.5-29 char as shown in Table 2.2. When chars are heated in nitrogen to 800 ^{0}C (at 25 K/min) before commencing CO_2 gasification in an atmospheric TGA, it was found that P-1000-0.5-2 char lost 21.8 wt% of its starting weight as volatiles with 10.8 wt% lost in the temperature range of 110-400 ^{0}C. On the other hand, P-1000-0.5-29 char lost only 5.6 wt% of its starting weight as volatiles with 1.5 wt% lost in the range 110-400 ^{0}C. Since pyrolysis of cellulose and hemicellulose is fast and happens below 400 ^{0}C, these observations suggest that a lot of volatiles are trapped inside the particle for P-1000-0.5-2. For P-1000-0.5-29, the volatiles inside the char have more residence time in the PEFR to undergo secondary reactions to form carbon deposits (and gases). Therefore, P-1000-0.5-29 has less volatiles inside the char but possibly higher carbon deposits. Higher carbon deposits are likely responsible for the reduced char pore volume and surface area at higher residence time. The carbon deposits can form an overlayer over the inorganic ash species (which provide catalytically active sites for gasification), and possibly reduce

the available active surface sites for gasification reactions and thus the overall char reactivity.

Zanzi et al. [16] reported that char reactivity decreased with an increase in residence time (0.6 to 2.7 sec) at 750-900 ^{0}C pyrolysis temperature and 0.26 to 0.30 MPa pyrolysis pressure in a free fall reactor. However, Biagini et al. [12] observed the opposite effect of higher reactor severity (higher residence time and high temperature) on char reactivity. They found that during pyrolysis in a DTF (drop tube furnace), the char reactivity increased with increasing severity of pyrolysis conditions from 600 ^{0}C and 0.05 sec residence time to 800 ^{0}C and 0.2-0.6 sec residence time. This is mainly due to the very short residence time range and atmospheric pressure used in that pyrolysis study which limited the char graphitization (surface area was not reported). These results suggest the need to explore a broader range of relevant operating conditions that may possibly be envisioned for a commercial scale biomass gasifier.

There is one important feature which makes P-1000-0.5-2 char highly reactive even though this char is heated again in N_2 to 800 ^{0}C (or 1000 ^{0}C) at a slow heating rate (25 K/min) before starting gasification, effectively making the residence time of P-1000-0.5-2 char nearly equal to P-1000-0.5-29 char at 1000 ^{0}C (by including the residence time during slow heating of char before commencing gasification). During slow heating of P-1000-0.5-2 char, volatiles are released *incrementally at a lower temperature* when the rates of coke forming reactions are negligible. Only a very small fraction of the weight loss (5 wt %) occurs at temperatures above 600^{0}C, thus limiting the extent of coking inside P-1000-0.5-2 char. On the other hand, for a high residence time char, like P-1000-0.5-29, *all* the volatiles generated by pyrolysis inside the char are exposed to a high

temperature due to the high heating rate inside the PEFR. A combination of high temperature and high residence time tends to enhance coking reactions inside the char and thereby reduce the surface area and char reactivity.

As discussed above, a higher residence time for char under high pressure gasification conditions would allow trapped volatiles to undergo secondary reactions such as PAH formation and/or coking reactions and reduce char gasification reactivity. This suggests that in order to maximize the reactivity of char obtained from a PEFR, the residence time of particles in the PEFR should be limited to only the time needed for complete initial pyrolysis of biomass, which is the time beyond which there is no change in char yield. Literature data shows this value to be 1.0 sec for pyrolysis of wheat straw in a PEFR at 1000 ^{0}C and at 1.0 to 2.0 MPa [5] and 1.0 sec for pyrolysis of rice husk and saw dust at 1000 ^{0}C and 0.1 MPa in an EFR and 1.5 sec for pyrolysis of rice husk and saw dust at 800 ^{0}C and 0.1 MPa in an EFR [9]. Any incremental residence time above this time would result in increased secondary reactions of volatiles inside char reducing the surface area and char reactivity as seen in Figure 2.4.

2.3.2.3 Effect of pyrolysis pressure

Figures 2.5a through 2.5c show the effect of pyrolysis pressure on the reactivity and physicochemical properties of chars prepared at different pressures (0.5 to 2.0 MPa) at a constant temperature and residence time of 800 ˚C and 26 sec, respectively. Figure 2.5a shows that the reactivity of char decreased with increasing pressure until 1.5 MPa and then increased at 2.0 MPa. The trend of surface area (S_{DR}) and XRD trend shown in Figures 2.5b and 2.5c and pore volume shown in Table 2.2 also follow the char reactivity

trend. Reduced surface area and pore volume for high pressure-high heating rate PEFR char are suggested to be due to carbon deposition and also likely due to melting of char structure, causing removal of surface imperfections and potential clogging of micropores. To compare the extent of coking of these chars due to higher pressure and heating rate, low heating rate-low pressure char surface area and pore volume were measured. The surface areas (S_{DR}) of Q-800-0.1-NA and Q-1000-0.1-NA chars were 401 and 399 m^2/g, respectively which are much larger than the ones of PEFR chars (Figure 2.5b). Also, the pore volumes of Q-800-0.1-NA and Q-1000-0.1-NA chars were more than twice the pore volume of PEFR chars (Table 2.2). Hanaoka et al. [14] also reported a drastic decrease in char BET surface area and pore volume with pressure increase from 0.02 MPa (gauge) to 1.0 MPa (gauge) during pyrolysis in a continuous downdraft fixed-bed reactor at 800 ^{0}C for 20 min.

In this study, there is significant decrease in char surface area and char reactivity with increasing pyrolysis pressure until 1.5 MPa (Figure 2.5a and 2.5b). The char reactivity decrease is proposed to be a combined effect of surface area loss and increase in polyaromaticity of carbon structure as shown by XRD. Also, there is a reversal in the char reactivity trend observed at 2.0 MPa (Figure 2.5a). However, Cetin et al. [10] concluded that there is only a slight decrease in surface area with increasing pressure based on pyrolysis studies using Radiata pine as feedstock in a wire mesh reactor (500 K/min heating rate) and attributed the char reactivity decrease to more aromatic carbon structure as measured by XRD peak intensity. Also, no reversal in the reactivity trend at 2.0 MPa was observed in that study. These observed differences can be at least partially

attributed to different reactor types and heating rates used in the two studies, thus leading to formation of different char morphologies.

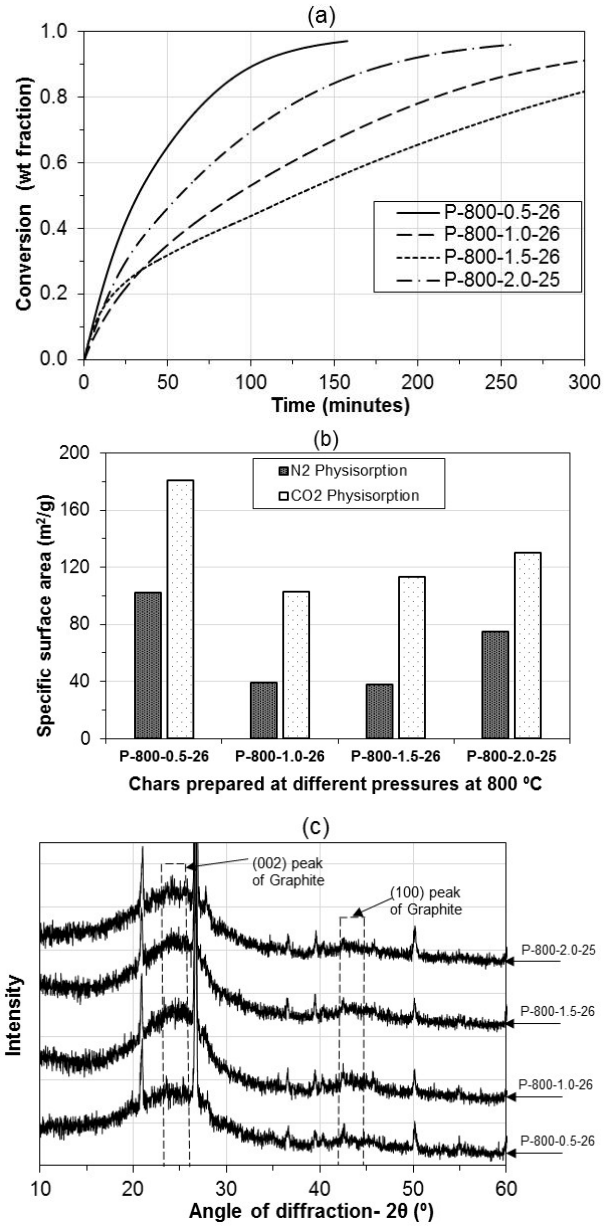

Figure 2.5 Effect of pyrolysis pressure on the reactivity and physicochemical properties of chars prepared at 800 ˚C and 26 sec residence time: (a) isothermal gasification conversion profile of chars in pure CO_2 at 800 ˚C, (b) specific surface area of chars, and (c) XRD spectra of chars

It is postulated that the reversal in char reactivity trend observed at 2.0 MPa is based on the combined effect of two opposing factors which affect char reactivity. On one hand, at higher pressure the secondary pyrolysis of tars is enhanced inside the char causing more coking and polyaromaticity of char. On the other hand, at higher pressure, self-gasification (by H_2O and CO_2 generated by pyrolysis) of volatiles and char would also be enhanced. This is because at higher pyrolysis pressures, more H_2O and CO_2 (generated by pyrolysis) is likely to be trapped in the char. This increases the partial pressure of H_2O and CO_2 in the char, thus enhancing the kinetics of char gasification. At higher pressure, the role of the second factor may be dominant, thus causing a reversal in the reactivity trend at higher pressures.

2.4 Conclusions

Char surface area measured by CO_2 physisorption is a good indicator of char reactivity. Higher pyrolysis pressure, temperature and residence time in the PEFR cause a decrease in char surface area as well as the formation of a more ordered char. These factors lead to a decrease in char gasification reactivity. However, char reactivity increased at 2.0 MPa compared to 1.5 MPa (for the test pressure range of 0.5 to 2.0 MPa at 800 °C - 26 sec). Experimental studies show that to maximize char gasification reactivity, carbon deposition from secondary pyrolysis of volatiles in the char should be minimized by limiting the residence time of the char at high temperature and high pressure to the time required for initial devolatilization.

2.5 References

[1] Eisentraut A. Sustainable Production of Second-Generation Biofuels: Potential and perspectives in major economies and developing countries. No 2010/1 OECD Publ 2010.

[2] Naik SN, Goud V V., Rout PK, Dalai AK. Production of first and second generation biofuels: A comprehensive review. Renew Sustain Energy Rev 2010;14:578–97.

[3] Martín C, Klinke HB, Thomsen AB. Wet oxidation as a pretreatment method for enhancing the enzymatic convertibility of sugarcane bagasse. Enzyme Microb Technol 2007;40:426–32.

[4] Joyce J, Dixon T, Diniz da Costa JC. Characterization of Sugar Cane Waste Biomass Derived Chars from Pressurized Gasification. Process Saf Environ Prot 2006;84:429–39.

[5] Fjellerup J, Gjernes E, Hansen LK. Pyrolysis and Combustion of Pulverized Wheat Straw in a Pressurized Entrained Flow Reactor. Energy Fuels 1996;10:649–51.

[6] Stevens C, Brown RC. Thermochemical processing of biomass: conversion into fuels, chemicals and power. John Wiley & Sons; 2011.

[7] Fermoso J, Stevanov C, Moghtaderi B, Arias B, Pevida C, Plaza MG, et al. High-pressure gasification reactivity of biomass chars produced at different temperatures. J Anal Appl Pyrolysis 2009;85:287–93.

[8] Biagini E, Cioni M, Tognotti L. Development and characterization of a lab-scale entrained flow reactor for testing biomass fuels. Fuel 2005;84:1524–34.

[9] Sun S, Tian H, Zhao Y, Sun R, Zhou H. Experimental and numerical study of biomass flash pyrolysis in an entrained flow reactor. Bioresour Technol 2010;101:3678–84.

[10] Cetin E, Moghtaderi B, Gupta R, Wall T. Influence of pyrolysis conditions on the structure and gasification reactivity of biomass chars. Fuel 2004;83:2139–50.

[11] Hu S, Xiang J, Sun L, Xu M, Qiu J, Fu P. Characterization of Char from Rapid Pyrolysis of Rice Husk. Fuel Process Technol 2008;89:1096–105.

[12] Biagini E, Simone M, Tognotti L. Characterization of high heating rate chars of biomass fuels. Proc Combust Inst 2009;32 II:2043–50.

[13] Yuan S, Chen XL, Li J, Wang FC. CO_2 gasification kinetics of biomass char derived from high-temperature rapid pyrolysis. Energy Fuels 2011;25:2314–21.

[14] Hanaoka T, Sakanishi K, Okumura Y. The effect of $N_2/CO_2/O_2$ content and pressure on characteristics and CO2 gasification behavior of biomass-derived char. Fuel Process Technol 2012;104:287–94.

[15] Okumura Y, Hanaoka T, Sakanishi K. Effect of pyrolysis conditions on gasification reactivity of woody biomass-derived char. Proc Combust Inst 2009;32:2013–20.

[16] Zanzi R, Sjöström K, Björnbom E. Rapid High-Temperature Pyrolysis of Biomass in a Free-Fall Reactor. Fuel 1996;75:545–50.

[17] Hansen LK, Fjellerup J, Stoholm P, Kirkegaard M. The pressurized entrained flow reactor at Risø. Design report. Risø-R-822(EN) 1995.

[18] Lozano-Castelló D, Cazorla-Amorós D, Linares-Solano A. Usefulness of CO_2 adsorption at 273 K for the characterization of porous carbons. Carbon 2004;42:1233–42.

[19] Dubinin MM. Theory of the bulk saturation of microporous activated charcoals during adsorption of gases and vapors. Russ J Phys Chem 1965;39:697–704.

[20] Dubinin MM, Radushkevich L V. Equation of the characteristic curve of activated charcoal. Proc Acad Sci USSR Phys Chem Sect 1947;55:331–3.

[21] Brunauer S, Emmett PH, Teller E. Adsorption of Gases in Multimolecular Layers. J Am Chem Soc 1938;60:309–19.

[22] Yu J, Harris D, Lucas J, Roberts D, Wu H, Wall T. Effect of pressure on char formation during pyrolysis of pulverized coal. Energy Fuels 2004;18:1346–53.

[23] Wu H, Bryant G, Wall T. The effect of pressure on ash formation during pulverized coal combustion. Energy Fuels 2000;14:745–50.

[24] Miura K, Nakagawa H, Nakai S, Kajitani S. Analysis of gasification reaction of coke formed using a miniature tubing-bomb reactor and a pressurized drop tube furnace at high pressure and high temperature. Chem Eng Sci 2004;59:5261–8.

[25] Qin K, Lin W, Jensen PA, Jensen AD. High-temperature entrained flow gasification of biomass. Fuel 2012;93:589–600.

[26] Baldwin RM, Magrini-Bair KA, Nimlos MR, Pepiot P, Donohoe BS, Hensley JE, et al. Current research on thermochemical conversion of biomass at the National Renewable Energy Laboratory. Appl Catal B Environ 2012;115-116:320–9.

[27] Wilson JM, Baeza-Romero MT, Jones JM, Pourkashanian M, Williams A, Lea-

Langton AR, et al. Soot Formation from the Combustion of Biomass Pyrolysis Products and a Hydrocarbon Fuel, n -Decane: An Aerosol Time Of Flight Mass Spectrometer (ATOFMS) Study. Energy Fuels 2013;27:1668–78.

[28] Chhiti Y, Peyrot M, Salvador S. Soot formation and oxidation during bio-oil gasification: Experiments and modeling. J Energy Chem 2013;22:701–9.

[29] Fitzpatrick EM, Jones JM, Pourkashanian M, Ross AB, Williams A, Bartle KD. Mechanistic Aspects of Soot Formation from the Combustion of Pine Wood. Energy Fuels 2008;22:3771–8.

[30] Kamishita M, Mahajan O, Walkerjr P. Effect of carbon deposition on porosity and reactivity of a lignite char. Fuel 1977;56:444–50.

[31] Fu P, Hu S, Xiang J, Sun L, Li P, Zhang J, et al. Pyrolysis of Maize Stalk on the Characterization of Chars Formed under Different Devolatilization Conditions. Energy Fuels 2009;23:4605–11.

CHAPTER 3

RECONCILIATION OF CHAR GASIFICATION PROFILE OF SUGARCANE TOPS/LEAVES AND BAGASSE BY CO_2 CHEMISORPTION

3.1 Background

Sugarcane is among the principal agricultural crops cultivated in many tropical countries [1]. Sugarcane harvesting and processing generates two kinds of agricultural wastes: (i) "bagasse", a residue obtained from sugarcane after it is crushed to obtain the juice used for sugar and ethanol production, and (ii) sugarcane leaves and tops, "SCT" (also known as cane trash or cane straw) [2]. With limited fossil fuel reserves and the need to reduce CO_2 emissions, the use of these biomass wastes through gasification represents a potentially attractive alternative to fossil fuel combustion/gasification for energy production [3]. Harvesting of chemical energy from sugarcane waste is attractive since it is a renewable source of energy, and is carbon neutral [2, 4].

Currently, sugarcane mills practically consume most of the bagasse in mill boilers to provide the mill energy demand with only 15% excess bagasse leftover [5]. This is due to the intentional bagasse burning at low efficiencies to avoid disposal issues [6-8]. SCT, on the other hand, is usually left in agricultural fields during sugarcane harvesting for disposal or is burned in the field during pre-harvest, which produces fly ash, severely damages soil microbial diversity, and raises environmental concerns [1, 7]. This leads to inefficient utilization of the energy content of these sugarcane wastes.

In the future, upgrades to the aging sugar mill boiler units and ancillary infrastructure could decrease the overall energy demand of sugar mills to 50% of the bagasse generated, leading to more bagasse availability [8]. Additionally, with the phasing out of cane pre-harvest burning and with an increased adoption of mechanical harvesting techniques, like in Brazil, about 50-66% of the total SCT produced in the field during mechanical harvesting would be potentially available at the sugar mill (the remaining SCT is left on the ground for soil and nutrient management) [6]. This would lead to an enhanced potential availability of these sugarcane wastes as shown in Figure 3.1. For the longer term, alternative technology based on the thermochemical conversion of sugarcane wastes into biofuels, chemicals and electricity are expected to be commercially available [6, 9]. This would enhance the overall energy value of these wastes and solve a substantial biomass disposal dilemma [2, 4, 8].

As seen from Figure 3.1, in terms of the potential availability of feedstock, SCT represents an equal or even higher proportion of the total sugarcane biomass residue available for gasification. Pippo et al. [7] also reported that SCT represents the largest and most important reserve of sugarcane residue. However, in the literature, bagasse is the more widely researched biomass for thermochemical conversion processes to produce renewable fuels and chemicals, with little emphasis given to identify the gasification characteristics of SCT. Deepchand [10] studied slow pyrolysis (10 K/min) of bagasse and SCT in a thermo-gravimetric analyzer (TGA), and found that SCT decomposes at a lower temperature than bagasse, and SCT has more ash content. Aguilar et al. [11] found that SCT chars were more reactive than bagasse char during the gasification of these chars in 10 vol% O_2. Gabra et al. [9], Keown et al. [12] and Leal et al. [6] found much higher

content of K, Ca, Mg, S and Cl in SCT compared to bagasse. This could be significant as K, Ca and Mg catalyze char gasification reactions, and could possibly explain the observed result of Aguilar et al. [11]. Since the char conversion is the slowest step in the biomass gasification process [2], this study is focused on sugarcane residue char gasification.

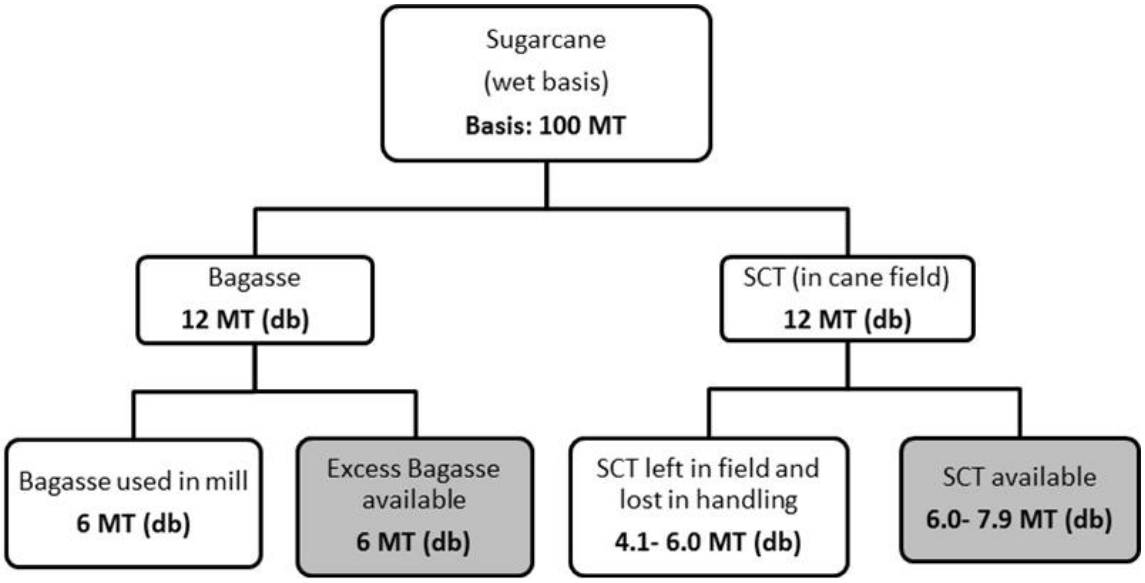

Figure 3.1 Potential future availability of excess bagasse and SCT feedstocks for the lignocellulosic conversion processes, on the basis of 100 MT (metric tons) of sugarcane production [5, 6, 8]. Estimated amount is calculated using the moisture content of bagasse and SCT to be 50 wt% and 32 wt%, respectively, and using the data that 50 - 66 % of the total SCT produced in the field could be potentially available [6]. "db" refers to dry basis.

Ideally, it is required that SCT and bagasse be processed in the same gasifier (either interchangeably or mixed together), which is designed for a set range of operating conditions. Thus, it is necessary to identify the extent of differences during char gasification of bagasse and SCT through extensive biomass characterization and

gasification reactivity tests, which is the first objective of this chapter. Additionally, it is important to see if these similarities/differences could be generalized for bagasse and SCT from any source, or whether it is dependent on the biomass source (i.e., inherent biomass heterogeneity due to different sugarcane species, soil and climatic conditions for sugarcane growth, etc.). For this study, bagasse and SCT from two different geographical locations is used. This is the second objective of this chapter. The third and final objective of this chapter is to rationalize the variation in observed char CO_2 gasification reactivity using a measurable char parameter that could help in predicting the reactivity differences between sugarcane wastes of different types and from different sources.

3.2 Experimental Methods

3.2.1 Experimental materials

Sugarcane bagasse and SCT from Louisiana (U.S.) and Brazil were used in this study. The two bagasse feedstocks and SCT sample from Brazil were dried in an oven at 105 ^{0}C for 6 hours and then ground and sieved to obtain 180-250 μm particles. Raw SCT samples from Louisiana had soil on its surface. Thus, this feedstock was soaked in water overnight, then dried in an oven at 105 ^{0}C for 6 hours, and then ground and sieved to obtain 180-250 μm particles. For all experiments, 180-250 μm size range particles were used. Sugarcane bagasse from Louisiana and Brazil are designated as Louisiana bagasse (LB) and Brazil bagasse (BB), respectively, while SCT from Louisiana and Brazil are designated as Louisiana leaves (LL) and Brazil leaves (BL), respectively. In addition, Avicel (model cellulose) is also used for a baseline study as it contains negligible

inorganic material to catalyze the char gasification reaction. Avicel® PH-101 (50 μm particle size) was purchased from Sigma-Aldrich.

3.2.2 Pyrolysis experiments

Pyrolysis of bagasse and SCT were performed in an atmospheric laminar entrained flow reactor (LEFR) to generate chars for further gasification tests. Iisa et al. [13] explains the schematic, components and operational details of this reactor. This LEFR provides a rapid heating rate for fast pyrolysis, and the residence time can be varied from < 1 sec to 15 sec. Since the bagasse and SCT particle sizes are small (180-250 μm), the particles move with the same velocity as the nitrogen gas (99.998 %) used for pyrolysis. Average velocity of the gas in the LEFR (V_{avg}, in m/s) and the particle residence time (t_R, in s) is calculated by:

$$V_{avg} = \frac{Q}{\pi r_i^2} \tag{3.1}$$

$$t_R = \frac{H}{V_{avg}} \tag{3.2}$$

where Q (in m^3/s) is total inlet gas flow rate at the reactor operating temperature and pressure (atmospheric); r_i (in meters) is inner radius of reactor tube; H (in meters) is the distance from the top of reaction tube to the top of the collector probe where reacted particles are collected. In this study, all pyrolysis experiments were performed at an average velocity of 13.5 cm/s (with full reactor length of 41 cm), which corresponds to a residence time of 3.0 sec, and at a reactor temperature of 1000℃. The chars collected were then characterized for physiochemical properties and also subjected to gasification

in an atmospheric thermogravimetric analyzer (TGA), and in an atmospheric horizontal quartz tube reactor (as shown in Figure 2.1b of Chapter 2) operated at a low heating rate (25 K/min) as discussed in Section 3.2.4. Avicel chars were generated in a horizontal quartz tube reactor by heating Avicel in N_2 at a heating rate of 25 K/min to 800 °C and then holding for 10 min.

3.2.3 Measurement of char CO_2 gasification reactivity in TGA

To measure the char gasification reactivity, isothermal gasification experiments (of chars generated by different pyrolysis runs) were carried out in an atmospheric TGA manufactured by TA Instruments (SDT Q-600) at a gasification temperature of 800℃ in pure CO_2. To ensure there was no external mass transfer resistance, the sample mass was varied in the gasification experiments until no change in reactivity was observed by further reducing the sample mass. To remove any internal mass transfer resistance, crushed char particles were used. The procedure for measuring char gasification reactivity is discussed before in Section 2.2.3 of Chapter 2. The carbon conversion (X) and reactivity (R) are defined as:

$$X = \frac{(m_o - m_t)}{(m_o - m_{ash})} \tag{3.3}$$

$$R = \frac{-1}{(m_t - m_{ash})} \frac{dm}{dt} \tag{3.4}$$

where m_o represents the initial mass of the char at the onset of gasification, m_t is the instantaneous mass of the char at any time t, m_{ash} is the remaining mass of ash after completion of gasification, and dm/dt is the rate of mass loss. Repeatability of data between the runs was good with a deviation of less than 5 %.

3.2.4 Intermediate conversion level chars generation in the quartz reactor

To understand the evolution of reactivity profile of char with conversion during gasification, the LEFR chars from BB and BL were gasified in pure CO_2 to different conversion levels (between 0 to 80 %) in a horizontal quartz tube reactor. The chars thus collected were characterized for N_2 and CO_2 physisorbed area, and CO_2 chemisorbed amount. This would elucidate the char properties responsible for a particular gasification profile. Briefly, LEFR chars were kept in a boat in a quartz tube reactor heated by a horizontal furnace. Then, the reactor was heated in N_2 at 25 K/min to the gasification temperature of 800 ^{0}C, and held there for 10 minutes (as in the TGA experiments). Then, the gas flow was switched to pure CO_2 (99.99 %) at 950 ml/min to start gasification. Chars were exposed to CO_2 for a predetermined time (found using the TGA experiments) to convert the char to a specific conversion level (shown in Section 3.3.3). The reactor gas was then switched to N_2 and cooled rapidly in N_2 to below 60 ^{0}C to collect the intermediate conversion level char.

3.2.5 Characterization techniques

Complementary N_2 and CO_2 physisorption techniques were conducted at 77 K and 273 K, respectively, to obtain the total surface area of chars. The measurements were performed in a Micromeritics ASAP 2020 instrument with an operating pressure range of 0 to 950 mm Hg. The Brunauer–Emmett–Teller theory (BET) method was used to obtain the BET surface area from N_2 physisorption data [14]. CO_2 physisorption was used to characterize micropore surface area [15-16]. The DFT method is used to obtain pore size

distribution [16-17]. Detailed descriptions of these methods are given in Section 2.2.4 of Chapter 2.

Ultimate analysis was performed by Huffman Laboratories (Colorado, US). Trace element analyses of biomass samples and chars were performed by the analytical testing lab located at the Renewable Bioproducts Institute (Atlanta, Georgia), by using a caustic fusion digestion method followed by ICP-OES analysis (Inductively coupled plasma-optical emission spectrometry). Elemental compositions are reported as corresponding oxides.

CO_2 chemisorption measurements were performed in a Micromeritics ASAP 2020 instrument using a procedure similar to the one followed elsewhere [18]. Char was outgassed in the ASAP 2020 instrument. The char was first outgassed for 4 hours at 300 °C at a residual pressure of 0.27 Pa. Then, the char was heated up to 800 °C at a pressure of 0.27 Pa for 30 min in order to remove the chemisorbed oxygen (oxygen adsorbed on the char from air during exposure to atmosphere). Char was then cooled down to 300 °C and the CO_2 chemisorption experiment initiated. The total CO_2 chemisorbed amount (in μmol of CO_2 adsorbed/gram of outgassed char) at equilibrium pressures of 100 mmHg was determined. After this first chemisorption experiment, the sample was outgassed again at 300 °C for 30 min at 0.27 Pa to remove any weakly chemisorbed CO_2 molecules. Then, the CO_2 adsorption procedure was repeated at an equilibrium pressure of 100 mm Hg to obtain the weakly CO_2 chemisorbed amount. The strong chemisorption amount is then calculated by subtracting the weakly chemisorbed amount from the total chemisorbed amount. The standard deviation of measurement of strong CO_2 chemisorbed amount is ± 0.9 μmol /g (at 100 mm Hg).

3.3 Results and Discussion

3.3.1 Characterization of bagasse, SCT and Avicel

Proximate and ultimate analyses, and ash composition of LB, LL, BB and BL are shown in Table 3.1. The proximate analysis of BB and BL are similar except that BL has higher ash content than BB. Similarly, LL has higher ash content than LB. Similar observations have been made in the past studies [6, 7, 9-12]. The ultimate analyses of these samples were also similar, typical of biomass feedstock, but leaves showed higher sulfur content compared to bagasse, as also observed in past studies [9, 12]. However, significant differences were observed for the ash content and composition of inorganics between the Brazil samples and the Louisiana samples. The Louisiana samples had much higher contents of ash, catalytically active alkali and alkaline earth metals (primarily K and Ca), and silicon compared to the Brazil samples. This has important consequences (as seen later in Section 3.3.2) since K and Ca increase the char gasification reactivity, while silicon in the biomass is known to inhibit the catalytic effect of K [19, 20]. It can also be seen that LL had much higher K and Ca than LB. On the other hand, BL had a smaller amount of K compared to BB, which was K rich. Many authors in the past found that SCT had more K, Ca and Mg compared to bagasse [6, 9, 12]. However, this study shows that such a generalized conclusion cannot be made. Avicel had similar proximate and ultimate analysis results as all sugarcane residues with an important difference that it had negligible contents of ash and catalytically active inorganics.

Table 3.1 Proximate analysis, ultimate analysis and ash composition of sugarcane residues (180-250 μm) and Avicel (~50 μm)

Feedstock[a]	LB	LL	BB	BL	Avicel
Parameters	*Proximate analysis (wt%), db[b]*				
Fixed carbon	11.6	15.1	13.5	13.4	6.2
Volatile	80.7	75.8	83.9	83.3	93.8
Ash	7.7	9.0	2.6	3.3	< 0.1
	Ultimate analysis (wt%), daf[b]				
C	49.87	NA	49.15	49.15	44.26
H	6.01	NA	6.02	6.18	6.19
N	0.38	NA	0.25	0.44	0.02
S	0.17	NA	0.05	0.07	0.02
O[c]	43.57	NA	44.53	44.16	49.51
	Ash composition in biomass (wt%), db[b]				
Al_2O_3	0.61	0.17	0.10	0.23	< 0.001
K_2O	0.38	0.93	0.21	0.11	0.008
CaO	0.38	0.72	0.07	0.36	0.010
MgO	0.12	0.27	0.06	0.10	0.003
Fe_2O_3	0.22	0.07	0.06	0.18	0.001
SiO_2	4.58	5.81	1.91	1.40	0.004
SO_3	0.30	0.19	0.05	0.12	< 0.020
P_2O_5	0.08	0.16	0.05	0.08	< 0.030

[a]LB = Louisiana bagasse, LL = Louisiana leaves, BB = Brazil bagasse, and BL = Brazil leaves; [b]db = dry basis, daf = dry and ash-free basis; [c]Calculated by difference; NA = Not analyzed

3.3.2 Comparison of char gasification reactivity of different sugarcane residues

Figures 3.2a and 3.2b show the conversion - time plot and reactivity - conversion plot, respectively, for the gasification of LB, LL, BB and BL chars. Gasification of these chars were performed in pure CO_2 at 800℃ in the TGA. For Avicel char, the gasification reactivity is negligible at 800 °C in CO_2 due to the negligible amount of catalytically active inorganics (K and Ca) in Avicel. It can be seen from Figure 3.2b that for calcium rich chars (LL and BL), the reactivity profile showed a sudden drop or discontinuity at low char conversion. This is because of the two opposing effects: Char conversion during gasification causes a weight loss. On the other hand, during the initial stages of char conversion (when CO_2 is fed for gasification at 800 °C), calcium oxide present in char reacts with CO_2 to form calcium carbonate causing a weight increase. This was determined by running a model experiment in TGA where pure calcium oxide was heated to 800℃ in nitrogen (at 25 K/min), and held there for 10 min. Then, the gas was switched to CO_2. The percent increase in weight of the sample was consistent with the carbonation of calcium oxide to calcium carbonate. Also, since calcium oxide reacted with CO_2 at a much faster rate compared to the char gasification rate, this discontinuity in reactivity profile was observed only temporarily.

Table 3.2 shows the ash content and ash composition of LEFR chars. Two measures of char gasification reactivity can be defined for correlating it to char physiochemical properties: a) Initial reactivity that is defined as the reactivity for the initial 5 to 10% conversion. Since char physiochemical properties are measured after the pyrolysis, it reflects only the initial char reactivity. b) Overall reactivity can be defined as average char reactivity between 5 to 80% conversion. Since char physiochemical

properties change during conversion, the overall char reactivity can be very different from the initial char reactivity. From a process point of view, overall char reactivity is much more important parameter than initial char reactivity.

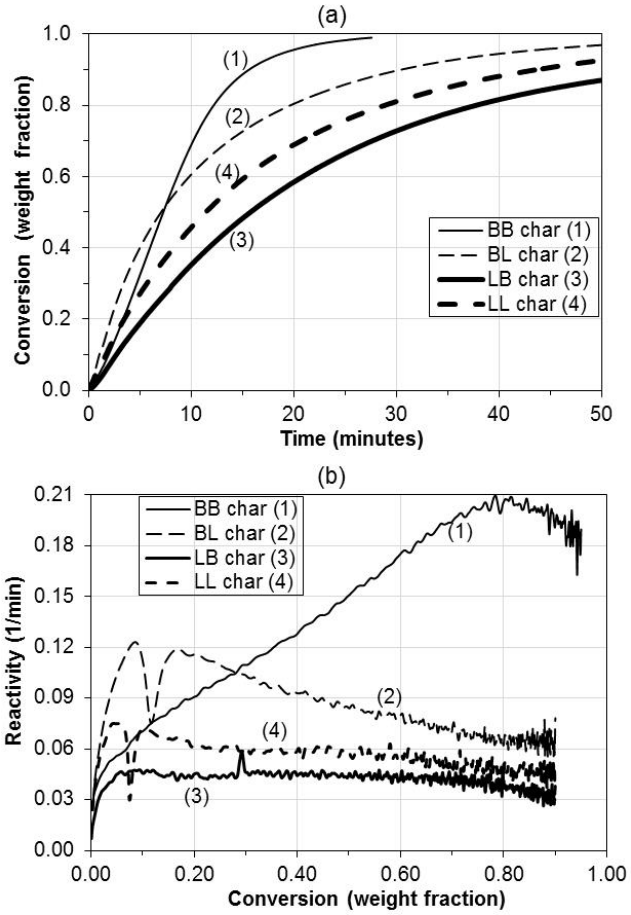

Figure 3.2 Isothermal gasification of LEFR chars from Brazil bagasse (BB), Brazil leaves (BL), Louisiana bagasse (LB) and Louisiana leaves (LL) at 800 °C in pure CO_2 in an atmospheric TGA. LEFR chars were generated by pyrolysis in nitrogen at 1000 °C and 3 sec. (a) Char conversion versus time, and (b) Char reactivity versus conversion.

The following observations can be made from Figure 3.2 and Table 3.2:

a) The initial char reactivities follow the following order BL > LL > BB > LB, while the overall char reactivities follow a different order BB > BL > LL > LB.

b) LB char, even with nearly equivalent wt% K_2O and much higher CaO than BB char, has lower overall char reactivity than BB char.

Table 3.2 Ash composition and ash content of LEFR chars from pyrolysis of sugarcane residues

	LB char	**LL char**	**BB char**	**BL char**
	Ash composition in char (wt%), dry and volatile-free char basis			
Al_2O_3	5.76	1.21	1.86	3.41
K_2O	4.37	5.31	4.71	2.30
CaO	2.83	3.66	1.44	5.54
MgO	1.29	1.36	1.15	1.61
Fe_2O_3	2.15	0.47	1.07	2.13
SiO_2	42	33	25	19
SO_3	1.52	0.75	0.94	1.23
P_2O_5	0.75	0.67	0.82	0.98
	Ash content in char (wt%), dry basis			
Total ash	61	55	36	32
	Atomic ratio of K/Si in char			
K/Si	0.133	0.208	0.240	0.154

The (K + Ca) content (in mmol/g of char) has been used in earlier literature studies to correlate the char reactivity of different biomass types [19, 20]. As can be seen from Figure 3.3a, the initial char reactivity does not correlate well with the (K + Ca) content of the char. This can be attributed to the high silica content in the Louisiana sample compared to the Brazil sample, which deactivates the active catalytic species. Thus, an attempt was made to correlate the char reactivity to (K + Ca)/Si (atomic ratio).

It was found that (K + Ca)/Si ratio correlated well (R^2= 0.98) with the initial char reactivity, but not with the overall char reactivity (Figure 3.3b and 3.3c). This can likely be explained as follows: It is known that for a calcium rich char, the char reactivity decreases drastically during the progress of gasification due to sintering of calcium as the char conversion progresses in CO_2 [21, 22]. Thus, the initial char reactivity will be high but the overall char reactivity is low. On the other hand, for a potassium rich char (in the absence of excess silica), the char reactivity increases during the progress of gasification due to an increase in the K/C ratio and the char exhibits a maximum reaction rate in the higher conversion range [20, 22]. Thus, the initial char reactivity will be small, but the overall reactivity is much higher than the initial reactivity. Based on these arguments, and since BB char has the highest K/Si ratio due to low silica and ash content (Table 3.2), BB char shows the highest overall reactivity. This is because in BB char not all K is likely to be deactivated, as seen by the reactivity profile, which is typical for a K catalyzed gasification reaction. However, since calcium is very low in BB char, its initial reactivity is low. Thus, in the (K + Ca)/Si ratio for BB char, the K/Si contribution is small during the initial reactivity but high for the overall reactivity. This explains why the same correlating parameter, (K + Ca)/Si, cannot be used for both the initial and overall reactivity due to a much larger increase in reactivity at the later stages of conversion for the K rich BB char. For all the other chars (from LB, LL and BL), the reactivity profile does not look to be dominated by potassium, as the reactivity does not increase with conversion for these chars. This can be explained by the low K/Si ratio in these samples, which is likely causing the deactivation of most of the potassium at higher conversion. Therefore, for these chars (LB, LL and BL chars), the reaction is dominated by the

catalytic effect of calcium over the entire range of conversion. Thus, the overall reactivity of these chars correlates well to calcium content (mmol/g char), as seen from Figure 3.3d. Thus, in absence of significant K in char, calcium content of char is a good indicator of overall reactivity. Therefore, different empirical correlating factors need to be used for predicting char reactivity during initial conversion compared to overall conversion. These correlations also agree well to the known catalytic effect of potassium and calcium on char gasification (with potassium being more catalytically active than calcium for overall char reactivity), and the inhibitive effect of silicon on char gasification.

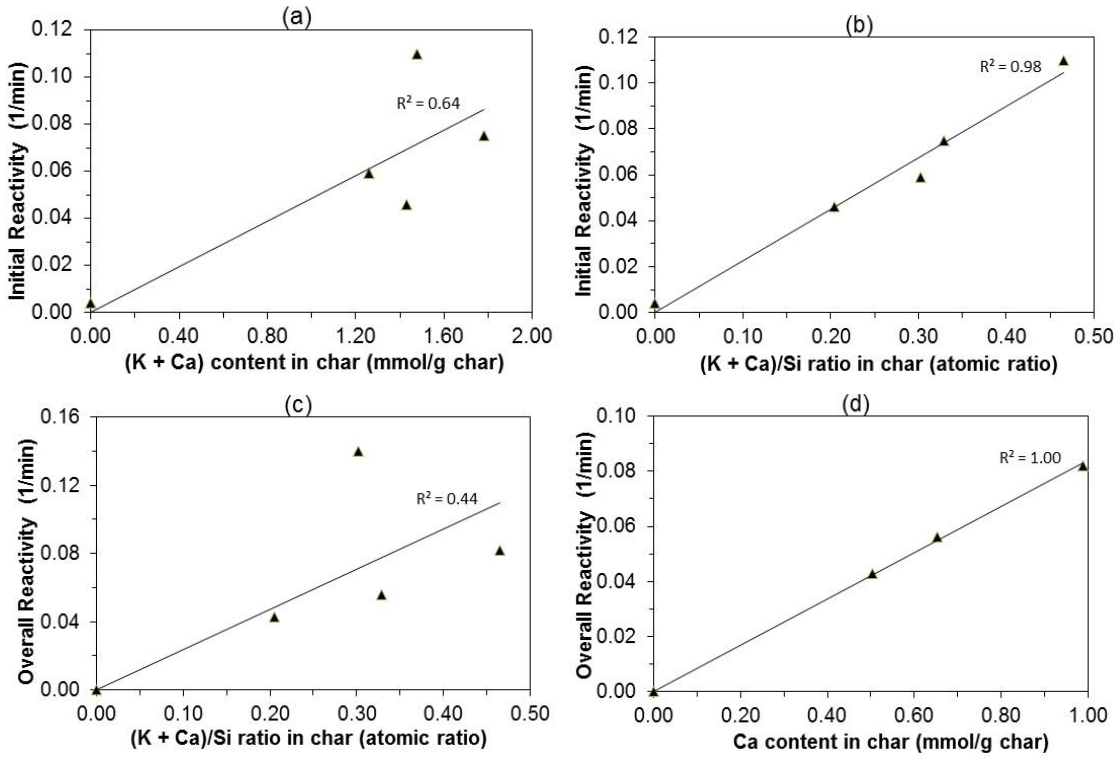

Figure 3.3 Correlations between the initial and overall gasification reactivity of LEFR chars from different sugarcane residues (BB, BL, LB and LL chars), and Avicel char as a function of char inorganic concentration. (a) and (b) show the initial char reactivity as a function of (K + Ca) content and (K + Ca)/Si ratio in char, respectively, and (c) and (d) show the overall char reactivity as a function of (K + Ca)/Si ratio and Ca content of char, respectively. The point near the origin corresponds to Avicel char with negligible K and Ca, and negligible char reactivity in CO_2 at 800 °C. Plot (d) does not include BB char.

Even though SCT and bagasse came from the same plant, their reactivity towards gasification was not the same. This could be attributed to the substantial difference in the inorganic composition of SCT and bagasse, since they belong to different parts of the plant and have undergone different harvesting and processing steps. During sugarcane processing, some elements are leached away from bagasse during the process of extraction of juice from sugarcane stalk, while SCT does not undergo such a processing step. LL had higher overall reactivity than LB, but BB had higher overall reactivity than BL. Therefore, no generalized conclusion, that SCT is more reactive compared to bagasse as observed by Aguilar et al. [11], can be made. Also, bagasse from two different sources (Brazil and Louisiana) was found to be widely different in its reactivity, thus, preventing any generalization. Even though chars from these sugarcane residues vary widely in their reactivities preventing any generalization, the reactivity can still be correlated to common measurable parameters as shown above.

It was shown that the reactivity of sugarcane residue depends not only on the type of residue (SCT or bagasse) but also the source of the sugarcane residue. This may be attributed to the wide variation in elemental concentrations between different species of a biomass [23]. Furthermore, for the same type of biomass, the mineral part of the biomass presents a large variation in composition depending on the growing conditions (soil, climate variations), and harvesting conditions [24]. This reinforces the need for analyzing the sugarcane residue feedstock, whenever changing the source or type of sugarcane residue, before feeding it to a gasifier. This analysis will assist in predicting the char gasification reactivity from the correlating char physiochemical properties. This will then aid in determining the adjustments required for the gasifier operating conditions to

maintain close to desired char conversion to syn-gas, when sugarcane residue feedstock quality changes. Alternatively, a slowly gasifying char can be burned for energy.

3.3.3 Correlating BB and BL char reactivity profile to measurable char properties

Figure 3.2b shows that the gasification reactivity profile of BB char was very different compared to BL char gasification. The reactivity of BB char increased by a factor by 3.5 during the progress of char conversion, while BL char reactivity decreased by a factor of 2.0 as char conversion increased. Qualitatively, it can be explained as follows: As mentioned above in Section 3.3.2, char reactivity decreases with increasing conversion for a calcium catalyzed char gasification, while the char reactivity increases with increasing conversion for a potassium catalyzed char gasification. BL char is calcium rich, and the small amount of potassium in BL char is likely deactivated by silica due to the low K/Si in this char. On the other hand, BB char is potassium rich (with a small amount of Ca) with a high K/Si, and thus the excess potassium can catalyze char gasification. However, since the char of BB and BL contained both K and Ca, and the total surface area of char also changed drastically during the char conversion (Figure 3.4a and 3.5a), it is difficult to predict whether surface area, K content or Ca content plays a major role in establishing a char reactivity profile. Alternatively, there may be an interplay of changes in char K and Ca content, and surface area that determines the reactivity profile. Thus, it is difficult to predict and correlate such a char reactivity profile *a priori*. Thus, the objective is to find measurable char properties that can correlate to the observed reactivity trend.

The char reactivity is determined by the char physical surface area, the content of K, Ca and Si (or the active inorganics which are not deactivated by minerals in biomass),

and the dispersion of K and Ca (all of which changes with char conversion). Thus, a parameter that combines all these factors into one measurable property is needed. The active site area (ASA) is one such parameter that combines these individual effects to measure the dispersion of active catalytic species on the char surface. In this study, the ASA is measured by CO_2 chemisorption at 300°C, as followed by many authors in the past [18, 21, 22, 25, 26]. The strong and total CO_2 chemisorbed (μmol/g of char), which determines the ASA of the char, is measured for different intermediate conversion level chars and is then correlated to char reactivity at that stage of conversion.

Many types of intermediates have been proposed as actives sites for catalyzed gasification [27]. Among all the intermediates, the clusters (or particles) of alkali and alkaline earth metals anchored to the carbon by phenolate group (C-O-M group, where M denotes metal) are the most active species, and is capable of chemisorbing CO_2 [27-30]. Dissociation of chemisorbed CO_2 on these active sites forms oxygen atom and CO gas. Oxygen atom binds to the edge carbon to form C(O) complex [28]. Higher active site concentration thus provides more C(O) complex, resulting in an increased gasification rate. Appendix A shows the detailed schematic of potassium-catalyzed CO_2 (or H_2O) gasification mechanism on the active sites, based on the literature studies [28-30].

Figure 3.4a compares the evolution of total surface area and reactivity of BL char with conversion. It shows that surface area increased during the initial stages of conversion, went through a maximum and then decreased. However, the reactivity continued to decrease with conversion. Therefore, char surface area alone does not explain the evolution of char reactivity with conversion. On the other hand, the total and strong CO_2 chemisorbed followed the reactivity profile closely as shown in Figure 3.4b,

indicating that the concentration of active sites measured using CO_2 chemisorption correlated well to the observed reactivity profile. Even though there was an increase in char surface area with conversion initially and a likely increase in calcium content in char with increasing conversion (due to carbon burn-off in char assuming negligible calcium loss), the reactivity and chemisorbed CO_2 still decreased. This is attributed to the sintering of calcium with increasing conversion during CO_2 gasification. Sintering would lead to less available active surface for gasification, even for a char with increasing total surface area and calcium content. The strong chemisorbed CO_2 is a better parameter than the total chemisorbed CO_2 for correlation because it does not include the weakly chemisorbed CO_2, as in the total chemisorption.

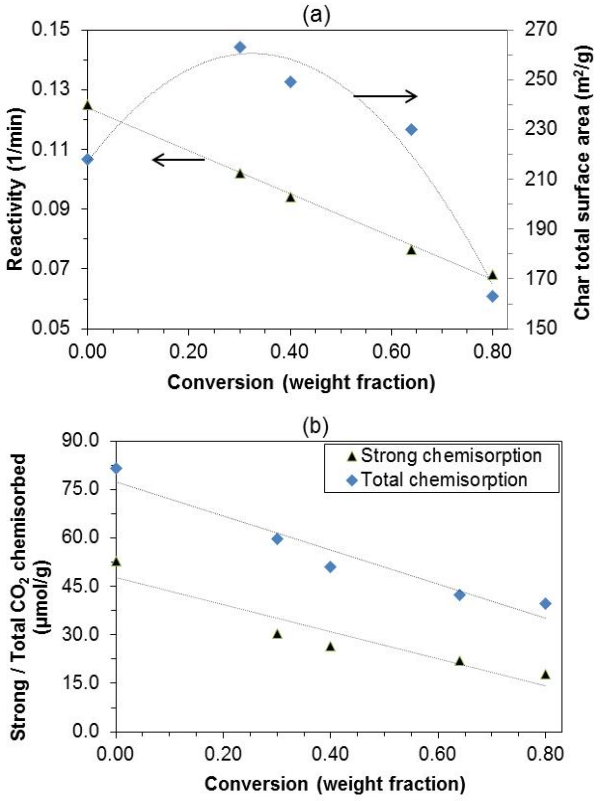

Figure 3.4 Evolution of reactivity profile and physiochemical properties of Brazil leaves char (BL char) during the progress of char conversion in pure CO_2 at 800 ˚C: (a) Reactivity profile and surface area as a function of char conversion, and (b) strong and total CO_2 chemisorbed as a function of char conversion.

For BB char, the char surface area, reactivity as well as the total and strong chemisorbed CO_2 increased with conversion with some deviation at 75% conversion (Figure 3.5a and 3.5b). As char conversion progressed, potassium becomes more concentrated in the char. This would lead to a higher K/C ratio with conversion. Also, K is mobile in the char [19]. Thus, the increasing concentration of potassium and the increasing surface area with conversion is likely causing the increase in ASA, and thus the increase in char reactivity with conversion. This would explain the much higher overall reactivity of BB char compared to BL char.

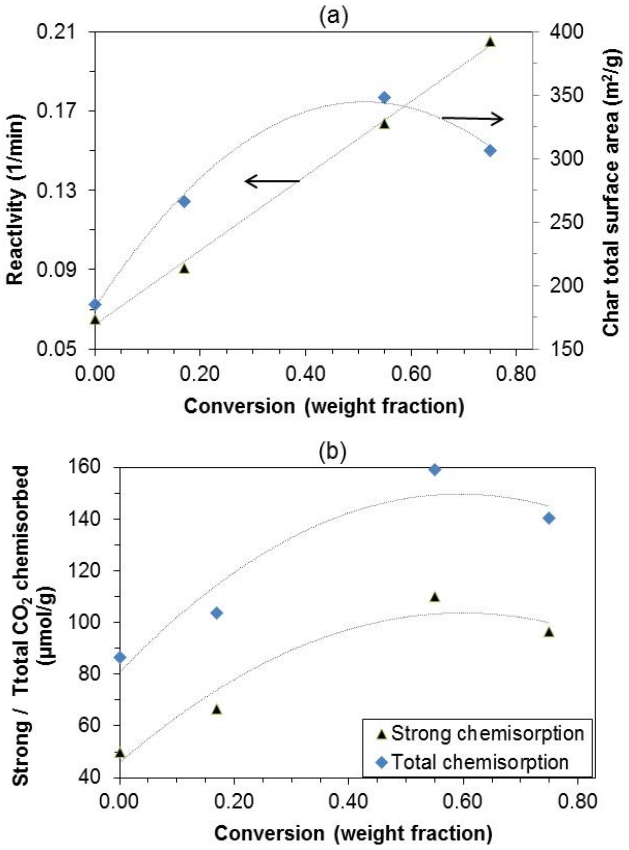

Figure 3.5 Evolution of reactivity profile and physiochemical properties of Brazil bagasse char (BB char) during the progress of char conversion in pure CO_2 at 800 ˚C: (a) Reactivity profile and surface area as a function of char conversion, and (b) strong and total CO_2 chemisorbed as a function of char conversion.

3.4 Conclusions

a) Even though bagasse and SCT came from the same plant, their reactivity towards gasification is not the same. Also, no generalized conclusion can be made that SCT char is more reactive compared to bagasse char. The reactivity of sugarcane residue is found to depend on both the type of sugarcane residue, and the source of the sugarcane residue.

b) LB char, even with nearly equivalent weight fraction of K_2O and much higher CaO content than BB char, has lower overall char reactivity than BB char. This is likely due to the high silica content in sugarcane residue from Louisiana compared to Brazil. Furthermore, (K + Ca)/Si ratio correlated well with the initial char reactivity, but not with the overall char reactivity.

c) The strong CO_2 chemisorbed quantity correlated well with the overall reactivity profile of BB and BL char, indicating that the concentration of active sites measured using CO_2 chemisorption determines char reactivity rather than the char physical surface area or the concentration of inorganics (K, Ca and Si). The active sites, where CO_2 strongly chemisorbs, are likely to be the clusters of active alkali and alkaline earth metals anchored to the carbon by phenolate group.

d) The drastic char reactivity differences between sugarcane residues of different types and from different sources require significant flexibility in gasifier design and operating conditions. When changing the sugarcane residue feedstock to the gasifier (from a different source or of a different type), the feedstock should be analyzed before feeding it to the gasifier to assess its predicted char gasification reactivity. This will assist in determining the adjustments required for the gasifier operating conditions to maintain

close to desired char conversion to syn-gas. Alternatively, slowly gasifying char can be burned for energy.

3.5 References

[1] Chandel AK, da Silva SS, Carvalho W, Singh O V. Sugarcane bagasse and leaves: foreseeable biomass of biofuel and bio-products. J Chem Technol Biotechnol 2012;87:11–20.

[2] Joyce J, Dixon T, Diniz da Costa JC. Characterization of Sugar Cane Waste Biomass Derived Chars from Pressurized Gasification. Process Saf Environ Prot 2006;84:429–39.

[3] Keown DM, Hayashi J, Li C-Z. Effects of volatile–char interactions on the volatilisation of alkali and alkaline earth metallic species during the pyrolysis of biomass. Fuel 2008;87:1187–94.

[4] Ahmed II, Gupta AK. Sugarcane bagasse gasification: global reaction mechanism of syngas evolution. Appl Energy 2012;91:75–81.

[5] Lau FS, Bowen DA, Dihu R, Doong S, Hughes EE, Remick R, et al. Techno-economic analysis of hydrogen production by gasification of biomass. Dep Energy Natl Renew Energy Lab, DE-FC36-01GO11089; 2003.

[6] Leal MRL V, Galdos M V, Scarpare F V, Seabra JEA, Walter A, Oliveira COF. Sugarcane straw availability, quality, recovery and energy use: a literature review. Biomass Bioenergy 2013;53:11–9.

[7] Pippo WA, Garzone P, Cornacchia G. Agro-industry sugarcane residues disposal: the trends of their conversion into energy carriers in Cuba. Waste Manag 2007;27:869–85.

[8] White JE, Catallo WJ, Legendre BL. Biomass pyrolysis kinetics: a comparative critical review with relevant agricultural residue case studies. J Anal Appl Pyrolysis 2011;91:1–33.

[9] Gabra M, Pettersson E, Backman R, Kjellström B. Evaluation of cyclone gasifier performance for gasification of sugar cane residue—Part 2: gasification of cane

trash. Biomass Bioenergy 2001;21:371–80.

[10] Deepchand K. A note on the pyrolysis behaviour of sugar cane fibrous products. Biol Wastes 1987;20:203–8.

[11] Aguilar PJ V, Suarez MQ, García JOP, Yurell JCL. Kinetic study of sugar cane mill fibrous wastes gasification. Afinidad 2004;61:139–46.

[12] Keown DM, Favas G, Hayashi J, Li C-Z. Volatilisation of alkali and alkaline earth metallic species during the pyrolysis of biomass: differences between sugar cane bagasse and cane trash. Bioresour Technol 2005;96:1570–7.

[13] Iisa K, Lu Y, Salmenoja K. Sulfation of potassium chloride at combustion conditions. Energy & Fuels 1999;13:1184–90.

[14] Brunauer S, Emmett PH, Teller E. Adsorption of gases in multimolecular layers. J Am Chem Soc 1938;60:309–19.

[15] Lozano-Castello D, Cazorla-Amoros D, Linares-Solano A. Usefulness of CO_2 adsorption at 273 K for the characterization of porous carbons. Carbon 2004;42:1233–42.

[16] Malekshahian M, Hill JM. Effect of pyrolysis and CO_2 gasification pressure on the surface area and pore size distribution of petroleum coke. Energy Fuels 2011;25:5250–6.

[17] Webb PA, Orr C. Analytical Methods in Fine Particle Technology, Micromeritics Instr. Corp, Norcross GA USA 1997.

[18] Molina A, Montoya A, Mondragón F. CO_2 strong chemisorption as an estimate of coal char gasification reactivity. Fuel 1999;78:971–7.

[19] Kannan MP, Richards GN. Gasification of biomass chars in carbon dioxide: dependence of gasification rate on the indigenous metal content. Fuel 1990;69:747–53.

[20] Zhang Y, Ashizawa M, Kajitani S, Miura K. Proposal of a semi-empirical kinetic model to reconcile with gasification reactivity profiles of biomass chars. Fuel 2008;87:475–81.

[21] Linares-Solano A, Almela-Alarcón M, de Lecea CS-M. CO_2 chemisorption to characterize calcium catalysts in carbon gasification reactions. J Catal 1990;125:401–10.

[22] Zhang Y, Hara S, Kajitani S, Ashizawa M. Modeling of catalytic gasification kinetics of coal char and carbon. Fuel 2010;89:152–7.

[23] Tanger P, Field JL, Jahn CE, DeFoort MW, Leach JE. Biomass for thermochemical conversion: targets and challenges. Front Plant Sci 2013;4.

[24] Froment K, Seiler J-M, Defoort F, Ravel S. Inorganic species behaviour in thermochemical processes for energy biomass valorisation. Oil Gas Sci Technol d'IFP Energies Nouv 2013;68:725–39.

[25] Jing X, Wang Z, Zhang Q, Yu Z, Li C, Huang J, et al. Evaluation of CO_2 gasification reactivity of different coal rank chars by physicochemical properties. Energy Fuels 2013;27:7287–93.

[26] Xu K, Hu S, Su S, Xu C, Sun L, Shuai C, et al. Study on char surface active sites and their relationship to gasification reactivity. Energy Fuels 2012;27:118–25.

[27] Chen SG, Yang RT. Unified mechanism of alkali and alkaline earth catalyzed gasification reactions of carbon by CO_2 and H_2O. Energy Fuels 1997;11:421-7.

[28] Chen SG, Yang RT. Mechanism of alkali and alkaline earth catalyzed gasification of graphite by CO_2 and H_2O studied by electron microscopy. J Catal 1992:138:12-23.

[29] Meijer R, Weeda M, Kapteijn F, Moulijn JA. Catalyst loss and retention during alkali-catalysed carbon gasification in CO_2. Carbon 1991;29:929-41.

[30] Chen SG, Yang RT. The active surface species in alkali-catalyzed carbon gasification: Phenolate (C-O-M) groups vs clusters (particles). J Catal 1993;141:102-13.

CHAPTER 4

UNDERSTANDING THE GASIFICATION REACTIVITY OF DIFFERENT BIOMASS DERIVED CHARS

4.1 Background

Biomass is a promising source of energy as it is widely available, renewable and a nearly CO_2-neutral resource. Biomass comprises a broad range of biomaterials, such as forest residues, agricultural residues, energy crops, grasses, waste from the wood and food industries, algae, etc. Biomass can potentially be used for many applications, such as power generation, fuels and chemicals [1], and gasification is one of the technologies to harness the energy content of the biomass. Biomass gasification consists of two processes in series: pyrolysis and gasification. Since char gasification is the slowest step, it determines the residence time required in a gasifier [2].

Utilization of biomass as a gasifier feedstock has associated challenges. The low bulk density and dispersed nature of biomass limits the quantity of a single biomass feedstock that can be collected economically within a reasonable transport distance. This factor, combined with the fact that different biomass has different growth seasons, would mean that a wide range of different biomasses would need to be utilized in a gasifier to ensure fuel supply security. In principal, all different types of biomass can be converted by gasification into syngas [3]. However, the use of different kinds of biomass results in different challenges for the operation of the gasifier [3]. One of the reasons is that the lignocellulosic biomasses differ greatly in their physical, chemical and morphological

properties, causing a wide variation in gasification characteristics between various biomass species [4-5]. Unlike coal, the variations in biomass compositions were found to be greater [6]. Fuel characteristics of biomass feedstock can be affected by harvesting time, growth locations, transportation, storage, and debarking processes [4]. Therefore, design and operation of a biomass gasifier requires understanding and correlating the effect of various types of biomass feedstock with the performance of the system [5]. Since char gasification is the slowest step in the overall biomass gasification process, the main objective of this study is to identify fundamental descriptors of char gasification reactivity that will reconcile the wide variation in char reactivity among different biomass chars. This will assist in formulating a correlation to predict the char gasification reactivity from a wide variety of biomass chars.

Extensive research has been conducted in the past to understand the fundamental descriptors of char reactivity [7]. However, different results are reported by different authors. Zhang et al. [8] concluded that the gasification reactivity of different biomass chars was predominantly governed by the concentration of (K + Na + Ca) in char (in mmol per 100 g of dry and ash free (daf) char), while Kannan and Richards [9] correlated the gasification reactivity of different biomass chars to the concentration of (K + Ca) in char, except for high silica containing biomass. Kannan and Richards [9] also speculated that the chemical and physical properties of the chars are remarkably similar, despite the wide range of plant species and morphologies from which they are derived. A similar argument was made by Di Blasi [7] who speculated that the nature of the lignocellulosic fuels does not significantly affect the char reactivity, and the differences among various samples can be attributed essentially to the inorganic composition (more specifically, to

the catalytic effects exerted on the heterogeneous reactions by alkali and alkaline earth metals, AAEM). On the other hand, Duman et al. [2] concluded that the char surface areas have a higher influence on char reactivity than mineral matter (based on a comparison of the observed gasification reactivity among different wood chars and agricultural residues chars). Thus, the first aim of this study is to identify whether the char total surface area, or the concentration of AAEM, or other factors determines the variation in reactivity of different biomass chars. One of the main hurdles in this study is that the concurrent variation in many char properties prevents the deconvolution of the effect of different char properties on its gasification reactivity. To partially overcome these limitations, four biomass feedstocks are specifically chosen in this study to segregate the effect of different inorganics, ash content and total surface area while still maintaining the inherent biomass feedstock properties. In this study, the biomass chars are generated by pyrolysis in a pressurized entrained flow reactor (PEFR) operating at high heating rates ($\geq 10^3$ ^{o}C/sec) and at short residence time (28 sec). Char reactivity was then studied in a thermogravimetric analyzer (TGA).

In a heterogeneous gas-solid reaction, the rate of reaction is generally assumed to be proportional to the accessible surface area of the solid. However, the total surface area (TSA) derived from physical adsorption may not reveal the actual number of reactive sites, because there are many sites that are reactive only under extreme conditions. Active surface sites only represent a fraction of the total surface area, called active surface area (ASA) [10]. Lizzio and Radovic [11] proposed an expression for the reaction rate (R) of catalyzed char gasification:

$$R = kC_{cs} = k * (TSA) * \frac{ASA}{TSA} * \frac{RSA}{ASA} \quad (4.1)$$

where C_{cs}, is the concentration of carbon (re)active sites and *TSA*, *ASA*, and *RSA* are the total, active, and reactive surface area of the char, respectively. RSA represents the concentration of active sites that form the reactive intermediate under gasification reaction conditions, while ASA represents the concentration of active sites that are measured by low-temperature chemisorption. The common approach is to implicitly assume that the ratio RSA/ASA is a constant, and to determine ASA by low temperature chemisorption, as is routinely done in heterogeneous catalysis [12]. Differences in reaction rates are then rationalized in terms of ASA differences (which are presumably proportional to RSA differences) [12]. Measurement of RSA was attempted before by Lizzio and Radovic [11] (by switching the reactive gas to inert gas at reaction temperature to quantify the CO released). However, RSA obtained by this method is well suited for K-catalyzed gasification, and not for Ca catalyzed gasification. RSA was also measured by Cazorla-Amoros et al. [13] using temperature programmed desorption (TPD) analysis after CO_2 chemisorption. However, this was tested only for Ca catalyzed gasification. In the absence of a reliable method for measuring the RSA, the common approach of measuring the ASA is followed. We hypothesize that the char reactivity is determined by the combined effect of char physical surface area, the type of minerals present and the dispersion of these minerals on the char surface. ASA could be one such parameter that combines these individual effects to measure the number of active sites on char surface. Thus, the second aim of this study is to probe if the ASA of char is a better descriptor of initial reactivity of different biomass chars, than the char TSA or the content and type of inorganics in char.

4.2 Experimental Methods

4.2.1 Experimental materials

Four different biomass feedstocks were specifically chosen in this study to segregate the effect of different char properties (inorganic types and composition, ash content and char total surface area) on its gasification reactivity. These feedstocks are: Sugarcane bagasse from Louisiana (U.S.), loblolly pine wood (debarked and chipped pine logs) from Georgia (U.S.), Switchgrass supplied by National Renewable Energy Laboratory (NREL, Golden, Colorado), and Avicel® PH-101 from Sigma Aldrich. Section 4.3.1 explains the rationale behind choosing these feedstocks. Since biomass particle size used in pyrolysis affects char structural evolution and gasification properties [14], small size range particles (180-250 μm) were used for all biomasses in this study, except for Avicel which was available as ~50 μm particle size from Sigma-Aldrich. Sugarcane bagasse ("bagasse"), loblolly pine ("pine") and switchgrass were dried in an oven at 105 ^{0}C for 6 hours and then ground and sieved to obtain 180-250 μm particles.

4.2.2 Pyrolysis experiments

Pyrolysis of bagasse, pine, switchgrass, and Avicel were performed in a pressurized laminar entrained flow reactor (PEFR) to generate chars for further gasification tests. The PEFR was originally designed and located at Risø National laboratory [15], and Fjellerup et al. [16] explains briefly about the operation of this PEFR. Figure 2.1a of Chapter 2 shows the schematic of the PEFR, and Section 2.2.2 explains the components of the PEFR.

In this study, all pyrolysis experiments (to generate chars) were performed at a residence time of 28 s, a temperature of 800 °C, and pressures of 5 and 20 bar (except for Avicel char which was generated at 5 bar only, and switchgrass char which was generated at 15 bar instead of 20 bar).

4.2.3 Measurement of initial char CO_2 gasification reactivity

To measure the char gasification reactivity, isothermal gasification experiments (of chars generated by different pyrolysis runs) were carried out in an atmospheric TGA manufactured by TA Instruments (SDT Q-600) at a gasification temperature of 800℃ in pure CO_2. To ensure there was no external mass transfer resistance, the sample mass was varied in the gasification experiments until no change in reactivity was observed by further reducing the sample mass. The initial gasification reactivity of chars did not change by crushing the char particles. The procedure for measuring char gasification reactivity is discussed before in Section 2.2.3 of Chapter 2. The carbon conversion (X) and reactivity (R) are defined as:

$$X = \frac{(m_o - m_t)}{(m_o - m_{ash})} \tag{4.2}$$

$$R = \frac{-1}{(m_t - m_{ash})} \frac{dm}{dt} \tag{4.3}$$

where m_o represents the initial mass of the char at the onset of gasification, m_t is the instantaneous mass of the char at any time t, m_{ash} is the remaining mass of ash after completion of gasification, and dm/dt is the rate of mass loss. The initial gasification reactivity is defined as the reactivity value averaged between 15 to 20% conversion. In this paper, we will focus on the correlation between char properties and the *initial* CO_2

gasification reactivity. This is because measured properties of char only represent its initial gasification behavior since the char properties will change as char conversion increases. Repeatability of data between the runs was good with a deviation of less than 5 %.

4.2.4 Characterization techniques

Complementary N_2 and CO_2 physisorption measurements were conducted at 77 K and 273 K, respectively, to obtain the total surface area of the chars. The measurements were performed in a Micromeritics ASAP 2020 instrument with an operating pressure range of 0 to 950 mm Hg. The Brunauer–Emmett–Teller theory (BET) is applied to obtain the BET surface area from N_2 physisorption data [17]. CO_2 physisorption is used to characterize micropore surface area [18-19]. The DFT method is used to obtain pore size distribution [19-20]. A detailed description of these methods are given in Section 2.2.4 of Chapter 2.

Ultimate analysis was performed by Huffman Laboratories (Colorado, US). Trace element analyses of biomass samples and chars were performed by the analytical testing lab located at the Renewable Bioproducts Institute (Atlanta, Georgia), by using a caustic fusion digestion method followed by ICP-OES analysis (Inductively Coupled Plasma-Optical Emission Spectrometry). For the analysis of sodium in biomass, an acid digestion method is used followed by ICP emission spectroscopy. Elemental compositions of biomass are reported as corresponding oxides.

CO_2 chemisorption measurements were performed in a Micromeritics ASAP 2020 instrument using a procedure similar to the one followed elsewhere [21]. A detailed description of the procedure is given in Section 3.2.5 of Chapter 3.

4.3 Results and Discussion

4.3.1 Characterization of bagasse, SCT and Avicel

The proximate and ultimate analyses, and ash composition of bagasse, pine, switchgrass and Avicel are shown in Table 4.1. Also, the surface areas of char generated from pyrolysis of these biomasses are shown in Table 4.2. It can be seen that for most of the chars, surface area measured by CO_2 physisorption (micropore surface area) is much larger than the surface area measured by N_2 physisorption. Pore size distribution (see Appendix B) showed that the contribution of meso and macropore surface area to the total surface area of these chars is only about 2 to 8 %. Thus, these chars are mostly microporous material, and the total surface area of these chars can be reasonably approximated to surface area measured by CO_2 physisorption. Comparison of surface area measured by CO_2 physisorption for the four biomass chars showed that Avicel char has the lowest surface area, the two pine chars have the highest surface areas, and intermediate surface areas are observed for bagasse and switchgrass chars.

The biomass chars chosen for this study cover a wide range of ash content, concentration of catalytically active inorganic metals and surface areas. Inherent potassium, sodium and calcium in biomass are known to be catalytically active metals that enhance the char gasification rate, while silica present in biomass is known to reduce the catalytic effect of catalytically active metals by reacting with these metals to form catalytically inactive silicates [8,9,22]. In this study, the chosen biomasses covered a broad range of K, Ca and Si content (Na content in all the biomasses are negligible compared to K and Ca). Avicel (model cellulose) was chosen for a baseline study because it contains a negligible amount of ash, negligible Si content and negligible

catalytically active inorganic metals. Also, the surface area of Avicel char is low. On the other hand, switchgrass represents an energy crop with moderate ash content, a high K content, and moderate amounts of Ca and Si, but it generates char with only moderate surface areas. Bagasse represents an agricultural residue containing high ash content with moderate amounts of K and Ca, but a high Si content. Also, chars from bagasse have moderate surface areas. Pine represents a forest residue, and it generates very high surface area chars. However, pine has very low ash content, low content of K and Ca, and negligible Si.

Ultimate analysis (Table 4.1) showed that C, H and O of these biomasses are very similar, with a small deviation for Avicel. This is because Avicel contains mostly cellulose whereas the other biomasses contain hemicellulose and lignin, in addition to cellulose.

Table 4.1 Ultimate analysis, proximate analysis and ash composition of bagasse, pine, switchgrass (180-250 μm) and Avicel (~50 μm)

Feedstock	Bagasse	Pine	Switchgrass	Avicel
Parameters	*Proximate analysis (wt%), db*[a]			
Fixed carbon	11.6	16.3	18.9	6.2
Volatile	80.7	83.4	76.9	93.8
Ash	7.7	0.3	4.2	< 0.1
	Ultimate analysis (wt%), daf[a]			
C	49.87	50.82	49.44	44.26
H	6.01	5.99	6.06	6.19
N	0.38	0.07	0.58	0.02
S	0.17	0.02	0.08	0.02
O[b]	43.57	43.10	43.84	49.51
	Ash composition in biomass (wt%), db[a]			
Al_2O_3	0.610	0.004	0.005	< 0.001
K_2O	0.383	0.065	0.890	0.008
Na_2O	0.013	0.002	0.006	0.004
CaO	0.380	0.103	0.316	0.010
MgO	0.124	0.045	0.256	0.003
Fe_2O_3	0.221	0.003	0.009	0.001
SiO_2	4.580	0.014	1.481	0.004
SO_3	0.304	< 0.020	0.122	< 0.020
P_2O_5	0.081	< 0.030	0.266	< 0.030

[a] db = dry basis; daf = dry and ash-free basis.
[b] Calculated by difference.

Table 4.2 Surface area of PEFR chars generated by pyrolysis of different biomass at 800℃ and 28 sec residence time

Adsorbent for surface area analysis	**Char surface area, m^2/g**						
	Bagasse char		Pine char		Switchgrass char		Avicel
	5 bar	20 bar	5 bar	20 bar	5 bar	15 bar	5 bar
N_2 Physisorption[a]	102	75	8	34	19	41	6
CO_2 Physisorption[b]	173	124	312	331	280	255	119

[a] BET surface area by N_2 physisorption
[b] DFT surface area (micropore surface area) by CO_2 physisorption

4.3.2 Correlating the initial char reactivity with H/C and char surface area

The C, H and O content can provide an indication of the the structural order (or polyaromaticity) of char. It is known that the carbon structure of char affects the char gasification reactivity, and one way of semi-quantification of carbon structure of char is by using the H/C (atomic) ratio, as commonly used in coal literature [23]. In biomass literature, it is shown that the loss of oxygen and hydrogen in biochar results in ordering/condensation of the biochar structure, and thus a reduction in char reactivity [24]. Thus, a higher H/C represents a more reactive char for gasification. Figure 4.1a shows the correlation of H/C with the initial reactivity of char. For all the chars, higher pressure chars (15/20 bar) have lower reactivity than char generated at 5 bar pyrolysis pressure. Also, higher pyrolysis pressure lowers the H/C ratio. It can be seen from Figure 4.1a that for similar values of the H/C ratio, the gasification reactivity varies widely. Therefore, H/C alone is not a good indicator of char reactivity.

The surface area of a solid is a common parameter that determines the reaction rate of a heterogeneous gas-solid reaction, like char gasification by CO_2. As discussed before, char total surface area is obtained by performing both nitrogen and CO_2 physisorption, and is close to micropore surface area (by CO_2 physisorption). Figure 4.1b shows the correlation of total char surface area with the initial reactivity of the chars. For all biomass chars, higher pressure chars (15/20 bar) have lower total surface area than char generated at 5 bar. It can be seen that even though Avicel char has a total surface area of 119 m^2/g, its reactivity is still negligible. Also, even though pine chars have the highest surface areas (more than 300 m^2/g), its reactivity is still lower than the switchgrass chars. This shows that not all the measured physical surface area is active. It

is likely because pine has low content of active inorganics which reduces the active portion of the total surface area. Thus, even though char surface area may be an important indicator of char reactivity, it cannot be used alone as a unifying parameter to reconcile the reactivity of a wide range of biomass chars. Therefore, active surface area (ASA) is measured for these chars in Section 4.3.4

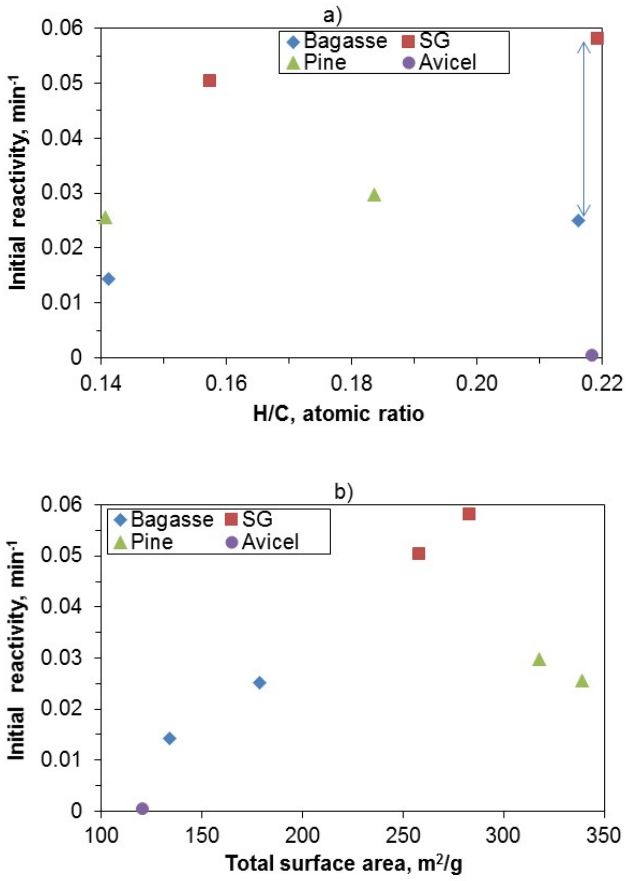

Figure 4.1 (a) Correlation between initial char gasification reactivity and H/C atomic ratio of chars, and (b) correlation between initial char gasification reactivity and total surface area of chars. SG refers to switchgrass char.

4.3.3 Correlating the initial char reactivity with (K + Ca) content and alkali index

Figure 4.2a show the correlation of the initial reactivity of char with total ash content. As expected, this correlation is not good because not all inorganics in ash contribute to enhancing char reactivity. In bagasse, a large proportion of the ash consists of inactive inorganic components, like Si and Al. A correlation of the reactivity with only active inorganics, K and Ca, is shown in Figure 4.2b. It can be seen from Figure 4.2b that even the (K + Ca) content of char does not correlate well with char reactivity. Bagasse chars, even with much higher K and Ca than pine, still have lower reactivity than pine chars. This could be attributed to two different arguments: 1) higher Si and Al in bagasse chars can reduce the catalytic activity of K and Ca by forming aluminosilicates, thus lowering the amount of active inorganics, and 2) high surface area and negligible Si in pine chars, compared to bagasse chars, may compensate for the lower amount of K and Ca content in pine, and thus lead to higher reactivity than bagasse chars. To test the first argument, a correlation of the char reactivity with the alkali index (equation 4.4) is presented in Figure 4.2c. This index accounts for the reduction in the activity of active inorganics by inactive Si and Al oxides. The Alkali Index (AI) expresses the ratio of the sum of the mole fractions of the basic compounds (CaO, MgO, Fe_2O_3, Na_2O, K_2O) to the sum of the mole fractions of the acid compounds (SiO_2, Al_2O_3) in the ash, multiplied by the ash content of the char [25].

$$Alkali\ Index = w_{ash}\frac{(Fe_2O_3 + CaO + MgO + Na_2O + K_2O)}{(SiO_2 + Al_2O_3)} \tag{4.4}$$

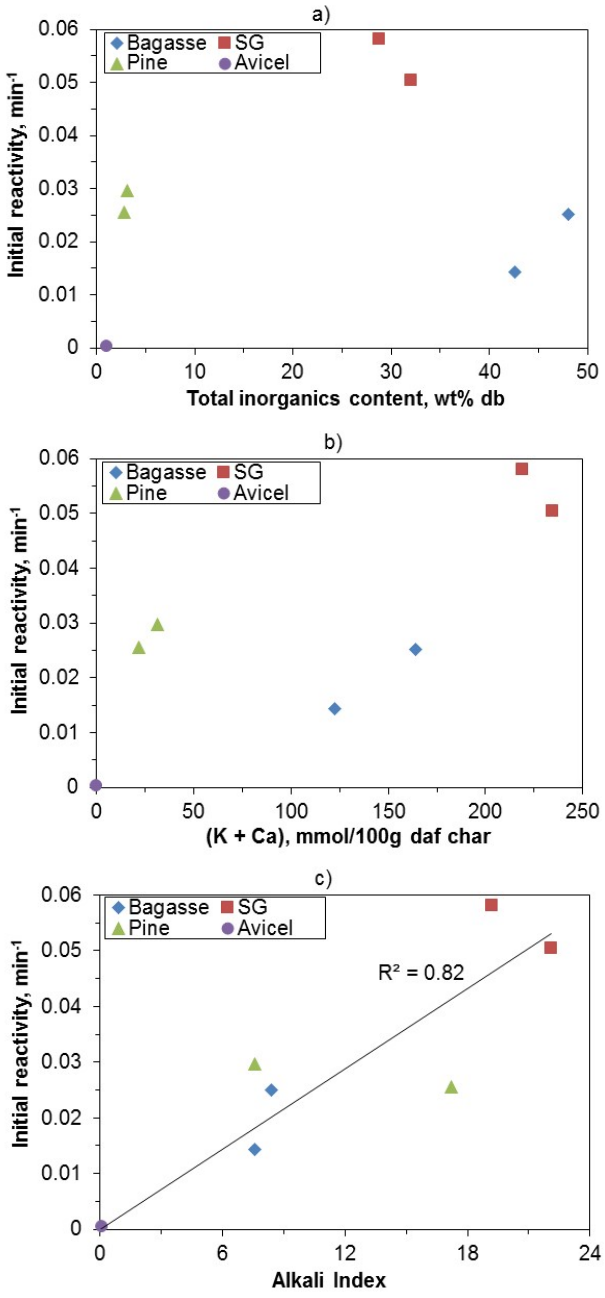

Figure 4.2 Correlation between initial char gasification reactivity and inorganics concentration of chars as represented by (a) Total ash content of char, (b) (K + Ca) content of char, and (c) Alkali Index of char. SG refers to switchgrass char. "db" and "daf" refers to dry basis, and dry and ash free basis, respectively.

In the prior studies, the AI has been correlated well with the gasification reactivity of different coal chars [26]. However, a good correlation was not obtained for chars from different woody and agricultural waste biomasses [2]. Figure 4.2c shows the correlation of biomass char initial reactivity with AI. It can be seen that even though this correlation is much better than all the other parameters shown before, it is still not acceptable. Thus, unlike coal chars, reactivity of biomass chars do not correlate well with AI. This is probably due to the large variation in biomass composition compared to coal.

Therefore, results from Section 4.3.2 and 4.3.3 suggest that both the char surface area, and the type and content of inorganic content together would likely help in better explaining the observed char reactivity. Therefore, to test this argument, the effect of surface area, the content and type of mineral matters, and the dispersion of these minerals on char surface are combined in a single parameter called the active surface area (ASA). ASA of char was measured and correlated to char reactivity in the next section (4.3.4)

4.3.4 Correlating the initial char reactivity with CO_2 chemisorption

There are different methods used in the past to measure ASA. This includes using different adsorbates (O_2, CO_2) and using different adsorption temperatures (250 to 300 ^{0}C) [10,21,27,28]. Also, different measurement techniques have been used. This includes a gravimetric method (by using a thermogravimetric analyzer, TGA, where the weight gain of char is measured during chemisorption of adsorbates at a fixed temperature). Another method is temperature programmed desorption, TPD (by adsorption of adsorbate onto char followed by measuring the total amount of adsorbate desorbed during temperature programmed heating of the char). A third method is volumetric

chemisorption (by measuring the volume of adsorbate adsorbed on the char at a fixed chemisorption temperature) [10].

In this study, the ASA is measured by CO_2 chemisorption at 300°C. This method of measuring ASA is used by many authors in the past to determine the effect of coal rank on the ASA, the effect of pyrolysis heating rate and temperature on the ASA of coal chars, and the effect of calcium and potassium on the ASA of coal chars and pure carbon [21,29-32]. However, this technique is not being utilized to determine the effect of different biomass chars on the ASA, and this is the aim of this section. In this study, gravimetric measurement of ASA using CO_2 chemisorption at 300^0C was attempted in a TGA (SDT Q-600), but the weight gain by the sample was too small to be detected accurately by TGA. In the TPD method, the absence of weakly chemisorbed adsorbate cannot be ascertained [10]. The char active surface area should be characterized using CO_2 chemisorption by an experimental method that can differentiate between strong and weak CO_2 chemisorption at 300°C. Therefore, the volumetric CO_2 chemisorption method is used for measurement of char ASA in this study. The strongly chemisorbed CO_2 (μmol/g of char), which determines the ASA of char, is measured and then is correlated to the initial char reactivity. The strongly chemisorbed CO_2 is a better parameter than the total chemisorbed CO_2 for correlation because it does not include the unreactive weakly chemisorbed CO_2, which desorbs easily [21]. The nature of active sites on carbon surface where CO_2 chemisorbs is shown in Section 3.3.3, and in Appendix A.

Figure 4.3 shows the correlation of the strongly chemisorbed CO_2 (a measure of ASA) with the initial reactivity of the char. This correlation is found to be much better than the earlier correlations presented in this study to reconcile the initial reactivity of the

wide range of biomass chars characterized. However, it can be seen from Figure 4.3 that the plot is broadly comprised of two zones. In the first zone, the initial increase in ASA leads to a large increase in reactivity. However, in the second zone, a large increase in ASA leads a much smaller, but linear, increase in reactivity. This can be explained by understanding what fraction of the measured ASA (by CO_2 chemisorption) is the reactive ASA which has contact with carbon (char), as shown schematically in Figure 4.4. In Figure 4.4, active inorganics are shown by a cube sitting on the char (carbon) surface. Cazorla-Amoros et al. [33] have shown that not all the active sites, as measured by CO_2 chemisorption, are reactive, and only the carbon-inorganic interfaces are the reactive sites. This reactive portion is shown as portion (1) in the inset of Figure 4.4, while the measured ASA corresponds to all portions of the inset shown in Figure 4.4. For Avicel char, the ASA and reactivity are negligible because there is a negligible amount of active inorganics in Avicel. For chars with a small amount of active inorganics, like for pine chars, the measured ASA by chemisorption is small, but most of the inorganics would likely have good contact with carbon, as shown schematically in Figure 4.4. So, the ratio of char-inorganic contact sites (or reactive sites) to the measured active sites would be much higher, and thus a large increase in reactivity is observed for nearly an incremental increase in the inorganic concentration in char. If the active inorganics content is high, like for switchgrass chars, then the ASA measured by chemisorption is high, but all the inorganics would not be in contact with carbon (Figure 4.4). So, the ratio of char-inorganics contact sites (or reactive sites) to measured active sites would be much smaller, and thus only a small increase in reactivity is observed even with a much larger increase in the inorganic content and the measured ASA. To summarize, the efficacy of

measured the ASA decreases at higher inorganic content due to the reduced char-inorganic contact. The schematic of Figure 4.4 thus explains the observed trend of the correlation of ASA with initial reactivity (Figure 4.3). Other reasons for the empirical nature of this correlation are that the turnover frequency of the K and Ca active sites is assumed to be the same, and the effect of small differences in the carbon structure of the chars on char reactivity is not considered in ASA. This empirical correlation can be used for predicting the gasification reactivity when processing different kinds of biomass chars. This correlation will assist in determining the adjustments required for the gasifier operating conditions to maintain close to the desired char conversion to syngas.

Future studies can be directed to test and improve this empirical correlation by testing more biomass species. This study was done by using CO_2 as the gasification medium. A similar study could be done for steam gasification. Also, in this study the initial char gasification reactivity is used as the measure of reactivity because measured properties of char only represent its initial gasification behavior. The char and ash properties change as the char conversion increases, as observed elsewhere [34].

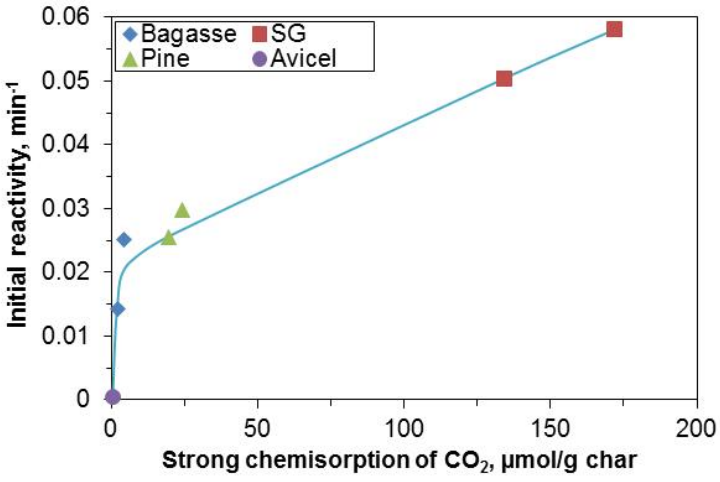

Figure 4.3 Correlation between initial char gasification reactivity and strong chemisorption of CO_2. SG refers to switchgrass char.

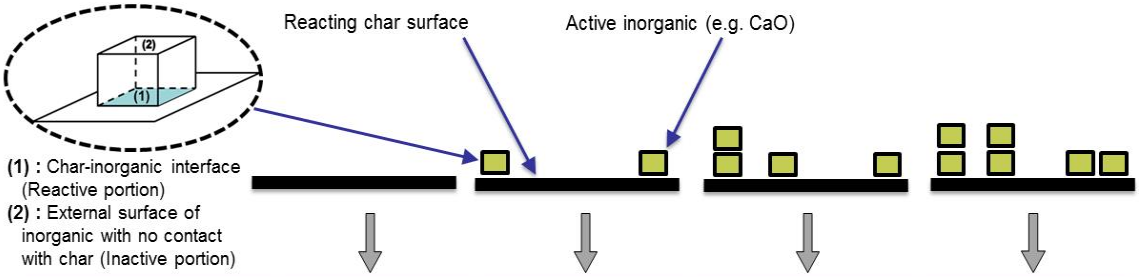

Active Inorganics content in char	None (Avicel char)	Low	Moderate	High
Measured active site (by CO_2 chemisorption)	Zero	Low	Moderate	High
Ratio of char-inorganic contact site to measured active site	Zero	High	Moderate	Low

Figure 4.4. Schematic showing the importance of char-inorganic contact for understanding the relation of char ASA to char reactivity, with increasing concentration of active inorganics. The efficacy of measured active site decreases at higher inorganic content due to reduced char-inorganic contact.

4.4 Conclusions

a) The char total surface area alone does not correlate well with the initial reactivity from different biomass chars, indicating that the concentration of specific active sites rather than the total surface area plays an important role.

b) The content of K and Ca do not correlate well to initial char reactivity. Bagasse chars had much higher content of K and Ca than pine chars, but still had lower initial reactivity due to the high Si and Al content in bagasse. Even the Alkali Index, which accounts for the inhibitive effect of Si and Al on gasification, does not improve the correlation with char gasification reactivity because the effect of surface area is not included in the Alkali Index.

c) The ASA measurements by strong CO_2 chemisorption on chars at 300 °C combine the effect of char physical surface area, inorganic content and composition, and the

dispersion of inorganics in one parameter. ASA is found to be a better descriptor to reconcile the char initial reactivity from different biomass chars. The empirical correlation between ASA of char and char reactivity can be used for predicting the gasification reactivity when processing different kinds of biomass chars in a gasifier.

d) The ASA measurement by strong CO_2 chemisorption is not a direct measurement of the true reactive sites. This is because at higher concentrations of active inorganics, even though the measured ASA increases, the contact between the inorganics and the char surface is likely to decrease. This reduces the effectiveness of inorganics (and the measured ASA) at higher concentration.

4.5 References

[1] Kirkels AF, Verbong GPJ. Biomass gasification: Still promising? A 30-year global overview. Renew Sustain Energy Rev 2011;15:471–81.

[2] Duman G, Uddin MA, Yanik J. The effect of char properties on gasification reactivity. Fuel Process Technol 2014;118:75–81.

[3] Heidenreich S, Foscolo PU. New concepts in biomass gasification. Prog Energy Combust Sci 2015;46:72–95.

[4] Moilanen A, Nasrullah M, Kurkela E. The effect of biomass feedstock type and process parameters on achieving the total carbon conversion in the large scale fluidized bed gasification of biomass. Environ Prog Sustain Energy 2009;28:355–9.

[5] Alauddin ZABZ, Lahijani P, Mohammadi M, Mohamed AR. Gasification of lignocellulosic biomass in fluidized beds for renewable energy development: A review. Renew Sustain Energy Rev 2010;14:2852–62.

[6] Vassilev S V, Baxter D, Andersen LK, Vassileva CG. An overview of the chemical composition of biomass. Fuel 2010;89:913–33.

[7] Di Blasi C. Combustion and gasification rates of lignocellulosic chars. Prog Energy Combust Sci 2009;35:121–40.

[8] Zhang Y, Ashizawa M, Kajitani S, Miura K. Proposal of a semi-empirical kinetic model to reconcile with gasification reactivity profiles of biomass chars. Fuel 2008;87:475–81.

[9] Kannan MP, Richards GN. Gasification of biomass chars in carbon dioxide: dependence of gasification rate on the indigenous metal content. Fuel 1990;69:747–53.

[10] Arenillas A, Rubiera F, Parra JB, Pis JJ. A comparison of ASA values determined by different methods. Carbon 2002;40:1381–3.

[11] Lizzio AA, Radovic LR. Transient kinetics study of catalytic char gasification in carbon-dioxide. Ind Eng Chem Res 1991;30:1735–44.

[12] Radovic LR, Lizzio AA, Jiang H. Reactive surface area: an old but new concept in carbon gasification. In Fundam. Issues Control Carbon Gasif. React., Springer; 1991, p. 235–55.

[13] Cazorlaamoros D, Linaressolano A, Gomis AFM, Delecea CSM. Calcium catalytic active-sites in carbon gas reactions- determination of the specific activity. Energy Fuels 1991;5:796–802.

[14] Asadullah M, Zhang S, Min Z, Yimsiri P, Li C-Z. Importance of biomass particle size in structural evolution and reactivity of char in steam gasification. Ind Eng Chem Res 2009;48:9858–63.

[15] Hansen LK, Fjellerup J, Stoholm P, Kirkegaard M. The pressurized entrained flow reactor at Risø. Design report. Risø-R-822(EN) 1995.

[16] Fjellerup J, Gjernes E, Hansen LK. Pyrolysis and Combustion of Pulverized Wheat Straw in a Pressurized Entrained Flow Reactor. Energy & Fuels 1996;10:649–51.

[17] Brunauer S, Emmett PH, Teller E. Adsorption of gases in multimolecular layers. J Am Chem Soc 1938;60:309–19.

[18] Lozano-Castelló D, Cazorla-Amorós D, Linares-Solano A. Usefulness of CO_2 adsorption at 273 K for the characterization of porous carbons. Carbon 2004;42:1233–42.

[19] Malekshahian M, Hill JM. Effect of pyrolysis and CO_2 gasification pressure on the surface area and pore size distribution of petroleum coke. Energy Fuels 2011;25:5250–6.

[20] Webb PA, Orr C. Analytical methods in fine particle technology. Micromeritics Instrument Corp; 1997.

[21] Molina A, Montoya A, Mondragón F. CO_2 strong chemisorption as an estimate of coal char gasification reactivity. Fuel 1999;78:971–7.

[22] Link S, Arvelakis S, Hupa M, Yrjas P, Kulaots I, Paist A. Reactivity of the Biomass Chars Originating from Reed, Douglas Fir, and Pine. Energy Fuels 2010;24:6533–9.

[23] Chan ML, Jones JM, Pourkashanian M, Williams A. The oxidative reactivity of coal chars in relation to their structure. Fuel 1999;78:1539–52.

[24] Yip K, Xu M, Li CZ, Jiang SP, Wu H. Biochar as a Fuel: 3. Mechanistic understanding on biochar thermal annealing at mild temperatures and its effect on biochar reactivity. Energy Fuels 2011;25:406–14.

[25] Sakawa M, Sakurai Y, Hara Y. Influence of coal characteristics on CO_2 gasification. Fuel 1982;61:717–20.

[26] Skodras G, Sakellaropoulos GP. Mineral matter effects in lignite gasification. Fuel Process Technol 2002;77:151–8.

[27] Laine NR, Vastola FJ, Walker PL. Importance of active surface area in carbon-oxygen reaction. J Phys Chem 1963;67:2030 – 2034.

[28] Koenig PC, Squires RG, Laurendeau NM. Effect of potassium carbonate on char gasification by carbon-dioxide . J Catal 1986;100:228–39.

[29] Linares-Solano A, Almela-Alarcón M, de Lecea CS-M. CO_2 chemisorption to characterize calcium catalysts in carbon gasification reactions. J Catal 1990;125:401–10.

[30] Zhang Y, Hara S, Kajitani S, Ashizawa M. Modeling of catalytic gasification kinetics of coal char and carbon. Fuel 2010;89:152–7.

[31] Jing X, Wang Z, Zhang Q, Yu Z, Li C, Huang J, et al. Evaluation of CO_2 gasification reactivity of different coal rank chars by physicochemical properties. Energy Fuels 2013;27:7287–93.

[32] Xu K, Hu S, Su S, Xu C, Sun L, Shuai C, et al. Study on char surface active sites and their relationship to gasification reactivity. Energy Fuels 2012;27:118–25.

[33] Cazorlaamoros D, Linaressolano A, Delecea CS. Calcium-carbon interaction study - its importance in the carbon-gas reactions. Carbon 1991;29:361–9.

[34] Umeki K, Moilanen A, Gomez-Barea A, Konttinen J. A model of biomass char gasification describing the change in catalytic activity of ash. Chem Eng J 2012;207:616–24.

CHAPTER 5

CO-GASIFICATION OF SUGARCANE BAGASSE WITH CANE TOPS/LEAVES

5.1 Background

Co-gasification of biomass with petroleum coke is known to enhance the reactivity of less reactive petroleum coke by the alkali and alkaline earth metals present in a more reactive biomass char (synergy) [1]. Co-gasification may also lead to an inhibitive effect; for example, addition of switchgrass to sub-bituminous coal reduced the reactivity of the mixture due to deactivation of mobile alkali species (present in switchgrass) by the reaction with aluminosilicates minerals in coal [2]. Tchapda and Pisupati [3] provides a review of different co-gasification studies.

Since biomass species differ in their ash content and composition, there is a possibility of enhancement in the reactivity of less reactive biomass char by a more reactive biomass char during co-gasification of two different types of biomasses. Also, an added incentive for co-processing of two or more biomasses (like bagasse with cane trash) is the potential improvement in the economy of scale and feedstock availability [4]. In this study, the focus is on co-gasifying chars from two kinds of sugarcane residue, bagasse and sugarcane leaves/tops (SCT). These residues are the agricultural wastes produced during sugarcane harvesting and processing [5]. SCT represents the largest and most important reserve of sugarcane residue [6]. However, in the literature, bagasse is the more widely researched biomass for thermochemical conversion processes, with little

emphasis given to SCT. The Brazilian bagasse used in this co-gasification study has a much higher content of potassium, and thus much higher overall char reactivity, than the Brazilian SCT char. Thus, co-gasification was expected to improve the reactivity of SCT char by the synergistic effect, which is the main focus of this study.

Contrary to expectations, it was observed that a combination of synergistic and inhibitive effects exists. Thus, the next part of this study was aimed at understanding the observed effect of combined synergistic and inhibitive effects during co-gasification by identifying the role of potassium redistribution during co-gasification on char reactivity. Based on these results, different flow schemes for co-processing of bagasse and SCT chars are suggested, qualitatively, to maximize the char reactivity. Finally, to reconcile the co-gasification reactivity data among different feedstocks, the conditions that leads to overall synergy, or inhibition, or additive effects are explained.

5.2 Experimental Methods

5.2.1 Experimental materials

Sugarcane bagasse and SCT from Brazil were used in this study. The bagasse and SCT feedstocks from Brazil were dried in an oven at 105 ^{0}C for 6 hours and then ground and sieved to obtain 180-250 μm particles. For all experiments, 180-250 μm size range particles were used. Sugarcane bagasse and SCT from Brazil are designated as Brazil bagasse (BB) and Brazil leaves (BL), respectively. In addition, Avicel (model cellulose) is also used for a baseline study as it contains negligible inorganic material to catalyze the

char gasification reaction. Avicel® PH-101 (50 μm particle size) was purchased from Sigma-Aldrich.

5.2.2 Pyrolysis experiments

Pyrolysis of bagasse and SCT was performed in an atmospheric laminar entrained flow reactor (LEFR) to generate chars for further gasification tests. Iisa et al. [7] explains the schematic, components and operational details of this reactor. BB char and BL char were generated in thus LEFR at 1000 °C, and the residence time was kept at 3 sec. In addition, Avicel char was generated by pyrolysis in a pressurized entrained flow reactor (PEFR) (at 800 °C - 5 bar - 28 s) to generate char for baseline studies. Fjellrup et al. [8] explains the flow scheme and operating details of this PEFR. The schematic of the PEFR is similar to the LEFR, except that the PEFR can be operated at higher pressure which generates Avicel char with a spherical morphology. This spherical morphology of char helps in easy identification of Avicel char in a mixture with BB char while performing SEM-EDX analysis. Details of the LEFR and the PEFR are explained in Section 3.2.2 and Section 2.2.2, respectively.

5.2.3 Measurement of char CO_2 gasification reactivity

To measure the char gasification reactivity, isothermal gasification experiments (of chars generated by different pyrolysis runs) were carried out in an atmospheric TGA manufactured by TA Instruments (SDT Q-600) at a gasification temperature of 800℃ in pure CO_2. To ensure there was no external mass transfer resistance, the char sample mass was varied in the gasification experiments until no change in reactivity was observed by further reducing the sample mass. To remove any internal mass transfer resistance,

crushed char particles were used. The procedure for measuring char gasification reactivity is discussed before in Section 2.2.3 of Chapter 2. The carbon conversion (X) and reactivity (R) are defined as:

$$X = \frac{(m_o - m_t)}{(m_o - m_{ash})} \tag{5.1}$$

$$R = \frac{-1}{(m_t - m_{ash})} \frac{dm}{dt} \tag{5.2}$$

where m_o represents the initial mass of the char at the onset of gasification, m_t is the instantaneous mass of the char at any time t, m_{ash} is the remaining mass of ash after completion of gasification, and dm/dt is rate of mass loss. Repeatability of data between the runs was good with a deviation of less than 5 %.

5.2.4 Ash generation in quartz reactor

To understand the effect of BB ash addition on the reactivity of BL char (and vice versa), BB and BL ash samples were generated by pure CO_2 gasification of the corresponding BB char and BL char to nearly complete conversion (~ X = 95 %) in a horizontal quartz tube reactor. Briefly, about 200 mg of LEFR char was placed in a quartz boat in a 2" diameter quartz tube reactor heated by a horizontal furnace. Then, the reactor was heated in N_2 at 25 K/min to the gasification temperature of 800 ^{0}C, and held there for 10 minutes (as in the TGA experiments). Then, the gas flow was switched to pure CO_2 (99.99 %) at 950 ml/min to start gasification. Chars were exposed to CO_2 for a predetermined time (found using the TGA experiments) to completely convert the char. The reactor gas was then switched to N_2 and cooled rapidly in N_2 to below 60 ^{0}C to collect the ash.

5.2.5 Characterization techniques

Ultimate analysis was performed by Huffman Laboratories (Colorado, US). Trace element analyses of biomass samples and chars were performed by the analytical testing lab located at the Renewable Bioproducts Institute (Atlanta, Georgia), by using a caustic fusion digestion method followed by ICP-OES analysis (Inductively coupled plasma-optical emission spectrometry). Elemental compositions are reported as corresponding oxides. SEM–EDX analysis of char was carried out in a LEO 1530 thermally-assisted field emission (TFE) scanning electron microscope (SEM) with energy dispersive X-ray analysis (EDX) capability.

5.3 Results and Discussion

5.3.1 Char reactivity profile of pure components

Proximate and ultimate analyses, and ash compositions of BB, BL and Avicel have been shown previously in Table 3.1. The ultimate analyses results of BB and BL are similar, which is typical of a biomass feedstock. Avicel had similar proximate and ultimate analysis results as BB and BL with an important difference that it had negligible contents of ash and catalytically active inorganics. Significant differences were observed in the composition of inorganics between the BB and BL samples. BL had a smaller amount of K compared to BB, and is mostly Ca rich. BB, on the other hand, is K rich. This has important consequences (as also seen earlier in Section 3.3.3) since evolution of char reactivity with conversion is different for a K-rich char than for a Ca-rich char [9]. Silicon (present in both BB and BL) in the biomass is known to inhibit the catalytic effect of K [10,11].

Figures 5.1a and 5.1b show the conversion - time plot and reactivity - conversion plot, respectively, for the gasification of BB and BL chars which were generated by pyrolysis in the LEFR at 1000 °C – 3 sec. Gasification of these chars was performed in pure CO_2 at 800℃ in the TGA. For Avicel char, the gasification reactivity is negligible at 800 °C in CO_2 due to the negligible amount of catalytically active inorganics (K and Ca) in Avicel.

The reactivity of BB char increased by a factor of 3.5 during the progress of char conversion, while BL char reactivity decreased by a factor of 2.0 as char conversion progressed. This is because for a calcium rich char (like BL char), the char reactivity decreases during the progress of gasification due to sintering of calcium as the char conversion progresses in CO_2 [9,12]. The reactivity of calcium-rich BL char was correlated to CO_2 chemisorption in Section 3.3.3. Thus, the initial BL char reactivity is high, but the overall char reactivity is low. On the other hand, for a potassium rich char (in the absence of excess silica), the char reactivity increases during the progress of gasification due to an increase in the K/C ratio and the char exhibits a maximum reaction rate in the higher conversion range [9,11]. The reactivity of potassium-rich BB char was correlated to CO_2 chemisorption in Section 3.3.3. Thus, the initial BB char reactivity is small, but the overall reactivity is much higher than the initial reactivity. Since BB char has higher reactivity than BL char, therefore co-gasification is expected to improve the reactivity of BL char by the synergistic effect from the K from BB char, which is tested experimentally in the next section.

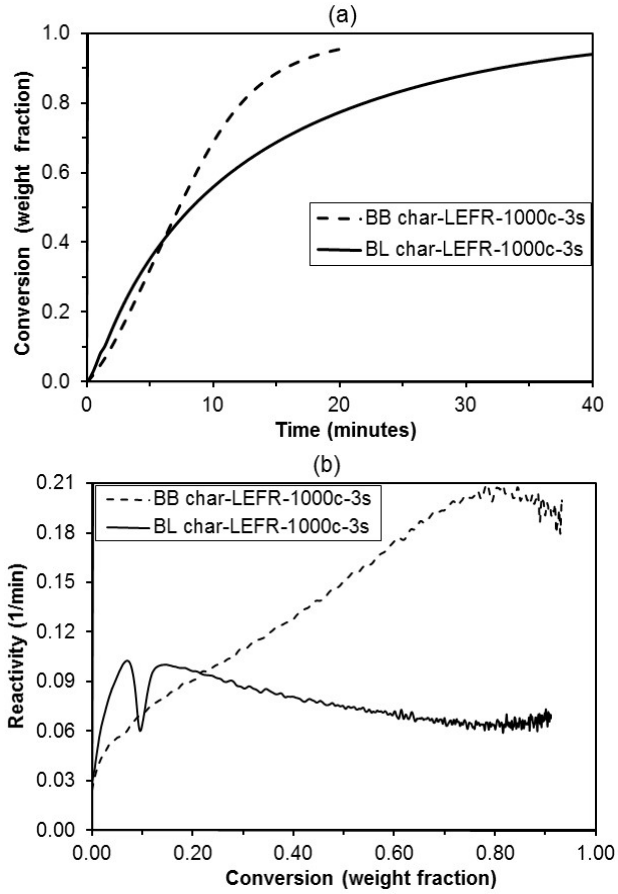

Figure 5.1 Isothermal gasification of LEFR chars from Brazil bagasse (BB) and Brazil leaves (BL) at 800 °C in pure CO_2. LEFR chars were generated by pyrolysis in nitrogen at 1000 °C and 3 sec. (a) Char conversion versus time, and (b) Char reactivity versus conversion.

5.3.2 Char reactivity of blends during co-gasification

To measure the experimental reactivity during co-gasification of BB char with BL char, different mixtures of BB char with BL char were tested. Figure 5.2 shows the experimental reactivity as a function of conversion for a mixture of 24 wt% BL char with 76 wt% BB char, and for a 53 wt% BL char with 47 wt% BB char. A similar result is observed for a mixture of 80 wt% BL char with 20 wt% BB char, but is not shown in Figure 5.2 for clarity purpose.

The experimental reactivity for the mixtures is compared with the calculated (or predicted) reactivity for the mixtures assuming no interaction between BB and BL. The calculated conversion and reactivity for the mixture of BB and BL char, assuming non-interacting mixtures, is computed from individual BB char and BL char reactivity as shown by equations 5.3 and 5.4

$$X_{calc} = w_{BB}X_{BB} + (1 - w_{BB})X_{BL} \tag{5.3}$$

$$R_{calc} = \frac{1}{(1-X_i)}\frac{(X_i - X_{i-1})}{(t_i - t_{i-1})} \tag{5.4}$$

where w_{BB} is weight fraction of BB char in mixture, and X_i's is the calculated value from equation 5.3 at every 2 sec time interval.

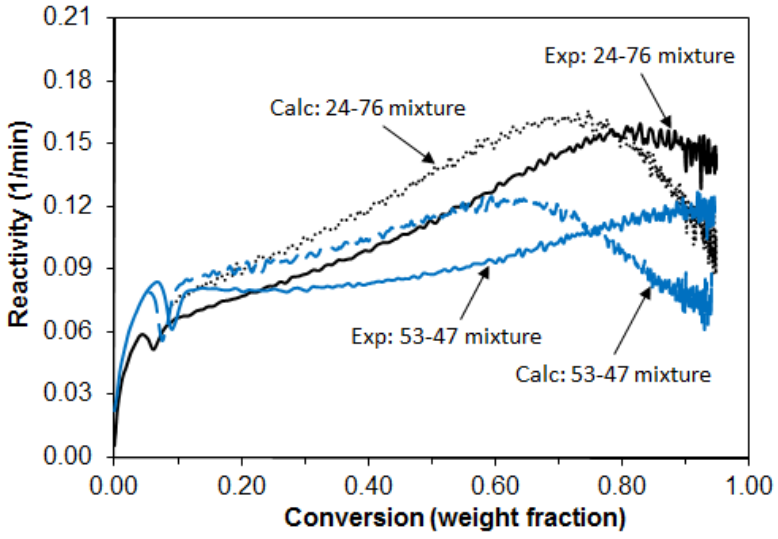

Figure 5.2 Isothermal co-gasification of various mixtures of Brazil bagasse (BB) char and Brazil leaves (BL) char at 800 °C in pure CO_2. Exp and Calc refers to the experimentally measured reactivity and calculated (predicted) reactivity, respectively. The first value in the mixture refers to wt % of BL char, and the second value refers to wt % of BB char in the mixture.

Contrary to the expectation, the experimentally measured reactivity during co-gasification of BB char with BL char showed that the overall reactivity of the mixture is lower than the calculated reactivity (Figure 5.2) for char conversions less than 75% (inhibition effect). For char conversion greater than 75%, the experimental reactivity of the mixture is higher than the predicted reactivity (synergistic effect). Thus a combined synergistic and inhibitive effect is observed during co-gasification. With respect to time for conversion, the time required for less than 75% conversion for co-gasification of mixtures is greater than the predicted time due to the inhibition effect. However, the time for 90 - 95 % conversion for various mixtures during co-gasification is about the same as the predicted time for co-gasification since the initial inhibition effect is overcome by later synergistic effect (see Figure C.1, Appendix C). To quantify the deviation between experimental and predicted reactivity (i.e., the intensity of interaction between two chars), root mean square (RMS) deviation is calculated as shown by equation 5.5

$$RMS\ deviation = \sqrt{\frac{\sum_{i=1}^{N}\left(\frac{R_{exp} - R_{calc}}{R_{calc}}\right)^2}{N}} \tag{5.5}$$

where N is the number of data points.

The RMS deviation calculated for the 24 - 76 mixture, 53 - 47 mixture, and 80 - 20 mixture (with the first value representing wt % of BL char in mixture) are 25%, 36% and 20%, respectively. The next section discusses the reasoning behind the combined inhibitive and synergistic effect.

5.3.3 Explanation of combined synergistic and inhibitive effect

Potassium migration into the amorphous carbon matrix is known to occur in the temperature range of 470-900 K [13]. A similar observation was made by Karimi and

Gray [14] who found that alkali metal compounds migrated in the bitumen coke particles at a temperature of 500 – 600 °C. On the other hand, calcium species did not migrate into the bulk of carbon during heat treatment up to 1123 K [15].

Based on these reports, it is hypothesized that the initial inhibition effect is attributed to the migration of potassium from K-rich BB char to BL char followed by scavenging of some of this K by aluminosilicates in BL char. This lowers the reactivity of BB char in the mixture and thus reduces the overall reactivity for char conversions less than 75%. The final synergistic effect is attributed to the enhancement of the reactivity of remaining BL char by the remaining K from the BB ash. This is shown schematically in Figure 5.3.

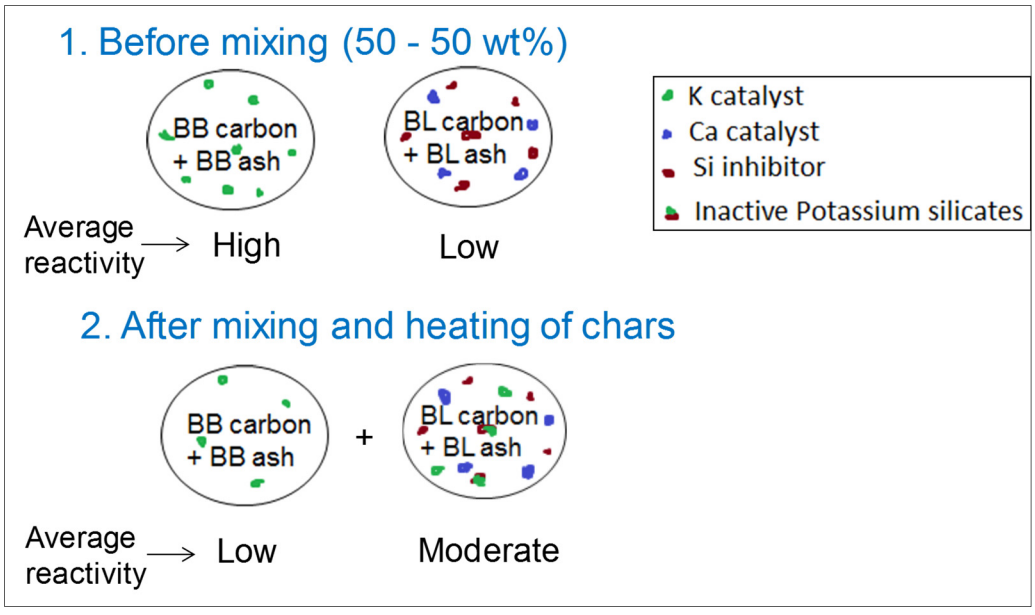

Figure 5.3 Schematic explaining the effect of potassium redistribution during co-gasification on the reactivity of the BB char portion and the BL char portion in the mixture.

After mixing of chars and heating of char, potassium migrates from BB to BL char leading to a reduction in potassium concentration in BB char, and thus a reduction of BB char reactivity in the mixture. In addition, some of the migrated K from BB char is scavenged by Si leading to reduced availability of active potassium in BL char. Thus, there is only a moderate increase in reactivity of BL char portion in the mixture as compared to a large decrease in BB char reactivity in the mixture. This causes an overall decrease in reactivity of the mixture, and thus the inhibitive effect is observed for moderate char conversions. Once nearly all the BB char is converted to BB ash, the remaining active potassium from BB ash catalyzes the reactivity of the remaining BL char, and thus the synergistic effect is observed at high char conversions.

The above hypothesis is tested by performing two sets of experiments as detailed below:

a. *Effect of BL ash on BB char reactivity, and vice-versa:* To test the effect of BL ash on BB char reactivity, different experiments were conducted where the concentration of BL ash in the mixture is varied from 0 wt% (i.e., 100% BB char) to 45 wt% (Figure 5.4a). As expected, the average reactivity (measured as reactivity averaged between 10 - 90% conversion) of BB char is reduced drastically by addition of BL ash. Even though BL ash enhances the reactivity of pure carbon (Avicel char in this study), potassium redistribution from BB char to BL char and scavenging of some of the K by Si causes a large reduction in the reactivity of BB char.

   On the other hand, a small linear increase in BL char reactivity is observed by the addition of BB ash to BL char (Figure 5.4b). The increase is only small since some of the K from BB ash is scavenged by Si present in BB ash as well by Si in BL

char. Thus, the decrease in reactivity of BB char by BL ash is much more drastic as compared to a small increase in reactivity of BL char by BB ash, which explains the overall reduction in reactivity of the mixture of BB char and BL char. This again explains the inhibition effect observed for moderate char conversions The implication of this result for choosing the favorable flow scheme for co-processing BB and BL char is discussed in the next section (5.3.4).

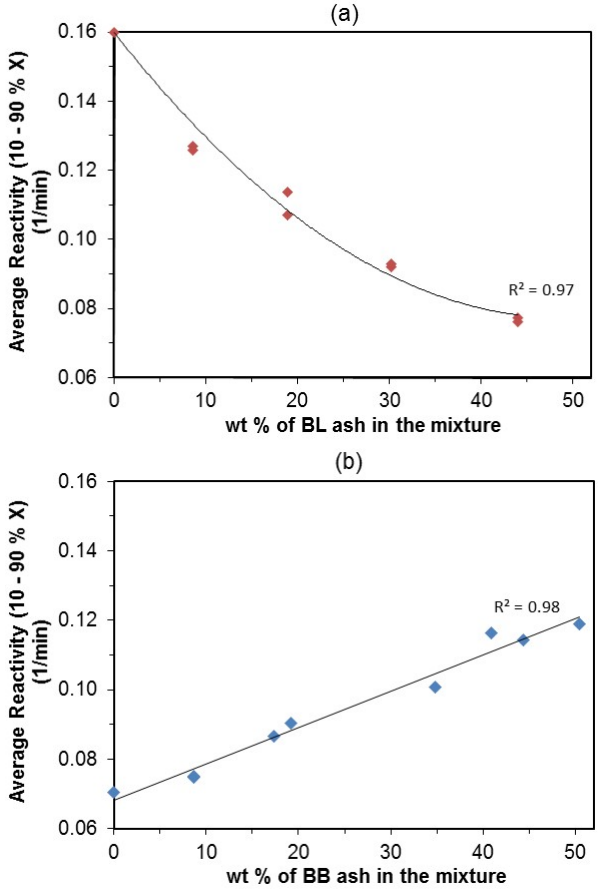

Figure 5.4 Effect of ash addition on the average reactivity of char at 800 °C in pure CO_2. (a) Effect of BL ash addition to BB char, and (b) Effect of BB ash addition to BL char.

b. *Role of potassium redistribution during co-gasification on char reactivity:* To confirm the potassium redistribution between chars, a physical mixture of BB char (LEFR-1000 °C-3s), which is 50% converted in pure CO_2, and Avicel char (PEFR-800 °C-5b-30s) was prepared. The physical mixture was heated at 25 K/min in pure N_2 to 800 °C and then cooled to room temperature to perform SEM - EDX analysis. 50% converted BB char was used because it contains a higher amount of potassium which makes it easier to quantify the potassium migration from BB char to Avicel char. SEM - EDX analysis of pure Avicel char and pure 50% BB char was measured separately (i.e., before physical mixing). This is shown in Table 5.1. Also, SEM – EDX analysis of the Avicel char portion in the mixture (after heating the mixture to 800 °C and cooling to room temperature) was performed to identify the potassium migration from BB char to Avicel char. As shown by Table 5.1, pure Avicel char has negligible potassium. Upon heating the Avicel char with 50% converted BB char, the potassium content of the Avicel char portion in the mixture increased to 1.5 wt%. This is also shown by EDX mapping (Figure 5.5). This confirms that BB char has sufficient active potassium which can migrate during co-gasification. This reduces the potassium concentration of BB char in the mixture which in turn causes a reduction in the reactivity of BB char portion in the mixture. This is also shown by the experimental measurement of the reactivities of mixtures comprised of BB char (LEFR-1000 °C-3s) and Avicel char (PEFR-800 °C-5b-30s) mixed in different proportions as shown in Figure 5.6. Pure Avicel char has negligible reactivity at 800 °C in pure CO_2 due to negligible inorganics. It can be seen from Figure 5.6 that the reactivity of the BB char in the mixture is lower than the predicted reactivity

(assuming no interaction between the components). The increase in reactivity of the Avicel char portion due to potassium migration is small (due to lower surface area of Avicel char and also because Avicel char is generated at higher pressure) compared to the large decrease in reactivity of the BB char (due to potassium migration) leading to the overall reduction in reactivity of the mixture (before complete conversion of BB char). Once nearly all the BB char is converted, the BB ash catalyzes the Avicel char reactivity, and thus the overall reactivity of the mixture (which is mostly remaining Avicel char) is higher than the predicted reactivity.

Table 5.1 SEM - EDX analysis showing potassium redistribution from 50% converted BB char to Avicel char after physical mixing of these two chars (60 - 40 mixture by weight %, respectively) and heating the mixture to 800 °C in N_2

Elements (in wt%)	Pure Avicel char (PEFR- 800 °C-5b-30s)	Pure 50% converted BB char (LEFR- 1000 °C-3s)	Avicel char portion in the mixture after heating to 800 °C
C	87.8	53.6	92.3
O	12.1	28.3	6.2
Si	0.07 ± 0.04	9.0	< 0.1
K	0.03 ± 0.06	4.5	1.5
other[a]	0	4.6	0
Total	100.0	100.0	100.0

[a] other major elements include Na, Mg, Al, P, Ca, Fe and Cl

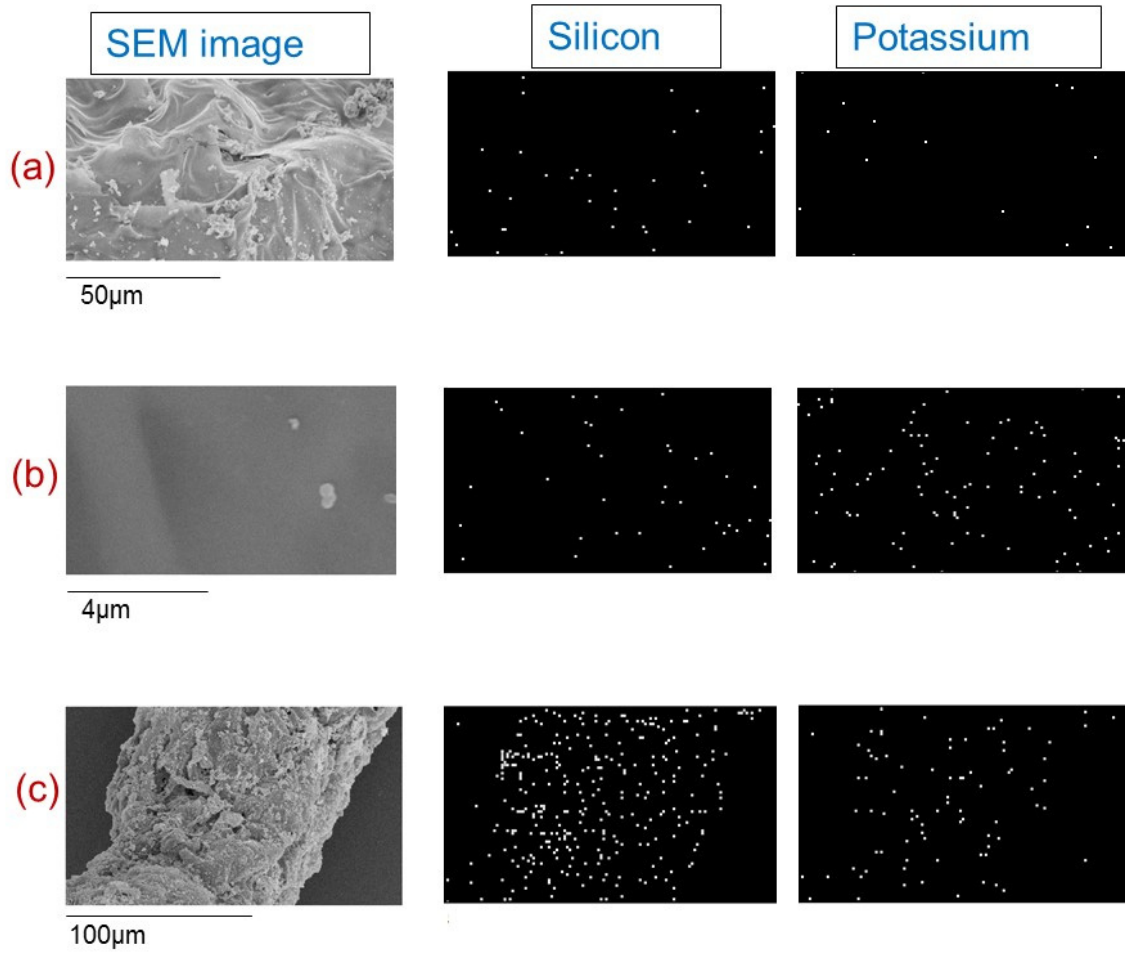

Figure 5.5 EDX mapping of silicon and potassium. (a) Pure Avicel char (PEFR-800 °C - 5 bar - 30 s), (b) Avicel char section in a mixture with 50% converted Brazil bagasse (BB) char (LEFR - 1000 °C - 3s) after heating this mixture to 800 °C in N_2 followed by cooldown in N_2, and (c) 50% converted BB char section in the same mixture (after heating the mixture to 800 °C in N_2 followed by cooldown in N_2). EDX tests was done at 10 KV (for 300 sec). Samples were coated with Au (7 nm Au layer thickness) by sputtering before performing SEM imaging and EDX mapping.

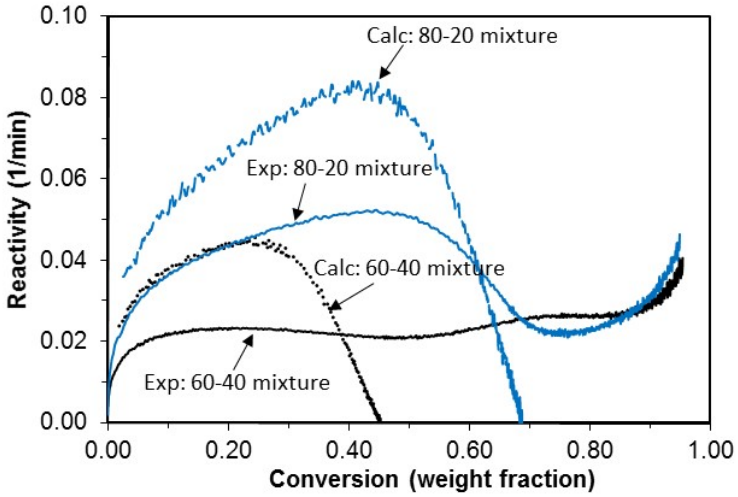

Figure 5.6 Isothermal co-gasification of various mixtures of Brazil bagasse (BB) char (LEFR-1000c-3s) and Avicel char (PEFR-800c-5b-30s) at 800 °C in pure CO_2. Exp and Calc refers to the experimentally measured reactivity and calculated (predicted) reactivity, respectively. The first value in the mixture refers to wt % BB char, and the second value refers to wt% Avicel char in the mixture.

5.3.4 Predicting the relative importance of the inhibitive effect versus the synergistic effect

The initial inhibition effect and a later synergistic effect is also reported in previous studies [2,16]. However, the authors attributed the inhibition effect to a different reason. Ding et al. [16] found that during co-gasification of corn-stalk char with Shenmu bituminous coal char (or with Jincheng anthracite coal char), the experimental conversion results were slightly smaller than the calculated conversion values below the conversion of around 0.55, which indicates the initial inhibition. The authors attributed this effect to the intimate contact of biomass char and coal char (physical effect), which leads to a change in the flow pathway of gasification reactants to the sample, so the gasification rate of Corn stalk char might decrease. However, the authors did not test this explanation. Also, since coal char reactivity was much smaller than corn-stalk char reactivity, the later

synergistic effect (due to ash from corn-stalk catalyzing coal char reactivity) was much more pronounced compared to the initial inhibition effect, thus leading to *overall synergy*.

A similar observation was made by Habibi et al. [2] who found that during co-gasification of switchgrass char with fluid coke char, the observed conversion of the mixture was slightly below the non-interacting predicted conversion (till 50% conversion), suggesting that there may have been some inhibition. Nevertheless, at conversions above 50%, a synergistic effect was observed (since fluid coke reactivity was negligible compared to switchgrass char), thus leading to an *overall synergistic effect*. But the authors did not provide any reason for the initial inhibition. We believe that the above hypothesis proposed in this study explains the initial inhibition observed in both of these two studies.

Unlike the two studies mentioned above where the reactivity differences between the two chars are very high, in our study the two chars used for co-gasification have similar reactivity. This caused the initial inhibition effect to be more pronounced as compared to the later synergistic effect in our study, thus leading to an *overall inhibition* for char conversion less than 75% and an *overall additive* effect for nearly complete (> 90%) char conversion (due to the cancellation of initial inhibitive effect by the later synergistic effect). This thus leads to different conclusions than the two previous studies [2,16] (which showed overall synergy), even though the underlying reasoning is the same. Thus, the relative reactivity and the ash composition of the two feedstocks for co-gasification play a major role in determining whether there is an overall synergistic effect, or overall inhibitive effect, or an additive effect.

If the alkali metal present in the first co-gasification feedstock is scavenged completely by silica present in second co-gasification feedstock, then *only* an inhibitive effect is likely to be observed over the complete conversion range, as is observed in the previous study during co-gasification of switchgrass and sub-bituminous coal [2].

5.3.5 Schematic of favorable flow schemes for sugarcane residue co-processing

Considering the experimental results of pure component (BB and BL char) gasification, co-gasification and the effect of ash on char gasification, four different flow schemes are possible for co-processing of sugarcane residue (Figure 5.7). Assuming that there is enough sugarcane residue available for feeding to a gasifier, co-gasification of sugarcane residue (BB + BL) does not offer any specific advantage over separate gasification. In addition, for char conversion up to 75%, co-gasification will require a bigger reactor size than the separate gasification case due to the inhibitive effect. As shown earlier in Figure 5.4b, addition of BB ash to BL improves BL reactivity. Therefore, a staged feeding scheme where BB char is converted in the first gasifier and ash from BB catalyzes BL char conversion in the second gasifier will offer the smallest reactor size and is the preferred flow scheme for co-processing (Figure 5.7c). In addition, a separate gasifier for processing the two feedstocks will offer operational flexibility as operating conditions can be adjusted independently for the two gasifiers when there are changes in feedstock quality and quantity. On the other hand, staged feeding where BL is converted first in a 1st gasifier and ash from BL catalyzes BB char conversion in a second gasifier will require the biggest reactor size (Figure 5.7d). This is because BL ash reduces

the reactivity of BB char due to potassium migration from BB char as seen from Figure 5.4a.

It should be noted here that the consideration of fixed capital cost of gasifier is only considered here for determining favorable flow schemes. In addition, this co-gasification study is applicable for a gasifier where there is intimate physical contact between the two feedstocks, for instance, a moving bed gasifier.

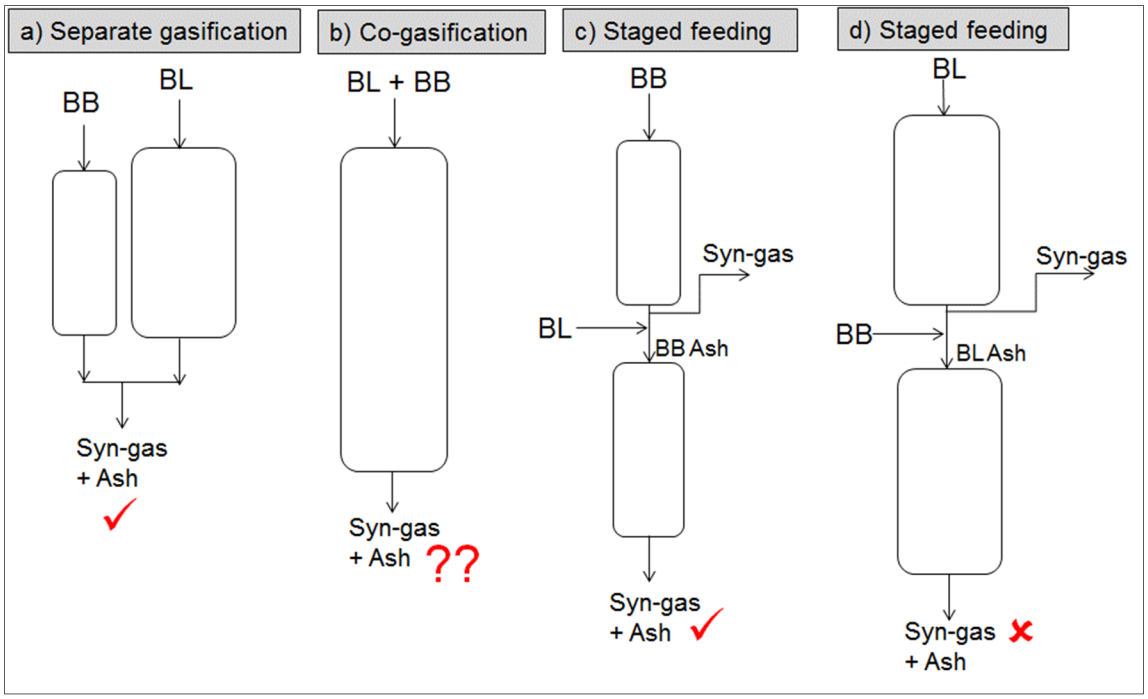

Figure 5.7 Schematic showing the favorable flow schemes for co-processing sugarcane residue

5.4 Conclusions

A combination of inhibitive and synergistic effects was observed during the progress of co-gasification of Brazilian sugarcane residue (BB and BL) in this study. The initial inhibition effect is attributed to the migration of potassium from potassium-rich BB char to BL char followed by the reaction of some of the migrated potassium with silica in SCT char to form inactive potassium aluminosilicates. This inhibition effect caused a reduction in the reactivity of BB char in the mixture which reduced the overall char reactivity of the mixture for char conversion less than 75%. The final synergistic effect is attributed to the ash from fully converted bagasse char catalyzing the reactivity of the remaining SCT char. An *overall* additive effect is observed for nearly complete char conversion during co-gasification due to cancellation of the initial inhibitive effect and the final synergistic effect.

This study showed that for enhancing the char gasification reactivity of the mixture of BB char and BL char, co-gasification does not offer any specific advantage. Staged feeding, where BB is fed first to gasifier 1 and the BB ash from gasifier 1 enhances the reactivity of the BL feed in gasifier 2, would likely result in better performance. This study thus provides a fundamental basis to qualitatively predict whether co-gasification of two different feedstocks would lead to overall synergy, or inhibition, or an additive effect.

5.5 References

[1] Nemanova V, Abedini A, Liliedahl T, Engvall K. Co-gasification of petroleum coke and biomass. Fuel 2014;117:870–5.

[2] Habibi R, Kopyscinski J, Masnadi MS, Lam J, Grace JR, Mims CA., et al. Co-gasification of biomass and non-biomass feedstocks: Synergistic and inhibition effects of switchgrass mixed with sub-bituminous coal and fluid coke during CO_2 gasification. Energy Fuels 2013;27:494–500.

[3] Tchapda A, Pisupati S. A Review of Thermal Co-Conversion of Coal and Biomass/Waste. Energies 2014;7:1098–148.

[4] Lau FS, Bowen DA, Dihu R, Doong S, Hughes EE, Remick R, et al. Techno-economic analysis of hydrogen production by gasification of biomass. Dep Energy Natl Renew Energy Lab, DOE contract no. DE-FC36-01GO11089; 2003.

[5] Joyce J, Dixon T, Diniz da Costa JC. Characterization of Sugar Cane Waste Biomass Derived Chars from Pressurized Gasification. Process Saf Environ Prot 2006;84:429–39.

[6] Pippo WA, Garzone P, Cornacchia G. Agro-industry sugarcane residues disposal: the trends of their conversion into energy carriers in Cuba. Waste Manag 2007;27:869–85.

[7] Iisa K, Lu Y, Salmenoja K. Sulfation of potassium chloride at combustion conditions. Energy Fuels 1999;13:1184–90.

[8] Fjellerup J, Gjernes E, Hansen LK. Pyrolysis and Combustion of Pulverized Wheat Straw in a Pressurized Entrained Flow Reactor. Energy Fuels 1996;10:649–51.

[9] Zhang Y, Hara S, Kajitani S, Ashizawa M. Modeling of catalytic gasification kinetics of coal char and carbon. Fuel 2010;89:152–7.

[10] Kannan MP, Richards GN. Gasification of biomass chars in carbon dioxide: dependence of gasification rate on the indigenous metal content. Fuel 1990;69:747–53.

[11] Zhang Y, Ashizawa M, Kajitani S, Miura K. Proposal of a semi-empirical kinetic model to reconcile with gasification reactivity profiles of biomass chars. Fuel 2008;87:475–81.

[12] Linares-Solano A, Almela-Alarcón M, de Lecea CS-M. CO_2 chemisorption to characterize calcium catalysts in carbon gasification reactions. J Catal 1990;125:401–10.

[13] Matsukata M, Fujikawa T, Kikuchi E, Morita Y. Interaction between potassium carbonate and carbon substrate at subgasification temperatures: Migration of potassium into the carbon matrix. Energy Fuels 1988;2:750–6.

[14] Karimi A, Gray MR. Effectiveness and mobility of catalysts for gasification of bitumen coke. Fuel 2011;90:120–5.

[15] Matsukata M, Fujikawa T, Kikuchi E, Morita Y. Auger electron spectroscopy and electron probe microanalysis observations of barium and calcium loaded on amorphous carbon under gasification conditions. Energy Fuels 1990;4:365–71.

[16] Ding L, Zhang Y, Wang Z, Huang J, Fang Y. Interaction and its induced inhibiting or synergistic effects during co-gasification of coal char and biomass char. Bioresour Technol 2014;173C:11–20.

CHAPTER 6

CHAR GASIFICATION REACTIVITY IN STEAM, CO_2 AND MIXTURES: ROLE OF IN-SITU HYDROGEN PRODUCT INHIBITION

6.1 Background

Gasification is a process which can convert most carbonaceous solids or liquids to syngas. Syngas can be further utilized for heating, industrial process applications, electricity generation, chemical production, and liquid fuels production [1]. Design and operation of biomass gasifiers requires knowledge of the reactivity of the biomass char in a gasification medium of some composition. The most commonly used gasification agents are steam, air, CO_2, and their mixtures. The product species (CO and H_2) may also affect gasification rate.

The choice of reacting gas, CO_2 or steam, is determined by the relative cost and availability of reacting gases as well as the relative reactivity of chars with these reacting gases. The benefit of using CO_2 is that it will lead to recycling of CO_2 stream from industrial processes, and thus reduce the greenhouse gas emissions. Additionally, thermal processing through CO_2 rather than steam avoids the use of large quantities of water [2]. On the other hand, it is commonly accepted that the gasification rate of chars in CO_2 is smaller than in steam [3], thus making steam gasification much more attractive than CO_2 gasification. However, the overall char gasification reactivity in steam is not always higher than CO_2 [4,5]. The relative reactivity ratio of steam to CO_2 depends on the

operating temperature [5] and feedstock properties, specifically the alkali index of char [6]. Thus, it is challenging to choose between steam and CO_2 (or to choose the relative percentage of steam and CO_2 for a mixture) as a gasification medium based on the consideration of maximizing char reactivity. This is because wide variations in properties of different feedstocks and gasifier operating conditions cause a higher or lower reactivity of chars in steam compared to CO_2.

The reactions for gasification of char in CO_2 and steam are as follows:

$$C + CO_2 \rightarrow 2CO \tag{6.1}$$

$$C + H_2O \rightarrow CO + H_2 \tag{6.2}$$

Since hydrogen is generated in-situ during steam gasification, char surfaces are exposed to significant hydrogen levels during steam gasification, even when hydrogen is not present in the initial reactant stream [7]. Huttinger and Merdes [8] showed the blocking of active sites by dissociative chemisorption of H_2 as C(H) with progressive gasification of pure carbon. This significant hydrogenation of the surface reduces the available active sites for the reaction, and so cannot be ignored in circumstances where H_2O is a reactant in high concentrations [7]. Pineda and Chen [7] provides a summary of literature studies with observed hydrogen inhibition.

Since biomass has inherently high active sites due to the catalytic effect of K and Ca present in biomass, the effect of hydrogen inhibition is likely to be severe in steam gasification of biomass chars. In addition, hydrogen inhibition of char gasification is more severe at low and moderate temperatures because the pseudo-activation energy associated with the hydrogen adsorption constant (in the Langmuir-Hinshelwood kinetic equation for steam gasification) is negative, meaning the inhibiting effect of product

hydrogen decreases with increasing temperature [9]. Since a typical fluidized biomass gasifier is likely to operate at moderate temperatures (typically less than about 870 °C to prevent ash-fusion [1]), hydrogen inhibition during steam gasification in a biomass gasifier may be significant. Past studies have shown a decrease in char reactivity with conversion in steam, hydrogen and its mixtures [8,10]. On the other hand, gasification in only CO_2 does not generate hydrogen. This can cause different gasification behavior in steam than in CO_2 for biomass gasification, as will be seen in this study.

The main aim of this study is to understand the fundamental difference in the evolution of the char reactivity profile in pure steam and in pure CO_2 for the gasification of biomass char. A potassium-rich sugarcane bagasse char is used in this study. This study will assist in defining the gasification medium for the design of a gasifier to maximize the overall char gasification reactivity for a K-rich biomass char. Also, it will be shown in this study that for the K-rich bagasse char, the inhibition effect of in-situ generated hydrogen leads to a very different reactivity profile in pure steam than in pure CO_2, and this affects the relative reactivity ratio of steam to CO_2. Thus, the second part of this study is to understand the role of hydrogen inhibition on the evolution of the char reactivity profile. Also, gasification in a mixture of steam and CO_2 will be studied to identify if the reactivity of gas mixtures is additive.

In summary, the specific objectives of this study are: 1. Determine the relative reactivity ratio of steam to CO_2 (both the *initial* and *overall* char gasification reactivity), and to rationalize the observed behavior, 2. Identify the role of hydrogen inhibition, by in-situ generated hydrogen in steam gasification, on the evolution of char reactivity with conversion during steam gasification, 3. Determine if the active sites are the same or

different for steam and CO_2 gasification, and to determine the effect of hydrogen inhibition on these sites, and 4. Find the gasification response for the reaction of char in a mixture of steam and CO_2. The feedstock used in this study is a potassium-rich sugarcane bagasse char which is generated by pyrolysis in a pressurized entrained flow reactor (PEFR) with heating rates of ~10^4 K/s and operated at 800 °C, 5 bar and 33 sec residence time. Char reactivity of pyrolysis char is then studied in an atmospheric pressure thermogravimetric analyzer.

6.2 Experimental Methods

6.2.1 Experimental materials

Sugarcane bagasse from Brazil (BB) was used in this study. Bagasse was dried in an oven at 105 ^{0}C for 6 hours and then ground and sieved to obtain 180-250 μm particles. In addition, Avicel (model cellulose) is also used for a baseline study as it contains negligible inorganic material to catalyze the char gasification reaction. Avicel® PH-101 (50 μm particle size) was purchased from Sigma-Aldrich. The properties of feedstock are shown earlier in Table 3.1.

Nitrogen gas used was ultra-high purity grade (99.999 %). CO_2 gas used was instrument grade (99.99 %). Air used was zero grade (20 - 22 % O_2). Additionally, custom made CO_2 gas containing 3.6 mol% H_2, and custom made N_2 gas containing 3.4 mol% H_2 were used for hydrogen inhibition studies. Ultra-high purity helium (99.999 %) was used for pressurization of the water tank of the steam generation unit. All the gases were supplied by Airgas. De-ionized water was used for steam generation.

6.2.2 Pyrolysis experiments

Pyrolysis of bagasse was performed in a pressurized laminar entrained flow reactor (PEFR) to generate char for further gasification tests. In the PEFR, heating rates as high as $10^3 - 10^4$ °C/s are achieved. Fjellrup et al. [11] explains the flow scheme and operating details of this PEFR. In this study, pyrolysis experiments to generate bagasse chars were performed at 800 °C - 5 bar - 33 sec. Avicel char was generated at 800 °C - 5 bar - 28 sec. A detailed description of the PEFR is presented in Section 2.2.2.

6.2.3 Measurement of char gasification reactivity in steam, CO_2 and mixtures

To measure the gasification reactivity (of chars generated by pyrolysis), isothermal gasification experiments were carried out in an atmospheric thermogravimetric analyzer (TGA) manufactured by Netzsch (STA 449 *F1 Jupiter*®). This TGA is equipped with a water vapor furnace with a maximum operating temperature of 1250 °C, and is suitable for a reactive atmosphere containing up to 100% steam.

The water vapor furnace of the Netzsch TGA is connected to a steam generator unit (by Bronkhorst High-Tech: Direct evaporator series ASTEAM DV2, model DV2MK) by a transfer line which is heated to 180 °C by electrical heat tracing to prevent steam condensation. Steam flow rate was controlled by an electronic liquid mass flow controller for water (by Bronkhorst, type Liqui-Flow). In this edition of the ASTEAM DV2MK, all components of the steam generator unit were installed in a 19” box, including the evaporator unit with a complete water dosing system, filter and Liqui-flow mass flow controller. For faster gas switchover response, a heated steam bypass line was added to stabilize the steam flow before the start of steam injection into the TGA. The

gas switchover response time to reach >95% of the steady state value was 30 sec for this TGA assembly. The mass flow rates of gases to TGA were adjusted by automatic gas mass flow controllers (by Omega) for each gas. Additionally, automatic on-off valves were added on N_2, CO_2 and steam lines for gas switching. The flow scheme for the gasification set-up is shown schematically in Figure 6.1. To ensure there was no external mass transfer resistance, the sample mass was varied in the gasification experiments until no change in reactivity was observed by further reducing the sample mass. To avoid internal mass transfer resistance, crushed char particles were used.

About 10 mg of sample was used in each run. In each experiment, the sample was kept on a 17 mm diameter flat-pan alumina sample holder. The TGA furnace was first evacuated and purged with N_2 three times to obtain an air-free atmosphere. Then the sample was heated to 150 °C and held there for 1 hour to stabilize weight and to purge out any traces of oxygen. Then the sample was heated to the desired gasification temperature in N_2 (flowing at 200 standard ml/min) at 20 K/min and held there for 30 minutes to stabilize the sample mass. Then, the gas flow was switched to a reactive gas like CO_2, steam or a mixture of CO_2/steam/H_2 (flowing at 200 standard ml/min) to start gasification. At the end of the run, completion of gasification was confirmed by injection of air for 20 minutes at the same gasification temperature. Product gas leaves the TGA via a heated line maintained at 160 °C to prevent steam condensation. The weight loss of the char sample was recorded continuously (every 3 s) as a function of gasification time till completion of char conversion. For slow reacting chars, data smoothening was done by taking a moving average (1 min) in such a manner so that the original curve is not affected. Repeatability between the runs was good with a deviation of less than 5 %.

The carbon conversion (X) and reactivity (R) are defined as:

$$X = \frac{(m_o - m_t)}{(m_o - m_{ash})} \tag{6.3}$$

$$R = \frac{-1}{(m_t - m_{ash})} \frac{dm}{dt} \tag{6.4}$$

where m_o represents the initial mass of the char at the onset of gasification, m_t is the instantaneous mass of the char at any time t, m_{ash} is the remaining mass of ash after completion of gasification, and dm/dt is rate of mass loss.

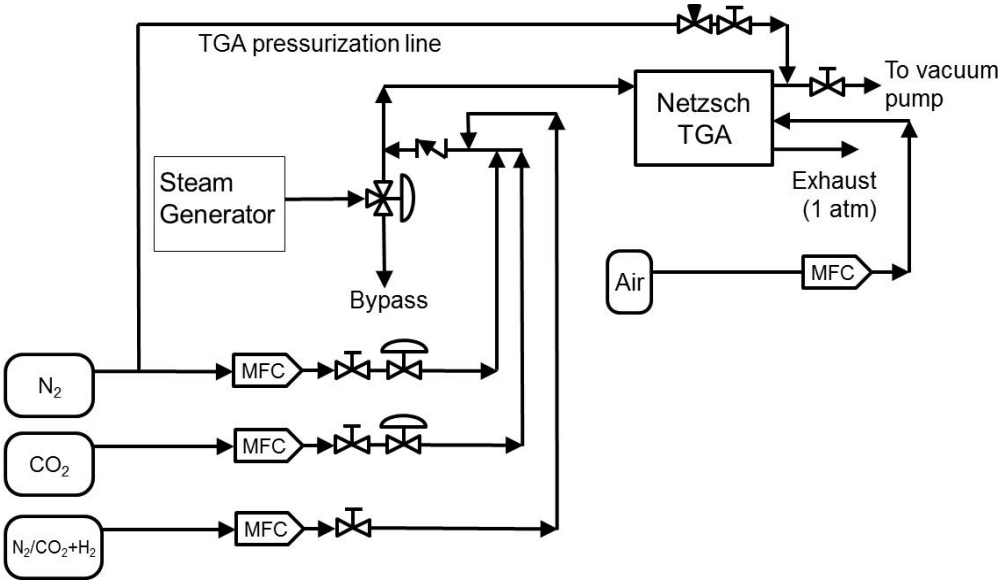

Figure 6.1 Schematic of char gasification set-up (MFC: mass flow controller; TGA: Thermogravimetric analyzer).

6.3 Results and Discussion

6.3.1 Evolution of char reactivity profile in steam and in CO_2

It is known that the relative gasification reactivity of char in steam can be an order of magnitude higher than in CO_2 when the alkali index of char is low (or for uncatalyzed

char gasification) [6]. Zhang et al. [6] has shown that the relative reactivity ratio of anthracite chars in steam to CO_2 is between 7 to 15, which is much higher than that of lignite and bituminous coal (about 2-5). In this study, Avicel char represents an uncatalyzed char gasification case which is analogous to anthracite char gasification, while the gasification of bagasse char (a K-rich biomass char) represents a catalyzed gasification case which is analogous to lignite char gasification. Therefore, one would expect similar range of relative reactivity ratios as observed in earlier studies.

Gasification of Avicel char (generated by pyrolysis in the PEFR at 800 °C - 5 bar - 28 sec) was performed at 800 °C in 100% CO_2 and 100% steam. As expected, it was found that the initial reactivity in steam is about 10 times the reactivity in CO_2, with the CO_2 reactivity being negligible (0.001 min^{-1}) (see Figure D.1 of Appendix D). On the other hand, for the case of bagasse char gasification at 800 °C, the reactivity profile in 100% steam is different than in 100% CO_2. As seen from Figure 6.2, the initial char reactivity in steam is about 2.4 times the reactivity in CO_2 which is expected for catalyzed gasification. However, the overall char reactivity, as measured by the time required for 90% conversion, is higher in CO_2 than in steam. Also, it is interesting to see the evolution of the bagasse char reactivity profile shown in Figure 6.2. There is an enhancement in char reactivity with conversion in CO_2, while there is retardation in char reactivity with conversion in steam. A similar trend was observed for gasification at 800 °C in 50% steam (50% N_2) and 50% CO_2 (50% N_2). Also, a similar trend was observed for gasification at 900 °C in 100% steam and 100% CO_2. This makes the overall char reactivity in CO_2 higher than in steam, making pure CO_2 a more attractive gasification medium than pure steam. This means that higher gasification reactivity in steam

compared to CO_2 is not universal, and it depends on the biomass type and the gasification conditions. Thus it is important to understand the fundamental reason for differences in char reactivity evolution in steam and in CO_2.

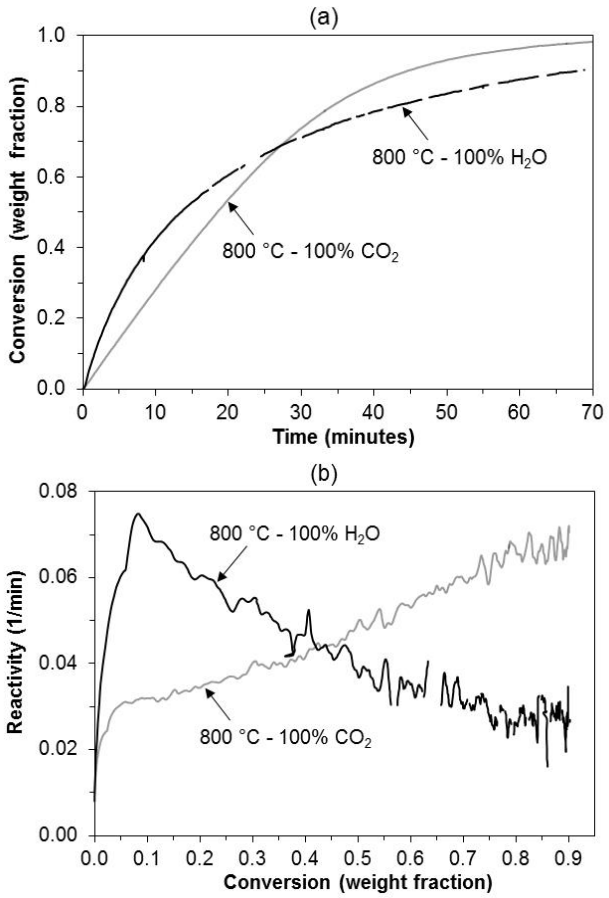

Figure 6.2 Evolution of reactivity profile of Brazilian bagasse char in 100% steam and in 100% CO_2 at 800 °C. (a) Conversion vs. time plot, and (b) reactivity vs. conversion plot.

It is known that CO_2 gasification reactivity increases with conversion for a K-rich biomass. This is because of the increase in the K/C ratio as char conversion increases. This increases the char active surface area, and thus CO_2 gasification reactivity of the

char with increasing conversion [12]. A similar result is also seen for CO_2 gasification of Brazilian bagasse in our earlier study for Brazil bagasse char (Chapter 3, Section 3.3.3). However, there is limited understanding of the evolution of char gasification reactivity in steam. The role of hydrogen, evolved during steam gasification but not during CO_2 gasification, has important implications for the evolution of char reactivity profile in steam, as will be seen in the next sections. Past studies have shown that the decrease in reactivity with conversion in steam, hydrogen and its mixtures is due to irreversible adsorption of hydrogen on carbon which blocks active sites [8,10]. The reactivity trend in this study suggests blockage of active sites on contact with steam due to *in-situ* generated H_2. Thus, to get a fundamental understanding of the differences in evolution of char reactivity in steam compared to CO_2, gas switchover experiments (Section 6.3.2) were conducted where char gasification was performed to intermediate conversion with the first gasification medium, and then the gas is changed over to another gasification medium. Also, hydrogen inhibition studies (Section 6.3.4) were performed to test the effect of hydrogen pretreatment of char on the subsequent char reactivity. The effect of hydrogen inhibition is also likely to affect the gasification when a gas mixture containing both steam and CO_2 is utilized (as is common in industrial gasifiers), and this is experimentally tested in Section 6.3.5.

6.3.2 Understanding the evolution of char reactivity profile by gas switchover experiments

Figures 6.3a and 6.3b show the effect of gas switchover gasification experiments on the evolution of the bagasse char reactivity profile at 800 °C. Plots of 100% steam and

100% CO_2 at 800 °C are shown in these figures for comparison. For Figure 6.3a, the initial char gasification until X = 32% was performed in 100% steam for 7 min, then the gas was switched over to 100% CO_2 for converting the remaining char. The following observations can be made from switchover experiment shown in Figure 6.3a: (a) Char exposure to steam reduces its subsequent initial reactivity in CO_2. This indicates a reduction in active sites for CO_2 gasification due to contact with steam. (b) Further reactivity in CO_2, however, increases with conversion even after steam exposure. Also, the increase in the reactivity in CO_2 with conversion for the switchover experiment is at a much faster rate compared to the 100% CO_2 run. This indicates that CO_2 gasification creates new active sites and also recovers the active sites which were blocked during steam gasification as will be seen later in Section 6.3.3.

For Figure 6.3b, the initial char gasification until X = 34% was performed in 100% steam for 7 min, then the gas was switched over to 100% CO_2 for 19 min for further converting the char until X = 65%. Finally, the gas was switched back to 100% steam for the remainder of the char conversion. In addition to the observations made from Figure 6.3a, there are two more important observations from Figure 6.3b. It shows that char exposure to CO_2 (after steam exposure) increases its subsequent *initial* reactivity in steam. This again suggests that CO_2 gasification recovers the active sites which were blocked during the prior steam gasification, and this causes an increase in the subsequent *initial* steam gasification reactivity at X = 65 to 70%. However, as expected, further gasification in steam decreases the char reactivity. This again suggests that the reactivity drop in steam is not due to drastic changes in char carbon structure.

This trend is repeatable when the gas switchover experiments are performed multiple times over the char conversion range, as shown in Figure 6.4. To get further insights into these results, the mechanism of char gasification reaction in the presence of CO_2, steam and hydrogen is discussed in the next section (6.3.3). Also, the hypothesis of hydrogen inhibition on reactivity evolution in steam is tested experimentally in Section 6.3.4

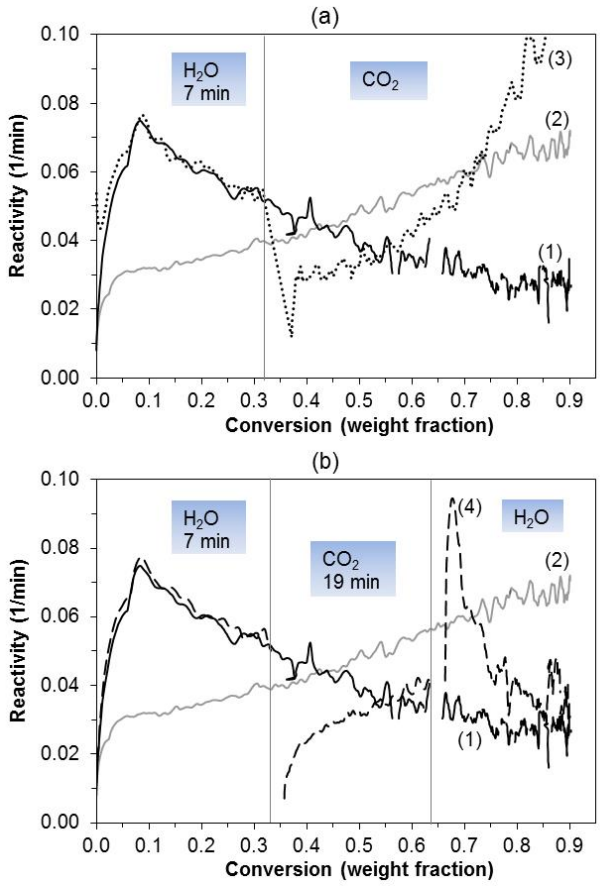

Figure 6.3 Understanding the evolution of gasification reactivity profile of Brazilian bagasse char by gas switchover experiments at 800 °C. (a) Gas switchover from 100% steam (for 7 min) to 100% CO_2, and (b) Gas switchover from 100% steam (for 7 min) to 100% CO_2 (for 19 min), and then to 100% steam. Designations for curves 1 to 4 are: (1) 100% steam; (2) 100% CO_2; (3) and (4) represents gas switchover experiments.

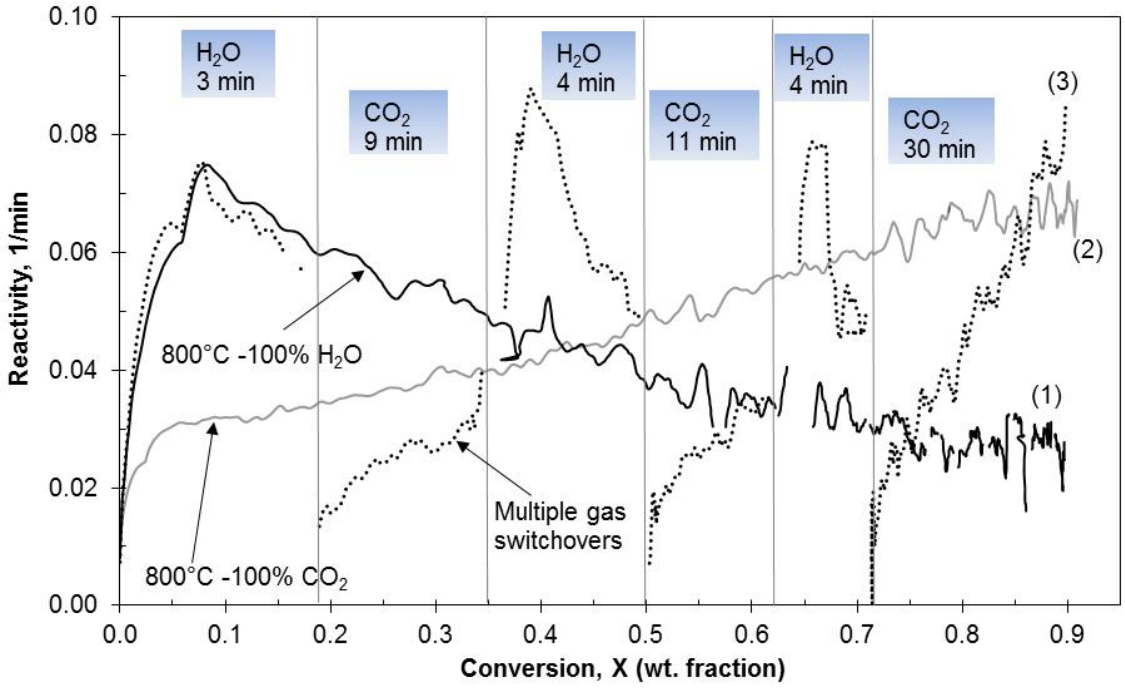

Figure 6.4 Understanding the evolution of gasification reactivity profile of Brazilian bagasse char by multiple gas switchover experiments at 800 °C. Both steam and CO_2 used in the switchover experiment are 100%. Gases used during different char conversion stage for gas switchover experiment are shown in highlighted boxes along with the gas exposure time. Designations for curves 1 to 3 are: (1) 100% steam, (2) 100% CO_2, and (3) gas switchover experiment.

6.3.3 Insights into the evolution of the char reactivity profile by understanding the gasification reaction mechanism

It has been shown that during steam gasification reaction of char, steam decomposes at high temperature on vacant active sites (C_f) to initially form an adsorbed hydrogen atom, C(H), and an adsorbed hydroxyl radical, C(OH). This is followed by the transfer of hydrogen atom from the adsorbed hydroxyl to another vacant site to form adsorbed C(O) and C(H) [13,14]. C(O) then reacts with edge carbon of char (C_b) to form gas phase CO and vacant site (C_f). Gasification in steam is shown by reactions 6.6, 6.7 and 6.8. Gasification reaction in pure CO_2 is shown by reactions 6.5 and 6.7 [15]. Here,

the vacant active sites, C_f, is likely to be the potassium clusters anchored to the carbon by phenolate group, as explained earlier in Section 3.3.3 and in Appendix A.

Hydrogen is known to be a strong inhibitor of the C - H_2O reaction [13]. Hydrogen, even at very low partial pressures, also inhibits the C - CO_2 reaction due to dissociative chemisorption of hydrogen on active sites (reaction 6.9) [16]. Dissociative adsorption is the observed mode of inhibition when quantities of hydrogen are limited (reaction 6.9), and reverse oxygen exchange (reaction 6.10) dictates rate dependence on hydrogen at elevated pressures where the char surface is essentially saturated in hydrogen by reaction 6.9 [17]. It is well known that dissociatively adsorbed hydrogen on the carbon surfaces requires temperatures approaching 1800 K to completely desorb [17,18].

$$CO_2 + C_f \leftrightarrow C(O) + CO \ (CO_2: oxygen\ exchange) \quad (6.5)$$

$$H_2O + 3C_f \leftrightarrow C(O) + 2C(H) \ (steam: oxygen\ exchange,\ H_2\ inhibition) \quad (6.6)$$

$$C(O) + C_b \rightarrow C_f + CO \ (carbon\ gasification) \quad (6.7)$$

$$2C(H) \rightarrow 2C_f + H_2 \ (hydrogen\ production) \quad (6.8)$$

$$H_2 + 2C_f \rightarrow 2C(H) (hydrogen\ inhibition: dissociative\ adsorption) \quad (6.9)$$

$$H_2 + C(O) \leftrightarrow C_f + H_2O \ (hydrogen\ inhibition) \quad (6.10)$$

In light of the above reactions, it can be seen that during pure CO_2 gasification of bagasse char, new active sites created during the progress of char gasification are not blocked by hydrogen, C(H), since there is no hydrogen generation in pure CO_2 gasification. However, in pure steam gasification (without any external hydrogen addition), the hydrogen formed in-situ during the reaction inhibits the reaction by occupying active sites as C(H), as shown by equation 6.6. Also, at higher hydrogen

partial pressure, hydrogen inhibits the reaction by reverse oxygen exchange reaction (reaction 6.10). When partially steam gasified char is further gasified in CO_2, then the subsequent *initial* CO_2 reactivity is reduced as compared to a char which is gasified in pure CO_2 from the start (Figure 6.3 and 6.4). This is likely because of hydrogen formed during steam gasification is strongly adsorbed as C(H) which reduces the active site for CO_2 gasification initially. However, as the char conversion in CO_2 progresses further, the gasification reactivity increases in CO_2 and it increases at a much faster rate, as shown by the slope of switchover gasification curve 3 of Figure 6.3a. This is because CO_2 gasification generates C(O) (reaction 6.5), and it reacts with C(H) (from prior steam gasification) to regenerate some of the blocked sites (as C(H)), as shown by the reverse of reaction 6.6. This also explains the subsequent higher *initial* steam reactivity at about X = 70% (curve 4 of Figure 6.3b) as compared to a char which is gasified in pure steam from the start. However, as the steam gasification progresses further, the reactivity again drops, as expected, due to the formation of in-situ surface hydrogen, C(H). This suggests that hydrogen inhibition is likely responsible for blocking the active sites during the progress of steam gasification and thus decreases char reactivity.

The role of hydrogen inhibition on reducing the char reactivity in steam is further tested experimentally in the next section (6.3.4). This is done by partially gasifying the bagasse char to some intermediate conversion level (e.g., 25% and 50%) in an atmosphere containing no hydrogen (100% CO_2 – "No hydrogen pretreatment case") and small added hydrogen (96.4% CO_2 + 3.6% H_2: "Hydrogen pretreatment case"), and then seeing the effect of hydrogen pretreatment and no hydrogen pretreatment on the subsequent initial reactivity in steam.

6.3.4 Testing the role of hydrogen inhibition on the evolution of steam gasification reactivity profile

To test the case of no hydrogen pretreatment on the initial char reactivity in steam, bagasse char was partially gasified at 800 °C to different intermediate conversion levels (e.g., 20% and 50%) in 100% CO_2 (i.e., no hydrogen). Then the char *initial* reactivity in steam was measured by switching the gas from 100% CO_2 to 100% steam. Results, as shown in Figure 6.5a, show that the *initial* reactivity in steam after CO_2 pretreatment is much higher as compared to the char reactivity in steam when the char is gasified in steam from the start. Also, the ratio of *initial* steam reactivity (for the intermediate CO_2 converted chars) to the CO_2 gasification reactivity at each of the char conversion level is about 2.4. Thus, the *initial* steam reactivity curve (for no hydrogen inhibition case- shown by the dotted line with an arrow) follows the CO_2 reactivity (curve 2), with steam being more reactive than CO_2 by a factor of 2.4. This indicates that the same active sites are likely responsible for steam and CO_2 gasification. For the same active sites, it is known that steam has higher reactivity than CO_2 because the gasification of chars in CO_2 and steam involves essentially the same pathway and intermediates, which is an oxygen transfer step (reaction 6.5 and 6.6) followed by a carbon gasification step (reaction 6.7), and since the structure of C(O) is consistent for both gasification media, the dissociation of steam or CO_2 is the governing step affecting the relative reactivity of steam to CO_2 [19]. And since the hydrogen bond of the water molecule is weaker than the carbon–oxygen double bond of the CO_2 molecule, it is easier to dissociate steam and form carbon–oxygen complexes [5,19,20].

However, as explained earlier, active sites are blocked by in-situ hydrogen product inhibition as steam gasification progresses. Therefore, to test the case of hydrogen pretreatment on the initial char reactivity in steam, bagasse char was partially gasified at 800 °C to different intermediate conversion levels (e.g., 25% and 50%) in an atmosphere containing a small percentage of hydrogen (96.4% CO_2 + 3.6% H_2). Then the char *initial* reactivity in steam was measured by switching the gas to 100% steam. Results, as shown in Figure 6.5b, show that the *initial* reactivity in steam after hydrogen pretreatment is similar to the char reactivity in steam when the char is gasified in steam from the start, and is much lower than the initial char reactivity in steam when the char was pretreated without hydrogen in 100% CO_2. For instance, at X= 50%, there is 45% drop in initial steam reactivity for the case of hydrogen pretreatment as compared to the no hydrogen pretreatment case, as shown in Figure 6.5b. This indicates that the hydrogen is blocking the active sites (by dissociative chemisorption), and thus the subsequent initial steam reactivity is reduced. A similar effect is also seen when the char was initially gasified in 100% CO_2 until X = 50% and then the char was exposed to 3.4% H_2 (rest N_2) for 15 min for hydrogen pretreatment. The subsequent initial steam reactivity was found to be reduced by about 37% after this pretreatment as compared to the initial steam reactivity when char was pretreated without hydrogen in 100% CO_2. Also, for a 20% gasified char in CO_2, the amount of CO_2 chemisorbed on this char (see Section 3.2.5 for CO_2 chemisorption procedure) was reduced after hydrogen treatment of the char (see Figure D.2 of Appendix D). This suggest that the number of potassium active sites, which are responsible for steam or CO_2 gasification in this study, is likely reduced by strong adsorption of hydrogen on active sites.

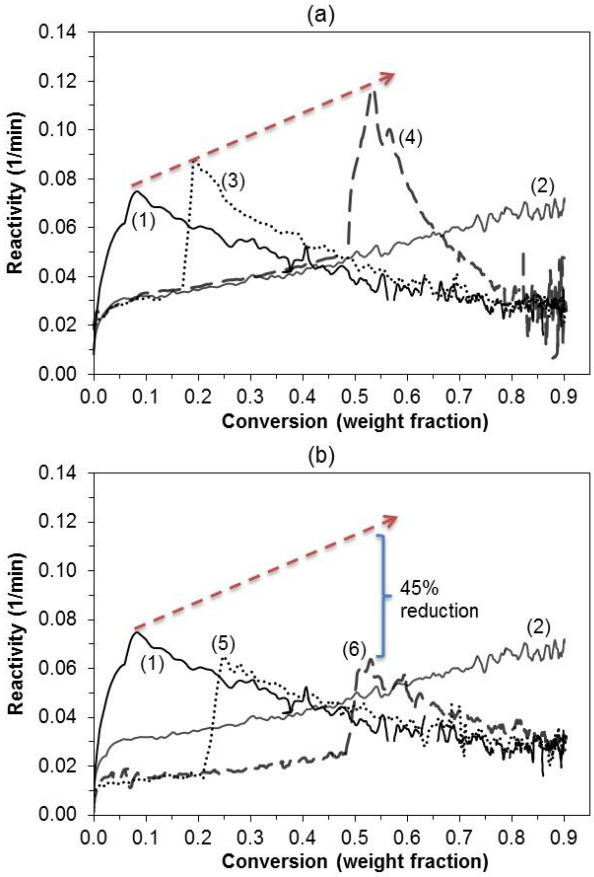

Figure 6.5 Brazilian bagasse char gasification at 800 °C. (a) No hydrogen pretreatment case, and (b) Hydrogen pretreatment case. Designation for curves 1 to 6 are: (1) 100% steam; (2) 100% CO_2; (3) switchover from 100% CO_2 (till X = 20%) to 100% steam; (4) switchover from 100% CO_2 (till X = 50%) to 100% steam; (5) switchover from gas containing 96.5% CO_2 with 3.5% H_2 (till X = 25%) to 100% steam; and (6) switchover from gas containing 96.5% CO_2 with 3.5% H_2 (till X = 50%) to 100% steam.

6.3.5 Reaction of char with CO_2 - steam mixtures

Experimental measurement of char reactivity in steam - CO_2 mixtures is of practical interest as it is important to identify if the reactivity measured separately in steam and in CO_2 can be added to get the reactivity in a mixture ("additive effect"). Guizani et al. [21] summarizes the past literature studies for gasification in a mixture of steam and CO_2 for coal and biomass char gasification, and they show that all three types

of effects are observed during mixed atmosphere gasification: a. Additive effect, where gases react on separate active sites; b. Competitive effect, where steam and CO_2 react on the same active sites (sharing of active sites) causing char reactivity in the mixed atmosphere gasification to be lower than the additive effect; and c. Synergistic effect, where there is synergy between gases causing char reactivity in the mixed atmosphere gasification to be higher than the additive effect.

It has been shown earlier in Section 6.3.4 that both steam and CO_2 are likely to react on the same active sites (sharing of active sites) causing competition between these gases for active sites. In addition, it has been shown that hydrogen evolved during steam gasification also inhibits the CO_2 gasification reaction. Based on this reasoning, it is expected that the char reactivity in a mixed atmosphere gasification would be lower than the additive effect. This is evident even from the experimental data of Figure 6.6a and 6.6b. Mixed atmosphere gasification for bagasse char at 800 °C is shown in Figure 6.6a and 6.6b for 50% steam – 50% CO_2 mixture and 50% steam- 15% CO_2 (rest N_2) mixture, respectively. The experimental measured reactivity for mixed atmosphere is lower than the predicted reactivity (calculated by assuming additive effect). Also, the mixed atmosphere reactivity is only about 10-15% higher than the equivalent steam reactivity for 50% steam – 50% CO_2 mixture. These results show that prediction of reactivity for gas mixtures ($H_2O/CO_2/N_2$) could not be obtained by the additive effect. Mixed atmosphere gasification reactivity should be measured experimentally by conducting experiments with different $H_2O/CO_2/N_2$ mixtures. A similar conclusion was reached by Barrio [22].

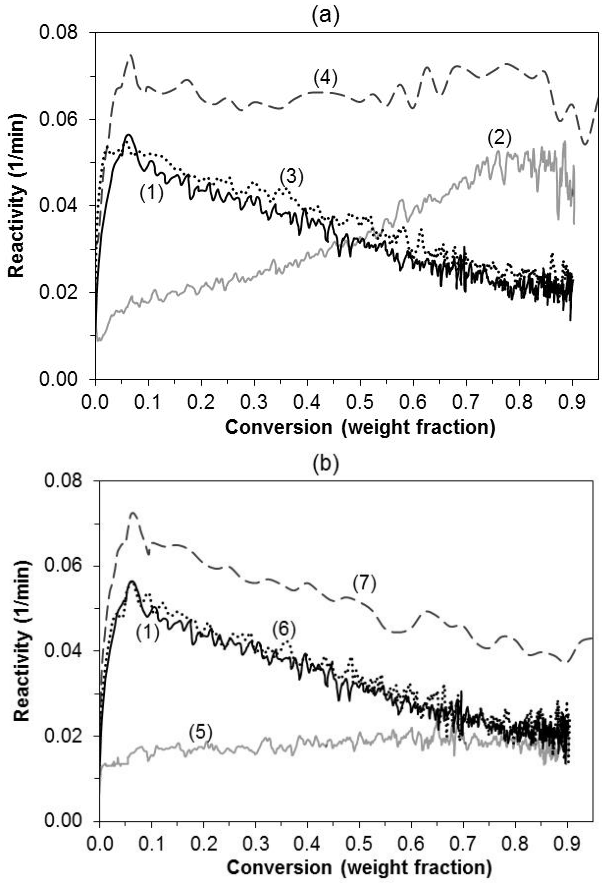

Figure 6.6 Mixed atmosphere gasification of Brazilian bagasse char at 800 °C for (a) 50% steam – 50% CO_2 mixture, and (b) 50% steam – 15% CO_2 mixture (rest N_2). Designation for curves 1 to 7 are: (1) 50% steam; (2) 50% CO_2; (3) experimental reactivity of 50% steam – 50% CO_2 mixture; (4) predicted reactivity of 50% steam – 50% CO_2 mixture; (5) 15% CO_2 (rest N_2); (6) experimental reactivity of 50% steam – 15% CO_2 mixture (rest N_2); and (7) predicted reactivity of 50% steam – 15% CO_2 mixture (rest N_2).

6.3.6 Effect of temperature on the steam gasification reactivity profile

As mentioned earlier, hydrogen is dissociatively chemisorbed on the carbon surface. The adsorbed hydrogen desorbs from the carbon surface in the temperature range of approximately 800 to 1350 °C [17]. Thus, it is expected that the inhibiting effect of adsorbed hydrogen on the char gasification reactivity in steam (due to in-situ hydrogen) is likely to be reduced at higher gasification temperature. This is tested experimentally by

performing gasification of Brazilian bagasse char in pure steam at three different temperatures: 800, 900, and 1050 °C. It is likely that char gasification reaction kinetics in pure steam at 1050 °C is not intrinsic due to mass transfer limitations at higher gasification temperatures.

Figure 6.7 shows that at a lower gasification temperature of 800 °C, char reactivity decreases as the char conversion progresses. At moderate gasification temperature of 900 °C, char reactivity remains nearly constant as the char conversion progresses. However, at high gasification temperature of 1050 °C, char reactivity increases as the char conversion progresses. This profile is typical of a potassium catalyzed char gasification in the absence of significant hydrogen inhibition. This result suggests that the effect of in-situ hydrogen inhibition on the char gasification reactivity in steam is reduced at higher gasification temperatures.

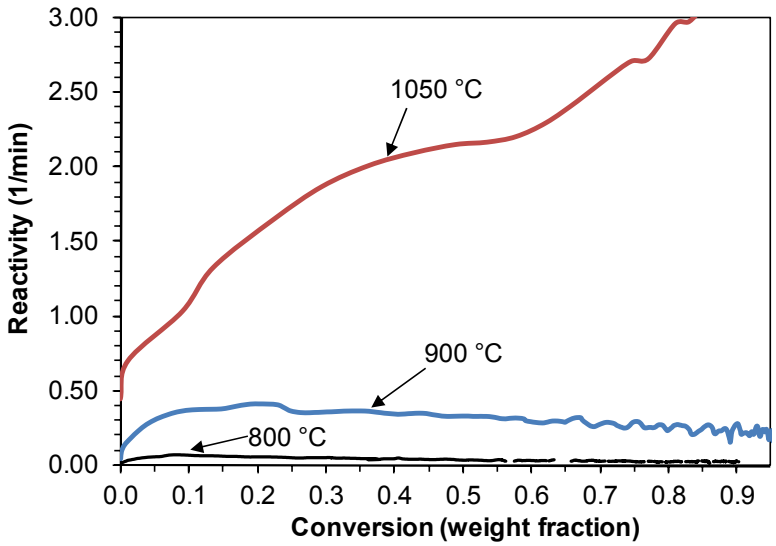

Figure 6.7 Evolution of reactivity profile of Brazilian bagasse char in 100% steam at different gasification temperatures

6.3.7 Effect of char oxidation on the steam gasification reactivity profile

Zhang et al. [23] has shown that low temperature oxidation of char (which is first partially gasified in hydrogen) enhances the subsequent hydrogasification reactivity of the char. They found that oxygen removes some amount, but not all, of the adsorbed hydrogen from the carbon surface at an oxidation temperature of 730 to 750 K [23]. This removal of adsorbed hydrogen from the surface by char oxidation led to an increase in the subsequent hydrogasification reactivity of the char [23].

In this study, char oxidation is performed at 390 °C for 10 min, after partial gasification of the char (until X= 40%) in pure steam at 800 °C, to verify if the low temperature char oxidation leads to an increase in the subsequent steam reactivity at 800 °C (Figure 6.8). In this experiment, char was cooled (from 800 to 390 °C) and heated (from 390 to 800 °C) in pure N_2 at a heating rate of 20 K/min. Results from this experiment, as shown in Figure 6.8, show that char oxidation leads to an enhancement in the subsequent initial steam reactivity. This again suggests that low temperature char oxidation regenerates some of the active sites that were blocked by adsorbed hydrogen. This causes an increase in the initial steam reactivity after char oxidation. However, as the char conversion progresses further in steam, the reactivity decreases due to in-situ hydrogen generation.

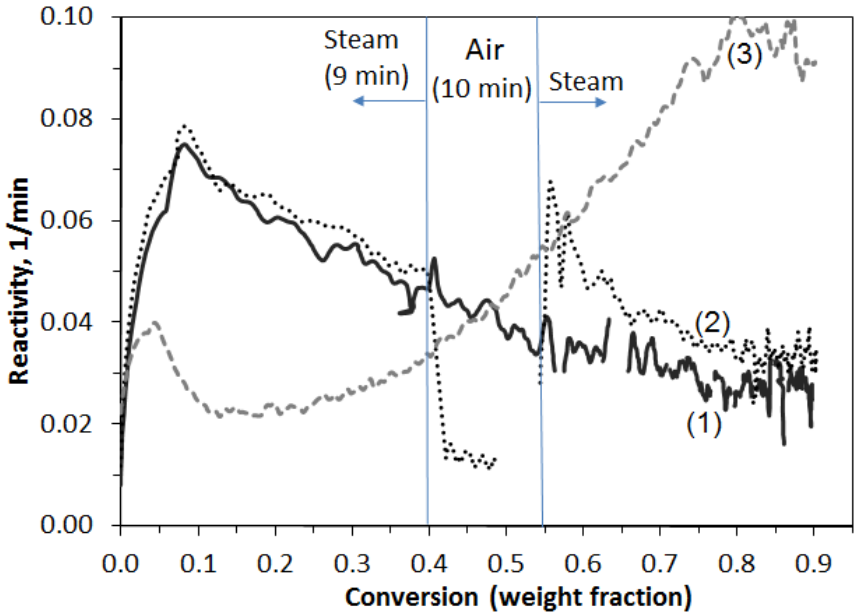

Figure 6.8 Effect of char oxidation (at 390 °C) on the subsequent gasification reactivity profile of Brazilian bagasse char in steam. Designations for curves 1 to 3 are: (1) 100% steam at 800 °C; (2) represent the gas switchover experiment. Gas switchover is done from 100% steam at 800 °C (for 9 min) to Air (for 10 min) at 390 °C, and then again to 100% steam at 800 °C; and (3) Char oxidation in air at 390 °C

To summarize, in this study the gasification of K-rich Brazilian bagasse char, which was generated by pyrolysis in the PEFR, showed a higher *initial* reactivity in steam compared to CO_2, and a lower *overall* reactivity in steam compared to CO_2 due to in-situ hydrogen product inhibition in steam gasification. However, this result is not universal for all biomass or coal chars, and at all gasification temperatures. At high gasification temperature, hydrogen desorbs causing reduced or no inhibition. Also, for uncatalyzed char gasification, CO_2 gasification reactivity at 800 °C is negligible compared to initial steam reactivity (order of magnitude difference). Thus, even with hydrogen inhibition in steam, it is likely that overall reactivity in steam will be still much more than the overall reactivity in CO_2. In addition, calcium catalyzed gasification (for

e.g., many biomass and coal char) is likely to behave differently in steam and in CO_2 than the present study. This is because it is known that calcium does not sinter in steam gasification with conversion, while calcium sinters in CO_2 gasification due to formation of calcium carbonate [24]. This additional parameter will thus also play a role in determining the overall reactivity in steam compared to CO_2 for a calcium rich char, or for a char containing both potassium and calcium. Thus future work should also focus on the above aspects. Also, the role of surface area evolution during steam gasification and the role of concentration of alkali metals on the observed trend should also be evaluated in future. Finally, more fundamental studies are required in future to understand how the active sites for K and Ca catalyzed gasification are blocked by in-situ hydrogen product formation and the type of surface species which are formed during hydrogen inhibition of these active sites.

6.4 Conclusions

This study provided a fundamental understanding of the differences in the evolution of the char reactivity profile in pure steam and in pure CO_2 due to *in-situ* hydrogen product inhibition during the gasification of potassium-rich sugarcane bagasse char. Following are the key conclusions that can be made from this study:

a) The evolution of char gasification reactivity with conversion is different in steam as compared to CO_2. The *initial* char gasification reactivity in steam is higher than in CO_2 (about 2.4 times), as is also observed in the literature. However, the *overall*

reactivity (as defined by time for 90% char conversion) is higher in CO_2 than in steam, thus making CO_2 as an attractive gasification agent compared to steam.

b) The active sites for steam and CO_2 gasification are likely to be the same for a potassium-rich char. The *initial* reactivity ratio in steam to CO_2 is the same for different intermediate conversion level chars, with steam being more reactive than CO_2 by 2.4 times. However, as the char gasification progresses in pure steam, the active sites are likely to be blocked by *in-situ* hydrogen product, which does not happen in pure CO_2 gasification. On the contrary, there is an enhancement in char reactivity with increasing conversion in CO_2 due to the increasing amount of K/C, thus creating more active sites. This explains why the *overall* reactivity in steam is lower than in CO_2.

c) Hydrogen pretreatment of partially gasified char (in CO_2) reduces its subsequent initial gasification reactivity in steam. This again indicates the inhibiting effect of hydrogen on steam gasification reactivity.

d) Gasification of bagasse char in a mixture of steam and CO_2 is not an additive effect. Therefore, mixed atmosphere gasification reactivity should be measured experimentally by conducting experiments with different $H_2O/CO_2/N_2$ mixtures.

6.5 References

[1] Stevens C, Brown RC. Thermochemical processing of biomass: conversion into fuels, chemicals and power. John Wiley & Sons; 2011.

[2] Butterman HC, Castaldi MJ. CO_2 as a carbon neutral fuel source via enhanced biomass gasification. Environ Sci Technol 2009;43:9030–7.

[3] Tomita A, Ohtsuka Y, Tamai Y. Low temperature gasification of brown coals catalysed by nickel. Fuel 1983;62:150–4.

[4] Ren L, Yang J, Gao F, Yan J. Laboratory study on gasification reactivity of coals and petcokes in CO_2/steam at high temperatures. Energy Fuels 2013;27:5054–68.

[5] Fan D, Zhu Z, Na Y, Lu Q. Thermogravimetric analysis of gasification reactivity of coal chars with steam and CO_2 at moderate temperatures. J Therm Anal Calorim 2013;113:599–607.

[6] Zhang L, Huang J, Fang Y, Wang Y. Gasification reactivity and kinetics of typical Chinese anthracite chars with steam and CO_2. Energy Fuels 2006;20:1201–10.

[7] Pineda DI, Chen J-Y. Modeling hydrogen inhibition in gasification surface reactions. Int J Hydrogen Energy 2015;40:6059–71.

[8] Hüttinger KJ, Merdes WF. The carbon-steam reaction at elevated pressure: Formations of product gases and hydrogen inhibitions. Carbon 1992;30:883–94.

[9] Hansen LK, Rathmann O, Olsen A, Poulsen K. Steam gasification of wheat straw, barley straw, willow and giganteus. Risø National Laboratory, Optics and Fluid Dynamics Department, Project No. ENS-1323/95-0010; 1997.

[10] Toomajian ME, Lussier MG, Miller DJ. Effect of oxidation and other treatments on hydrogasification rate of coal char. Fuel 1992;71:1055–61.

[11] Fjellerup J, Gjernes E, Hansen LK. Pyrolysis and Combustion of Pulverized Wheat Straw in a Pressurized Entrained Flow Reactor. Energy Fuels 1996;10:649–51.

[12] Zhang Y, Hara S, Kajitani S, Ashizawa M. Modeling of catalytic gasification kinetics of coal char and carbon. Fuel 2010;89:152–7.

[13] Long FJ, Sykes KW. The Mechanism of the Steam-Carbon Reaction. Proc R Soc London A Math Phys Eng Sci 1948;193:377–99.

[14] Tay H-L, Kajitani S, Zhang S, Li C-Z. Inhibiting and other effects of hydrogen during gasification: Further insights from FT-Raman spectroscopy. Fuel 2014;116:1–6.

[15] Ergun S. Kinetics of the reaction of carbon with carbon dioxide. J Phys Chem 1956;60:480–5.

[16] Biederman DL, Miles AJ, Vastola FJ, Walker PL. Carbon-carbon dioxide reaction: Kinetics at low pressures and hydrogen inhibition. Carbon 1976;14:351–6.

[17] Lussier MG, Zhang Z, Miller DJ. Characterizing rate inhibition in steam/hydrogen gasification via analysis of adsorbed hydrogen. Carbon 1998;36:1361–9.

[18] Redmond JP, Walker Jr PL. Hydrogen sorption on graphite at elevated temperatures. J Phys Chem 1960;64:1093–9.

[19] Linares-Solano A, Mahajan OP, Walker PL. Reactivity of heat-treated coals in steam. Fuel 1979;58:327–32.

[20] Huo W, Zhou Z, Wang F, Wang Y, Yu G. Experimental study of pore diffusion effect on char gasification with CO_2 and steam. Fuel 2014;131:59–65.

[21] Guizani C, Escudero Sanz FJ, Salvador S. Influence of temperature and particle size on the single and mixed atmosphere gasification of biomass char with H_2O and CO_2. Fuel Process Technol 2015;134:555–68.

[22] Barrio M. Experimental investigation of small-scale gasification ofwoody biomass (PhD Thesis). The Norwegian University of Science and Technology; 2002.

[23] Zhang Z, Lussier MG, Miller DJ. Stability of hydrogen adsorbed on Saran char. Carbon 2000;38:1289–96.

[24] Linares-Solano A, Almela-Alarcón M, de Lecea CS-M. CO_2 chemisorption to characterize calcium catalysts in carbon gasification reactions. J Catal 1990;125:401–10.

CHAPTER 7

CONCLUSIONS AND RECOMMENDATIONS FOR FUTURE WORK

7.1 Conclusions

Biomass is expected to play an important role in the future because the lignocellulosic components in biomass can be gasified to produce syngas for the sustainable production of electricity, chemicals, and fuels. However, one of the major challenges involved in commercialization of a biomass gasifier is the lack of fundamental studies which can help in generalization of results for different biomass feedstocks and for different gasification studies, and this is main focus of this dissertation. The research theme of this project focuses on providing a fundamental understanding of four important parameters that affect char gasification kinetics in a gasification reactor – pyrolysis conditions, biomass feedstock properties, interaction between two biomasses when co-fed together, and the gasifying media.

In Chapter 2, it was shown that for a biomass pyrolysis under commercially relevant gasifier operating conditions, increased pyrolysis severity causes a decrease in char surface area and the formation of more polyaromatic char. This led to a decrease in char gasification reactivity. Also, a complex char reactivity dependence on pyrolysis pressure was observed with a minimum char reactivity at 1.5 MPa and at high pyrolysis residence time. This parametric study of the effect of operating conditions on the gasification performance variables will help in making an informed decision for choosing

gasification reaction conditions for commercial scale gasifiers. Additionally, using process and kinetic data obtained from a lab scale reactor set-up that mimics a commercial gasifier, like the pressurized entrained flow reactor used in this study, provides data relevant for process design.

In Chapters 3 and 4, the reactivity of a wide variety of biomass chars are reconciled by determining a fundamental parameter that combines the effect of char physical surface area, inorganic content and composition, and the dispersion of inorganics into a single parameter called the active surface area (ASA). The initial reactivity of different types of biomass chars correlated well with its active surface area measured by CO_2 chemisorption. This empirical correlation can be used for predicting the gasification reactivity when processing different kinds of biomass chars, and it would also direct towards changes required in gasifier operating variables when processing varying feedstocks. More work needs to be done in the future to expand this study, and this will be highlighted in the next section.

In Chapter 5, it was found that the co-gasification of bagasse with cane leaves led to a lower than expected gasification performance due to potassium redistribution between chars. This was contrary to the expectation that co-gasification of sugarcane residue would lead to a potential synergistic increase in mixture reactivity due to interaction between these two different biomass chars. A staged gasification flow scheme was identified that was more suitable for co-processing these biomasses than co-gasification. Additionally, this study provides a fundamental understanding that helps qualitatively predict whether co-gasification of two different feedstocks would lead to overall synergy, or inhibition, or an additive effect. This study is important because co-

processing of different biomasses is required to potentially improve the economy of scale and fuel availability. Thus, it is important to understand if there is any interaction between the feedstock components rather than assuming additive effect.

In Chapter 6, it was shown that the evolution of char reactivity in steam is very different than in CO_2 for a potassium rich bagasse char. The *initial* char gasification reactivity in steam is higher than in CO_2 (about 2.4 times), as is commonly observed in literature. However, as the char gasification progresses in pure steam, the active sites are likely to be blocked by in-situ hydrogen product formation. This does not happen in pure CO_2 gasification. On the contrary, there is an enhancement in char reactivity with increasing conversion in CO_2 due to the increasing amount of K/C, thus creating more active sites. This causes higher *overall* char reactivity in CO_2 than in steam. Since this study is focused only for a potassium rich biomass, a future study is recommended for calcium and (K + Ca) based biomass to identify the differences in steam reactivity compared to CO_2 reactivity. This is discussed in the next section. Finally, this study showed that gasification of bagasse char in a mixture of steam and CO_2 is not additive. Therefore, mixed atmosphere gasification reactivity should be measured experimentally by conducting experiments with different $H_2O/CO_2/N_2$ mixtures.

In conclusion, this dissertation provides a more fundamental understanding of how char gasification kinetics in a gasification reactor is affected by the choice of pyrolysis conditions, variation in biomass feedstock characteristics, and interaction between two biomass chars, and the type of gasification medium employed for char gasification (steam compared to CO_2).

7.2 Recommendations for future work

7.2.1 Understanding char gasification reactivity of different biomass in steam

In Chapter 4, it was shown that active surface area (ASA) measured by CO_2 chemisorption at 300 °C is found to be a good descriptor to reconcile the initial char reactivity in CO_2 of different biomass chars. This empirical correlation between ASA of char and char reactivity can be used for predicting the initial gasification reactivity when processing different kinds of biomass chars in a gasifier.

However, this study was done with a limited set of biomass feedstocks. In addition, the variation in the carbon structure between these different biomass chars was assumed to be small in this study. Future studies should be directed to test and improve this empirical correlation by testing more biomass species and by incorporating the effect of differences in the carbon structure of different biomass chars on char reactivity. In addition, this study was done by using CO_2 as the gasification medium. A similar study could be done for steam gasification to determine if the same correlation is applicable for the initial char reactivity in steam. Since the active sites are likely to be same for steam and CO_2 gasification for a K-rich biomass char, as shown earlier in Chapter 6 (Section 6.3.4), it is expected that the same correlation may likely work for steam gasification.

7.2.2 Evolution of char reactivity profile in steam compared to CO_2 for calcium and (K + Ca) catalyzed reaction

In Chapter 6, it was shown that for a potassium rich bagasse char, the *initial* char gasification reactivity in steam is higher than in CO_2. However, the *overall* reactivity (as defined by the time for 90% char conversion) is higher in CO_2 than in steam, thus making

CO_2 a more attractive gasification agent compared to steam. However, calcium catalyzed gasification (for e.g., many biomass and coal chars) is likely to behave differently in steam and in CO_2 compared to the present study. This is because calcium does not sinter during steam gasification with conversion, while calcium sinters in CO_2 gasification due to formation of calcium carbonate [1]. This additional parameter will thus also play a role in determining the overall reactivity in steam compared to CO_2 for a calcium rich char, or for a char containing both potassium and calcium. Additionally, the role of concentration of potassium and calcium on the char reactivity trends in steam should be evaluated. Future work should focus on evaluating all these aspects experimentally.

7.2.3 Model to predict char gasification in a mixture of CO_2 and steam

In Chapter 6, it was shown that gasification of bagasse char in a mixture of steam and CO_2 is not additive, and that the mixed atmosphere gasification reactivity should be measured experimentally by conducting experiments with different gas mixtures. While there are models for shared active sites (during mixed atmosphere gasification) to predict char gasification reactivity [2], there is an additional complication of in-situ hydrogen inhibition that affects CO_2 gasification reactivity during mixed atmosphere gasification. This is not considered in the shared active site model. Thus, future work requires more experimental data for mixed atmosphere gasification at different temperatures (with different $H_2O/CO_2/H_2/CO/N_2$ mixtures) to propose a model to predict char gasification reactivity in a gasifier.

7.3 References

[1] Linaressolano A, Almelaalarcon M, Delecea CSM. CO_2 chemisorption to characterize calcium catalysts in carbon gasification reactions. J Catal 1990;125:401–10.

[2] Zhang R, Wang QH, Luo ZY, Fang MX, Cen KF. Competition and inhibition effects during coal char gasification in the mixture of H_2O and CO_2. Energy Fuels 2013;27:5107–15.

APPENDIX A

SUPPLEMENTARY INFORMATION FOR CHAPTER 3

A.1 Detailed mechanism of CO_2 gasification of char on potassium active sites

a) $* + CO_2 \leftrightarrow (CO_2)*$ *(CO_2 chemisorption on active site, *)*

b) $(CO_2)* \leftrightarrow O-* + CO\ (g)$ *(CO_2 dissociation on active site)*

c) $O-* + C \leftrightarrow C(O) + *$ *(Binding of oxygen to the edge carbon of char)*

d) $C(O) \rightarrow CO\ (g)$ *(Carbon gasification - Rate limiting step)*

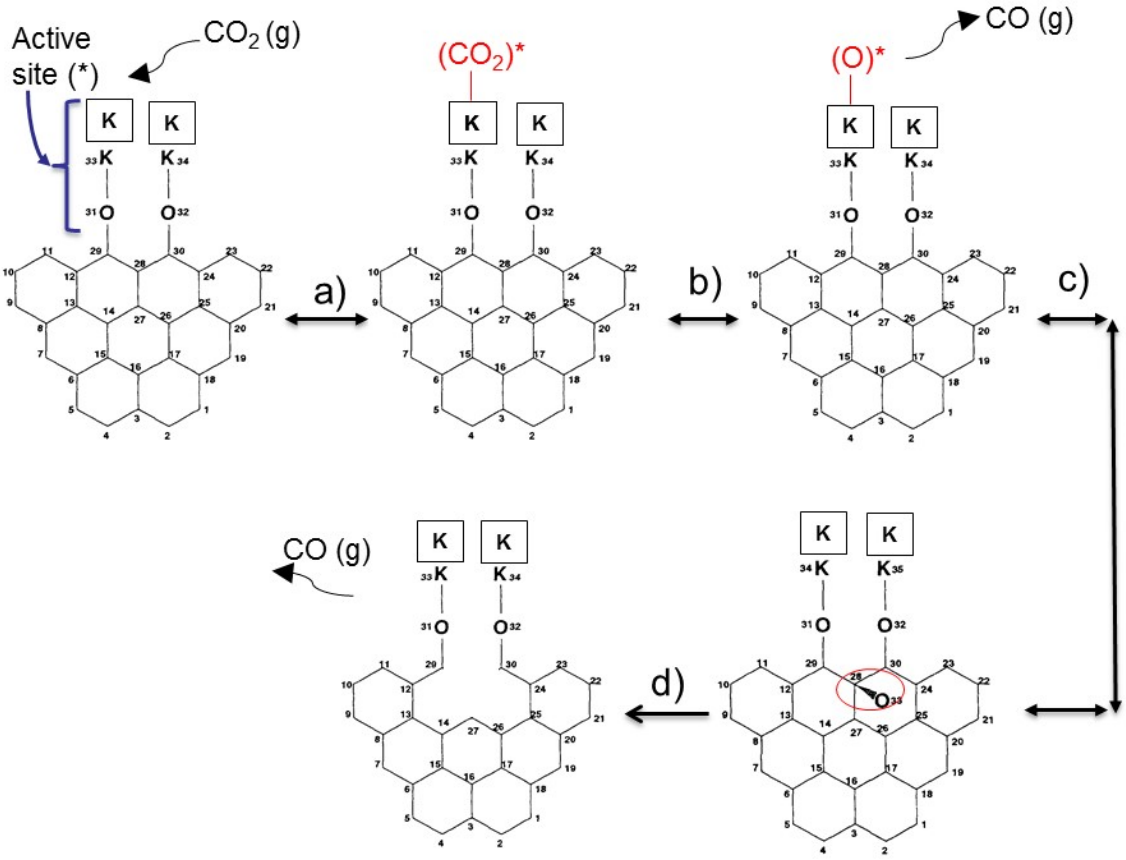

Figure A.1 Schematic showing the CO_2 gasification of char (shown as model substrate with zigzag face) on the potassium actives sites. The actives sites are the clusters (or particles) of alkali (or alkaline earth metals) anchored to the carbon by phenolate group.

APPENDIX B

SUPPLEMENTARY INFORMATION FOR CHAPTER 4

B.1 Distribution of pore surface area

Table B.1 shows the distribution of surface area in different size range pores (namely, micropores, mesopores and macropores). It can be seen that more than 90% of the total surface area of char is due to micropores.

Table B.1 Distribution of pore surface area in different biomass chars generated by pyrolysis of different biomass at 800℃ and 28 sec residence time

Surface area of different size range pores	**Char surface area, m^2/g**						
	Bagasse char		Pine char		Switchgrass char		Avicel
	5 bar	20 bar	5 bar	20 bar	5 bar	15 bar	5 bar
Micropore area (< 2nm)[a]	173	124	312	331	280	255	119
Mesopore area (2 - 50 nm)[b]	3	5	5	6	1	1	1
Macropore area (> 50 nm)[b]	4	4	1	2	1	2	1

[a] by DFT method using CO_2 physisorption

[b] by DFT method using N_2 physisorption

APPENDIX C

SUPPLEMENTARY INFORMATION FOR CHAPTER 5

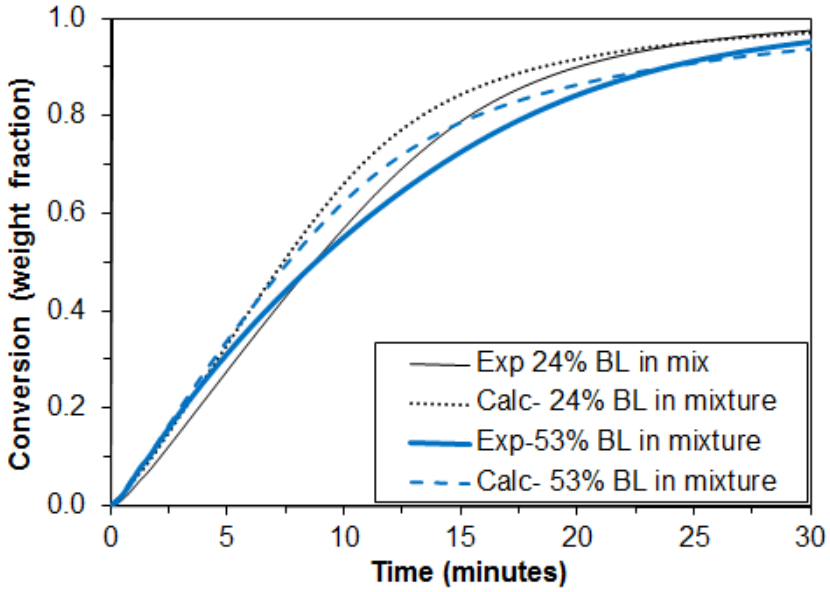

Figure C.1 Isothermal co-gasification of various mixtures of Brazil bagasse (BB) char and Brazil leaves (BL) char at 800 °C in pure CO_2. Exp and Calc refers to the experimentally measured reactivity and calculated (predicted) reactivity, respectively.

APPENDIX D

SUPPLEMENTARY INFORMATION FOR CHAPTER 6

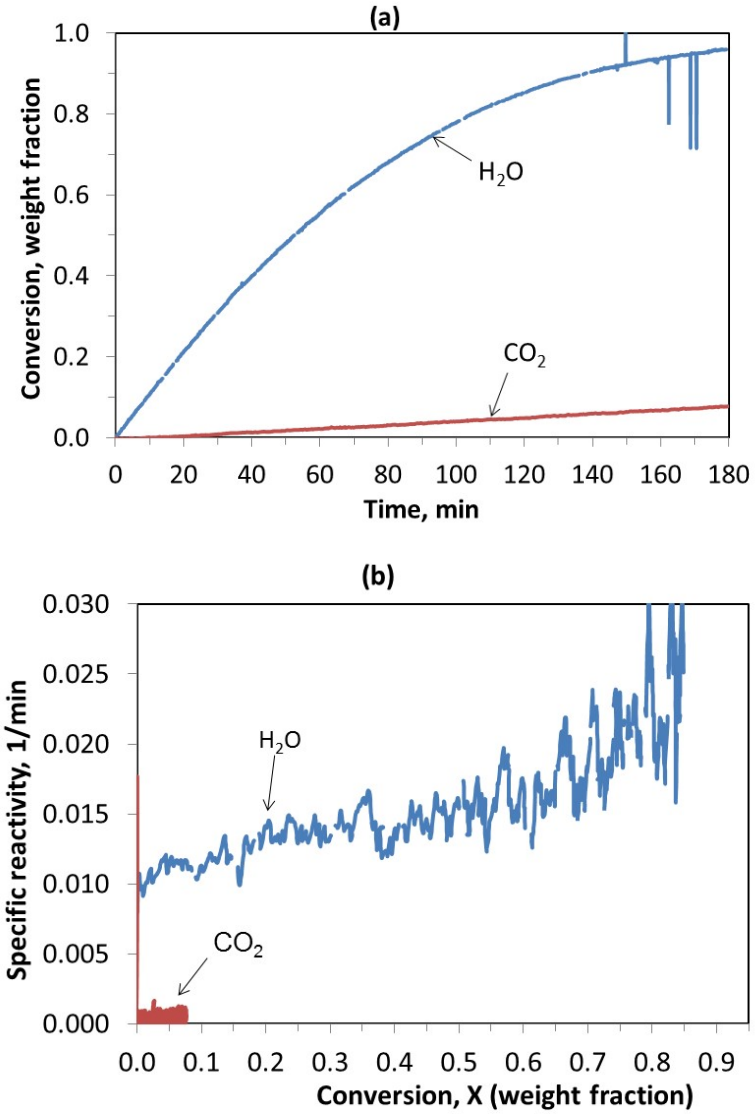

Figure D.1 Reactivity of Avicel char (generated by pyrolysis in the PEFR at 800 °C - 5 bar - 28 sec) in 100% steam and in 100% CO_2 at 800 °C. (a) Conversion vs. time plot, and (b) reactivity vs. conversion plot.

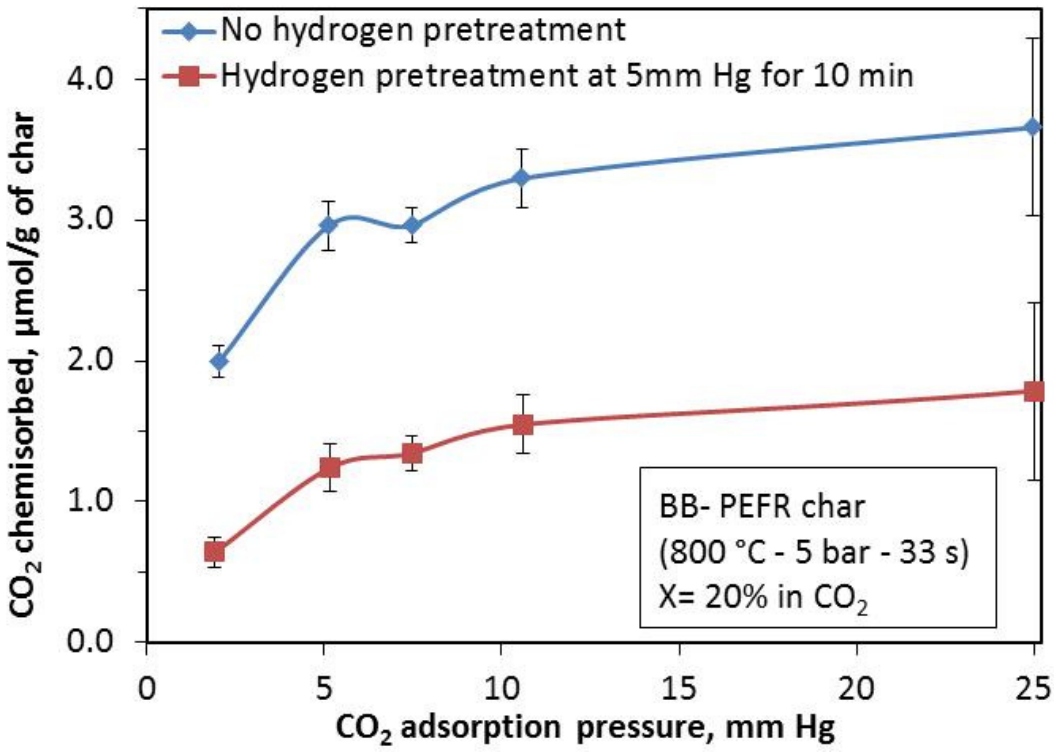

Figure D.2 Effect of hydrogen pretreatment of char (at 800 °C for 10 minutes with H_2 pressure of 5 mm Hg) on the subsequent CO_2 chemisorption quantity (at 300 °C). The char used is BB char from the PEFR at 800 °C – 5 bar – 33 sec which is then 20% converted by CO_2 gasification. CO_2 chemisorbed amount on this char is reduced after hydrogen pretreatment compared to no hydrogen pretreatment of this char.

VITA

MOHMED AKIL SYED

Mohmed Akil Syed was born in India on March 27, 1986. He attended primary and secondary school in Mumbai, India and graduated with 1st rank from high-school in May 2003 from Kendriya Vidyalaya Karanja, located in Mumbai, India. He then received an undergraduate degree in Chemical Engineering in May 2007 from the Institute of Chemical Technology (formerly UDCT), located in Mumbai, India. He received the Gold medal in 2007 from Mumbai university for scoring the highest marks in Chemical engineering exam. He then worked with UOP (A Honeywell Company) for 5 years – one year as assistant R&D engineer in Chicago (US) and four years as Field Technical advisor involved in start-up and troubleshooting of various petroleum refining and petrochemical process units located in India, China and Poland. He then moved to Atlanta, Georgia in August 2012 to pursue M.S. and Ph.D. degree in Chemical Engineering at Georgia Institute of Technology. When he is not working on his research, Akil enjoys watching and playing different sports and traveling.